

ALGEBRAIC RECONSTRUCTION TECHNIQUE FOR COMPUTERIZED TOMOGRAPHY WITH PARALLEL BEAM PROJECTION DATA

A Thesis submitted to
SHOBHIT UNIVERSITY, MEERUT
for the award of the degree of
DOCTOR OF PHILOSOPHY
in
COMPUTER ENGINEERING

By

Nirvikar

Under the Supervision of
Prof. (Dr.) Raghuvir Singh
&
Dr. Tanuja Srivastava



**Faculty of
Electronics, Informatics and Computer Engineering
Shobhit University, Meerut – 250110**

2012

Candidate's Declaration

I hereby certify that the work which is being presented in thesis entitled
**“ALGEBRAIC RECONSTRUCTION TECHNIQUE FOR COMPUTERIZED
TOMOGRAPHY WITH PARALLEL BEAM PROJECTION DATA”** in
fulfillment of requirement for the award of the Degree of Doctor of Philosophy
(D.Phil.) submitted in the **Faculty of Electronics, Informatics and Computer
Engineering at Shobhit University, Modipuram, Meerut** is an authentic record of
my own work under the supervision of **Prof. (Dr.) Raghuvir Singh** (*Academic
Advisor Shobhit University, Modipuram, Meerut and Director General, Shobhit
Institute of Engg. and Technology, Gangoh*) and **Dr. Tanuja Srivastava** (*Associate
Professor, Department of Mathematics, Indian Institute of Technology, Roorkee*).

I also declare that the work embodied in the present thesis

- (i) is my original work and has not been copied from any Journal/thesis/book, and
- (ii) has not been submitted by me for any other Degree/Diploma.

(Nirvikar)

Certificate of the Supervisor(s)

This is to certify that the thesis entitled "**ALGEBRAIC RECONSTRUCTION TECHNIQUE FOR COMPUTERIZED TOMOGRAPHY WITH PARALLEL BEAM PROJECTION DATA**" submitted by **Mr. Nirvikar** for the award of Degree of Doctor Philosophy in the **Faculty of Electronics, Informatics and Computer Engineering at Shobhit University, Modipuram, Meerut** is a record of authentic work carried out by him under our supervision.

The matter embodied in this thesis is the original work of the candidate and has not been submitted for the award of any other degree or diploma.

It is further certified that he has worked with us for the required period in the **Faculty of Electronics, Informatics and Computer Engineering at Shobhit University, Modipuram, Meerut and College of Engineering Roorkee.**

Prof. (Dr.) Raghuvir Singh
Academic Advisor
Shobhit University
Meerut – 250 110

Dr. Tanuja Srivastava
Associate Professor
Department of Mathematics
Indian Institute of Technology Roorkee
Roorkee 247667

Acknowledgement

I express my deeply indebted gratitude to **Prof. (Dr.) Raghuvir Singh** (*Academic Advisor Shobhit University, Modipuram, Meerut and Director General, Shobhit Institute of Engg. and Technology, Gangoh*). The immense convincing power, methodology of teaching, vast experience in research and above all, critical comments for improvement helped me at every step of my research work. I am proud to get necessary guidance from him in my research work. I also express my profound gratitude to **Dr. Tanuja Srivastava** (*Associate Professor, Department of Mathematics, Indian Institute of Technology, Roorkee*) for her advice, encouragement and guidance throughout the course of this research work.

I would also like to thanks **Prof. R.P. Agarwal**, (*Vice-Chancellor Shobhit University Meerut and Dean, Faculty of Electronics, Informatics and Computer Engineering*), an eminent professor in the field of Microelectronics, who helped me during the course of my research work in Shobhit University. He has shown me the right path which led me toward my goal. I am really thankful to him from my heart for his necessary guidance and help.

I would also like to thanks **Prof. J.B.Singh**, Professor, in the field of Statistics, who helped me during the course of my research work in Shobhit University. The simplicity and always ready to help has shown me the right path which led me toward my goal. I am really thankful to him from my heart for his necessary guidance and help.

Another simple, hardworking and eminent academician in the area of computer science, **Prof. A. K. Sharma**, who guided me through the minute details of the

research. He is ready to help and guide the researcher, day and night. I express my deep sense of gratitude to him.

I would also like to thanks **Brig. S.K. Sareen**, (*Registrar, Shobhit University, Meerut*), I have discussed several times with registrar sir, and he always encouraged me for my research work.

I also express my thanks to the office member of Shobhit University, Meerut for their help time to time.

I wish to place on record my deep sense of gratitude toward my parents, sisters, brother and my friends for their continuous encouragement. Also, I wish to acknowledge my wife as a great source of strength.

(**Nirvikar**)

CONTENTS

Candidate's Declaration	<i>i</i>
Supervisor(s) Certificate	<i>ii</i>
Acknowledgement	<i>iii</i>
Contents	<i>v</i>
List of Tables	<i>viii</i>
List of Figures	<i>ix</i>
List of abbreviations	<i>x</i>
Mathematical symbols	<i>xi</i>

Chapter No.	Page No.
1. CHAPTER I: INTRODUCTION 1	
1.1 Introduction	1
1.2 Mathematical Statement of the Problem	3
1.3 Objectives	7
1.4 Plan of Thesis	9
2. CHAPTER II: LITERATURE REVIEW 11	
2.1 Introduction	11
2.2 Transformation Methods	12
2.3 Finite Series Expansion Reconstruction Methods	19
2.4 Statistical Methods	22
2.5 Limited View Methods	23
3. CHAPTER III: FINITE SERIES EXPANSION RECONSTRUCTION METHODS 32	
3.1 Introduction	32
3.2 The Formulation of Discretized Model for Image Reconstruction	32

3.3 Methodology of the Series Expansion Approach	35
3.4 Basic Approaches and Methods of Finite Series Expansion	41
3.5 The Algebraic Approach	41
3.5.1 Algebraic Reconstruction Technique	42
3.5.2 Multiplicative ART	43
3.5.3 Generalized ART	45
3.5.4 Kackmarz's Relaxation Method	47
3.5.5 Algebraic Reconstruction with one Intermediate step (ART2)	48
3.6 The Feasibility Approach	48
3.6.1 Algebraic Reconstruction for Inequalities	49
3.6.2 ART3	50
3.6.3 ART with Damping Factor	52
3.6.4 Constrained ART	53
3.6.5 ART with Binary Constraint	53
3.7 The Optimization Approach	54
3.7.1 Entropy Optimization	54
3.7.2 Quadratic Optimization	55
3.8 Least Square Regularization Approach	57
4. CHAPTER IV: MODIFIED SIMULTANEOUS ALGEBRAIC RECONSTRUCTION TECHNIQUE	59
4.1 Introduction	59
4.2 Mathematical Principle of ART	60
4.2.1 Principle of Method of Projection	61
4.2.2 Example Explaining Projection Method	64
4.2.3 Geometric Interpretation	76
4.2.4 Efficiency	79
4.3 Modified Simultaneous Algebraic Reconstruction Technique (MSART)	82
4.3.1 Mathematical Explanation and Convergence of MSART	86

5. CHAPTER V: IMPLEMENTATION OF MODIFIED SIMULTANEOUS ALGEBRAIC RECONSTRUCTION TECHNIQUE	88
5.1 Introduction	88
5.2 Test Objects	89
5.2.1 Test Images	89
5.2.2 Projection Data	90
5.2.3 Errors	91
5.3 MSART Algorithms	92
5.4 Results of Numerical Implementation	94
6. CHAPTER VI: DISCUSSION AND COMPARISON	115
6.1 Introduction	115
6.2 Comparison with CBP	116
6.2.1 Error Analysis	116
6.2.2 Pictorial Quality of Reconstruction	121
6.2.3 Convergence with few projections	125
7. CHAPTER VI: CONCLUSION AND FUTURE RESEARCH	131
7.1 Conclusion	131
7.2 Future Research	132
REFERENCES	133
LIST OF REPRINTS	144

List of Tables

Table No.	Table Details	Page No.
Table 4.2.1:	Projection Value (p)	69
Table 4.2.2:	Initial Image Data ($f^{(0)}$)	69
Table 4.2.3:	Reconstructed Image	70
Table 4.2.4:	Projection data at each iteration	70
Table 4.2.5:	Error calculated in Image pixel values for every iteration	71
Table 5.4.2:	Convergence with projection data in PIC1	96
Table 5.4.2(contd):	Convergence with projection data in PIC1	97
Table 5.4.3:	Convergence in consecutive estimates in PIC1	98
Table 5.4.3(contd.):	Convergence in consecutive estimates in PIC1	99
Table 5.4.5:	Convergence with projection data in PIC2	101
Table 5.4.5(contd):	Convergence with projection data in PIC2	102
Table 5.4.6:	Convergence in consecutive estimates in PIC2	103
Table 5.4.6(contd.):	Convergence in consecutive estimates in PIC2	104
Table 5.4.8:	Convergence with projection data in PIC3	106
Table 5.4.8(contd):	Convergence with projection data in PIC3	107
Table 5.4.9:	Convergence in consecutive estimates in PIC3	108
Table 5.4.9(contd.):	Convergence in consecutive estimates in PIC3	109
Table 5.4.11:	Convergence with projection data in PIC4	111
Table 5.4.11(contd):	Convergence with projection data in PIC4	112
Table 5.4.12:	Convergence in consecutive estimates in PIC4	113
Table 5.4.12(contd.):	Convergence in consecutive estimates in PIC4	114
Table 6.1:	L_1 and L_2 errors for PIC1	117
Table 6.2:	L_1 and L_2 errors for PIC2	118
Table 6.3:	L_1 and L_2 errors for PIC3	119
Table 6.4:	L_1 and L_2 errors for PIC4	120
Table 6.4.1:	Given Projection Value (p)	125
Table 6.4.2:	Initial Image Data ($f^{(0)}$)	125
Table 6.4.3:	Reconstructed Image after 55 iterations	126
Table 6.4.4:	Error calculated in projection values in each iteration	127
Table 6.4.5:	Error calculated in Image pixel values in each iteration	128

List of Figures

Figure No.	Figure Description	Page No.
Figure 1.1:	Reconstruction Region of Image	4
Figure 1.2:	Showing angular direction θ and perpendicular distance S	5
Figure 1.3:	Projection data along perpendicular line (s, θ)	6
Figure 3.1:	Digitization of image and projection data	35
Figure 3.2:	Projection as sum of intersecting pixels	35
Figure 3.3:	Methodology of series expansion approach [Censor (1983)].	40
Figure 4.1(a):	The reconstruction problem as a system of linear equation (2×2) .	65
Figure 4.1(b):	The reconstruction problem as a system of linear equation (3×3) .	68
Figure 4.2:	Showing two hyper planes H_1 and H_2 Equation (4.3.1) and their intersection f^*	76
Figure 4.3:	Showing plane H_1 , point f^0 and its projection on H_1	77
Figure 4.4:	Showing plane H_1, H_2 and point f^0 with the projections	78
Figure 4.5:	Digitization with square grid.	84
Figure 5.2.1:	Digitized test images are 64×64 digitized images.	89
Figure 5.2.2:	100×64 digitized image of projection data Digitized projection data for test image PIC1-PIC4.	90
Figure 5.4.1:	Reconstruction of PIC1 at different iterations	95
Figure 5.4.4:	Reconstruction of PIC2 at different iterations	100
Figure 5.4.7:	Reconstruction of PIC3 at different iterations	105
Figure 5.4.10:	Reconstruction of PIC4 at different iterations	110
Figure 6.1:	Comparison of reconstruction with CBP for PIC1	121
Figure 6.2:	Comparison of reconstruction with CBP for PIC2	122
Figure 6.3:	Comparison of reconstruction with CBP for PIC3	123
Figure 6.4:	Comparison of reconstruction with CBP for PIC4	124
Figure 6.5:	Reconstructed Image at different iterations	126
Figure 6.4.7-6.4.10:	Image as a line Graph using ART at different iterations	129

List of Abbreviations

ART	:	Algebraic Reconstruction Techniques
BP	:	Back Projection
CAT	:	Computerized Transmission Tomography
CBP	:	Convolution Back Projection
CT	:	Computerized Tomography
DFTs	:	Discrete Fourier Transforms
DT	:	Diffraction Tomography
EM	:	Expectation Maximization
FBP	:	Filtered Back Projection
FFT	:	Fast Fourier Transform
IRR	:	Iterative Reconstruction-reprojection
MART	:	Multiplicative ART
MLS	:	Multilevel Scheme
MPI	:	Message Passing Interface
MRI	:	Magnetic Resonance Imaging
MSART	:	Modified SART
NDE/NDT	:	Nondestructive Evaluation/Testing
PART	:	Parallel ART
PET	:	Positron Emission Tomography
RPS	:	Random Permutation Scheme
SART	:	Simultaneous ART
SAS	:	Sequential Access Scheme
SIRT	:	Simultaneous Iterative Reconstruction Technique
SMART	:	Simultaneous MART
TV	:	Total Variation
VSR	:	Virtual Symmetry Reconstruction

Mathematical Symbols

f	:	unknown density function
\mathbb{R}	:	set of real numbers
\int	:	integral
\leq	:	less than or equal to
\geq	:	greater than or equal to
\parallel	:	mod
\in	:	is an element of
Σ	:	summation
\forall	:	for all
\neq	:	not equal to
i	:	subscript for reconstruction elements
j	:	subscript for projection elements
k	:	subscript for projections
m	:	number of projection elements
n	:	number of reconstruction elements
p_j	:	density measurement of the j^{th} projection element
w_{ij}	:	fraction of reconstruction element
R	:	reconstruction space
r_θ	:	width of a parallel ray at angle θ
q	:	iteration counter

CHAPTER I: INTRODUCTION

1.1 INTRODUCTION

There are many situations of real world, when it is desired to determine some structural (internal) properties of an object or substance, using the measurements, called data, obtained by methods that do not damage or disturb the conditions of the object or substance under investigation. Tomography is a method used to reconstruct cross-section of the internal structure of an object without having cut or damaging the object. The term occurs in the combination of computer referred Computerized Tomography (CT) or Computer Assisted Tomography (CAT) or Image Reconstruction. Most important application of Tomography is in industries and research activities in areas such as medical sciences, metallurgical engineering, material science, earth sciences for mapping of underground resources such as the search of oil depends upon the analysis of seismic data etc. The most revolutionary applications of tomography are in medical diagnosis such as ultrasound, X-ray, CAT, PET scanning, MRI etc.

In order to determine complete information for the image reconstruction, projection data for the complete object are needed. The Projection data is obtained by a smaller angle rotation around the object. It is not possible to measure a large number of projections in every situation, and it may also happen that they are not uniformly distributed on complete angular distance i.e. on 180^0 or 360^0 (used in 3D). For transform methods, large number of projections at all angular distances distributed uniformly is a necessary condition to get the solution. Thus in all these situations transform methods becomes inapplicable for image reconstruction problem. The

example for such kind of situations arises in earth sciences, in earth resources imaging using cross boreholes methods from monitoring reflection of radiation or energy flows. In astronomy also the measurements on complete rotation of celestial bodies is not possible many times, because it is reconstructed in 3D. The data for determining the internal structure or properties of the objects or materials under investigation are obtained by passing energies through them from different directions at different angles and measuring the transmitted energy at the other end. In medical or industrial applications, the illumination is done by X-rays and/or gamma rays. Measurements (data) are determined as energy loss (i.e. absorbed energy) with the help of a source of energy and detector setup. Here the source emits the energy as X-rays and/or gamma rays and the detector detects the energy escaped from the object. The properties or the internal structure of the object is determined from the pattern of the absorbed energy at different locations of the object covering the complete object. These kinds of determinations are known as image reconstruction from projection data. [Deans (1983), Herman (1980), Kak and Slaney (2001) Natterer (1986, 2001), Srivastava (1992)].

The problem of Image Reconstruction in two dimensions mathematically has been investigated and reported in this thesis. In other words a parallel algorithm for Computed Tomography based on the Algebraic Reconstruction Technique (ART) algorithm for reconstructing pictures from projections has been reported in this thesis that is useful for applications such as Computed Tomography (CT or CAT) to produce an image of comparable or better quality. The structure is identified as

absorption (or attenuation) coefficient of X-ray or gamma ray as a real valued function defined in two dimensions.

Fundamentally, tomographic imaging deals with reconstruction of an image from projections of different directions specified by the angle. The measurements known as projection data are obtained as total energy loss (or absorption or attenuation) of X-rays and/or gamma rays along a strip or a line (explained in chapter III, figure 3.1), identified by the direction and distance from the center of the image. Hence projection data are the line or strip integral of function f . [Deans (1983), Herman (1980), Kak and Slaney (2001) Natterer (1986, 2001), Srivastava et al (1992, 1994), Srivastava (2004)].

1.2 MATHEMATICAL STATEMENT OF THE PROBLEM

It is assumed that the domain of the function ' f ' is confined to a finite region of a plane. Determination of the function from its line integral was first solved by Radon (1917). After a big gap of several years some other mathematicians John (1955), Bureau (1955), Deans (1983) etc extended Radon's work, which was based on limited angles to find the image function. The solution of the problem for real world applications in astronomy was reported by Bracewell (1956). He also reconstructed sun spots from multiple views of the Sun from the Earth. The computational solution of ill-posed problems of the form arising in the general area of tomography is a very active research topic in computational mathematics.

The value of the image function within the range of the image is finite, while it is zero outside the range of the image function. Let image be defined on unit square or unit circle as shown in Figure 1.1.

$$S = \{(x_1, x_2) \in \mathbb{R}^2 : -1 \leq x_i \leq 1, \quad \} \text{ for unit square}$$

Or

$$S = \{(x_1, x_2) \in \mathbb{R}^2 : x_1^2 + x_2^2 = 1\} \text{ for unit circle}$$

and range is any closed interval $[a, b], a, b \in \mathbb{R}$.

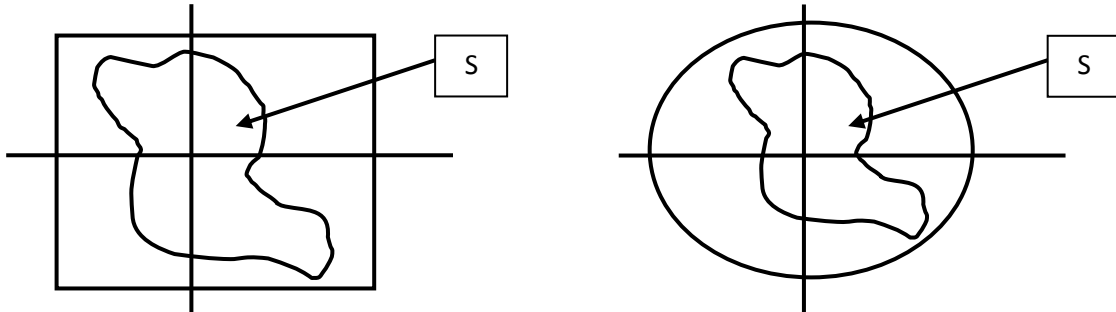


Figure1.1: Reconstruction Region of Image

The projection data known as Radon transform is identified by angular direction ' θ ' and perpendicular distance 's' from the centre of the image as shown in Figure 1.2. The projection data along perpendicular line (s, θ) shown in Figure 1.3 by rotation of the axis and is represented mathematically as follows

$$B = (s \cos \theta, s \sin \theta) \text{ is a fixed point on L}$$

$$OC = s \cos \theta$$

$$CE = -t \cos(90 - \theta) = -t \sin \theta$$

$$\text{So, } x_1 = s \cos \theta - t \sin \theta$$

$$OD = s \cos(90 - \theta) = s \sin \theta$$

$$DF = t \cos \theta$$

$$\text{So, } x_2 = t \cos \theta + s \sin \theta$$

Hence, the Radon transform can be written as

$$\begin{aligned}
 p(s, \theta) &= \int_{-L(s, \theta)}^{L(s, \theta)} f(x_1, x_2) dt \\
 &= \int_{-L}^L f(s \cos \theta - t \sin \theta, s \sin \theta + t \cos \theta) dt
 \end{aligned}$$

In general, Radon transform of a function $f(x_1, x_2)$ of two variables is the set of line integrals, used widely in a large class of applications which are in the area of image reconstruction. It is the problem of finding f from the above mentioned line integrals(s, θ) and is related to the inversion of the Radon transforms. Line integrals are obtained by moving the source and detector through the object. Then an appropriate inversion or reconstruction algorithm is applied to recover an approximation to the attenuation coefficient distribution over a transverse section of some portion of the object.

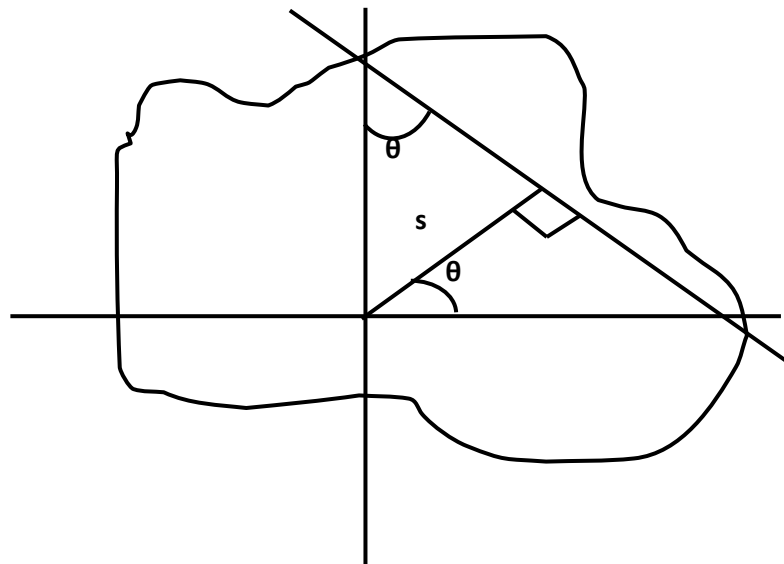


Figure 1.2: Showing angular direction θ and perpendicular distance S

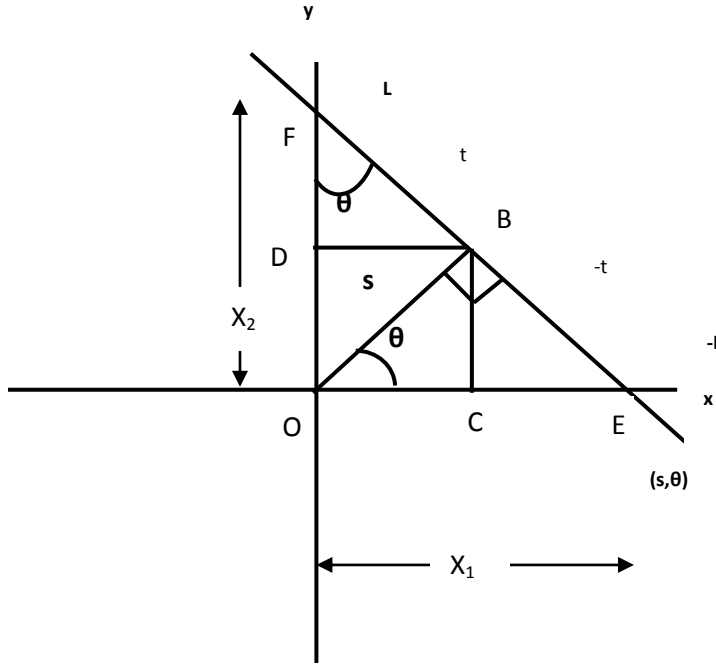


Figure 1.3: Projection data along perpendicular line (s, θ)

In real world problems, the measurements are taken for a finite number of angular distance and a finite number of perpendicular distances in the interval [-1 to 1], thus we have $p(s, \theta)$ for $s \in [-1, 1]$ and $\theta \in [0, \pi]$ for say K distances and L number of angles from 0 to π . Now from this projection data which is $K \times L$ line integrals, we determine $f(x_1, x_2) \in S$. These projection data are not actually integrals but approximation of these integrals and contains noise as well as set up disturbances or we can say that the inversion of Radon transform is an ill-posed problem (especially when the data are not complete or not accurate) and the number of projection data is limited. Practically the problem of Image Reconstruction is much more complicated than the theoretical solution provided by Radon [John (1955)].

1.3 OBJECTIVES

The main aim of this research work is to develop an algorithm for image reconstruction using the methods of solving the highly ill posed (small change in the input data can cause large change in the results) system of linear equation ($Af = P$), which is fast, efficient, accurate, and easy to implement.

where

A_{mxn} is the projection matrix,

f_{nx1} is the image vector and

P_{mx1} is the measurement vector.

To meet out the above mentioned objective we followed the following steps:

- (a) Study of various methods available in literature for image reconstruction problem.
- (b) Analysis of the methods used for solving the problem of image reconstruction to select a suitable method for image reconstruction.
- (c) Development of an algorithm named “Modified Simultaneous Algebraic Reconstruction Technique (MSART)”, better than the existing algorithms for image reconstruction.
- (d) Implementation and evaluation of MSART algorithm on some images for which the projection data were available. The comparison is done with the CBP algorithm and the convergence is also shown with limited number of projections.

All the above mentioned steps are described one by one as follows:

a) Study of various methods available in literature for image reconstruction problem

Image reconstruction has been used in various fields such as in medical diagnosis, referred as Computerized Tomography or Computerized Transmission Tomography (CT or CAT), in Nuclear Medicine as Positron Emission Tomography (PET), in optics as Optical Methods, in Molecular Biology as Electron Microscopy, in Acoustic as Ultrasound, in Astronomy and Astrophysics, Geophysics etc as Magnetic Resonance Imaging (MRI). The methods employed for image reconstruction for one field may not be suitable for the image reconstruction in other fields. The required accuracy of the results, amount of the input data, and the time for image reconstruction are the factors which have been kept in mind for developing the algorithm for different situations. Therefore we critically studied several methods and the critical review on these methods is reported in chapter II.

b) Analysis of the methods used for solving the problem of image reconstruction to select a suitable method for image reconstruction.

The applications are very much varied and for many applications quite a few methods have been developed. All these methods, when transformed to mathematical algorithms, are required to be digitized for implementation on computers. On analyzing the merits and demerits of all the methods of image reconstruction reported in Chapter – II, “Finite Series Expansion Reconstruction Method” was selected to solve the problem of image reconstruction. The review of the work done on Finite Series Expansion Reconstruction Method is given in Chapter – III with its variations and limitations.

c) Development of an algorithm named “Modified Simultaneous Algebraic Reconstruction Technique (MSART)”, better than the existing algorithms.

The method “Modified Simultaneous Algebraic Reconstruction Technique (MSART)” was developed by incorporating the properties of ART and SART methods described in chapter - III, along with some mathematical modifications for better convergences. The details of the MSART algorithm are given in Chapter - IV.

d) Implementation and evaluation of MSART algorithm on some images for which the projection data were available.

The computer program for MSART algorithm was developed and the program was implemented on four images named Chromosomes, Saturn, Smooth and Thorax respectively for which the projection data were available to check the validity of the algorithm. The algorithm and results are discussed in Chapter - IV and V respectively.

1.4 PLAN OF THESIS

The material embodied in this research work has been presented into seven chapters of this thesis. First chapter is introduction in which the subject has been introduced describing the progressive history, importance and the statement of the problem along with its objectives of the research work.

In second chapter, the literature review on image reconstruction is provided, for deciding the method to prepare mathematical algorithm for the purpose of present research work. After discussion of several methods finally “Finite Series Expansion Reconstruction Method” was selected for detailed critical analysis.

The third chapter deals with Finite Series Expansion Reconstruction Methods. The formulation of the problem in digitized form and the methodology of approach along

with the basic approaches and their methods such as algebraic approach, feasibility approach, optimization approach and least square regularization approach etc have been discussed in this chapter.

In chapter four, the development of the algorithm “Modified Simultaneous Algebraic Reconstruction Technique (MSART)” for algebraic reconstruction method has been described. The convergence of this algorithm has also been discussed because we are interested in knowing whether the iterative process is approaching towards actual solution, and if it is approaching towards correct solution, then how fast it is reaching there or how many iterations steps it requires to get the solution.

In chapter five, according to the convergence criteria of two MSART algorithms with their numerical implementations have been given. Further these algorithms are tested on images named Chromosomes, Saturn, Smooth and Thorax and the results of MSART algorithm with convergence are reported.

In chapter six, gives the discussion on MSART algorithm and its results have been compared with the results of other algorithm. The reconstruction and error are compared and reported.

In chapter seven, conclusions and future research scope have been discussed.

CHAPTER II: LITERATURE REVIEW

2.1 Introduction

The basic of image reconstruction from projection was introduced by Herman, (1980), Natterer and Wubbeling (2001) and Kak and Malcolm (2001). Recently image reconstruction has become very important for determining the internal structure of objects from its projection. There is a wide scope of carrying out theoretical as well as applied work in the area of image reconstruction. The determination of internal structure or properties of an object is known as image reconstruction or computed tomography. The basic principle of image reconstruction is that the two dimensional reconstruction space is divided into small pixels R_i ($i=1, 2, \dots, n$) each of which is assigned a value f_i . The radiation after passing through a very narrow strip (line) gives a projection P_i of the two dimensional space.

The solution of the problem to reconstruct a function from its projections was proposed by Radon (1917). The current excitement in the field of image reconstruction originated with the Hounsfield's invention of the x-ray computed tomographic scanner for which he received a Nobel prize in 1972. Allan Cormack independently discovered some of the algorithms of image reconstruction and shares the Noble prize with Hounsfield in 1972. His invention showed that it is possible to compute high-quality cross-sectional images with an accuracy now reaching one part in thousand in spite of the fact that the projection data do not strictly satisfy the theoretical models. The invention also showed that it is possible to process a very large number of measurements, a million for the case of x-ray tomography with fairly

complex mathematical operations. This image reconstruction problem, after a discretization of the image domain, leads to a system of linear equations which is inevitably inconsistent, due to noise, inaccurate measurements, and the discretization process.

Different work done in the area of image reconstructions for which several types of algorithms have been developed, these can be grouped in four main categories:

1. Transformation Methods,
2. Finite Series Expansion Reconstruction Methods,
3. Statistical Methods, and
4. Limited View Methods

A literature review of all these methods of reconstruction is described in this chapter.

2.2 Transform Methods

In this category of methods of image reconstruction from projections is formulated mathematically to obtain the image function $f: \mathbb{R}^2 \rightarrow \mathbb{R}$, which are the line integrals along the line $(s, \theta); p(s, \theta)$ given as the projection data,

$$p(s, \theta) = \int_{-L}^{L} f(s \cos \theta - t \sin \theta, s \sin \theta + t \cos \theta) dt$$

The image is reconstructed by obtaining analytic inversion of Radon transform in some manner with assumption of continuity on both the image functions f and projection data $p(s, \theta)$. For application on real problems in this procedure the obtained

analytic formulae are digitized. Some of the major work reported in this area is given as follows.

Direct inversion of Radon transform known as radon inverse formula was first given by Radon (1917) himself

$$[R^{-1} p](r, \theta) = \frac{1}{2\pi^2} \int_0^\pi \int_{-\infty}^\infty \frac{1}{rcos(\theta-\phi)-l} p_1(s, \theta) d\theta ds \quad (2.2.1)$$

But it was not practically applied. Theoretically some more inversion of radon transform were reported recently such as Nievergelt (1986), Van Schie et al (1989), Lautsch (1989). The physical problems which make these direct inverse formulae not applicable were discussed by Joseph (1981) and by Macovaski (1983). The mathematical aspect of image reconstruction problem is discussed by Louis and Natterer (1983).

The practical solution and application of that solution was first done by Bracewell (1956) in radio astronomy using the relation of projection data with the image function in Fourier domain, which is popularly known as ‘Projection Slice Theorem’. In this work direct Fourier inversion was used which required certain filtering. This method and some more modification in fine manner with more applications are given by Bracewell (1978). Crowther et al (1970) used Fourier inversion for 3 dimensional reconstructions in Electron Microscopy, while Hinshaw and Lent (1983) applied this technique in NMR. One of such methods known as Linogram method was published by Herman et. Al (1992) and Edholm et. Al (1988).

The basic result of this method justifies the well-known *projection theorem* which

says that “taking the two-dimensional Fourier transform is the same as taking the Radon transform and then applying the Fourier transform with respect to the first variable” by Herman (1980). The method was first proposed by Edholm et. Al (1987). The merit of this method is its speed of execution. The paper deals with three-dimensional problems; but we will apply this approach for two-dimensional problems.

For the linogram approach we assume that the data were collected in a special way (that is, at points whose locations will be precisely specified); if they were collected otherwise, we need to interpolate prior to reconstruction. If the function is to be estimated at an array of points which covers the object for reconstruction with rectangular coordinates $\{(id, jd) / -N \leq i \leq N, -N \leq j \leq N\}$, then the data function p needs to be known at points

$$(nd_m, \theta_m), -2N - 1 \leq n \leq 2N + 1, -2N - 1 \leq m \leq 2N + 1 \quad (1)$$

and at points

$$\left(nd_m, \frac{\pi}{2} + \theta_m\right), -2N - 1 \leq n \leq 2N + 1, -2N - 1 \leq m \leq 2N + 1, \quad (2)$$

Where

$$\theta_m = \tan^{-1} \frac{2m}{4N+3} \text{ and } d_m = d \cos \theta_m \quad (3)$$

Two facts about the linogram method can be described as, One is the most expensive computation that needs to be used in any of the stages is taking of *discrete Fourier transforms* (DFTs). Secondly, the output of any stage produces estimates of function values at exactly those points where they are needed for the discrete computations.

These two facts which indicate why the linogram method is computationally efficient and accurate.

The linogram method using a multi-stage procedure. We now list these stages,

1. Fourier transformation of the data— For each value of the second variable, we take the DFT of the data with respect to the first variable in Eq. (1) and Eq. (2). By the projection theorem, this provides us estimates of the two-dimensional Fourier transform F of the object at the points (in a rectangular coordinate system)

$$\left(\frac{k}{(4N+3)d}, \frac{k}{(4N+3)d} \tan \theta_m \right), -2N - 1 \leq k \leq 2N + 1, \quad (4)$$

$$-2N - 1 \leq m \leq 2N + 1$$

and at points (also in a rectangular coordinate system)

$$\left(\frac{k}{(4N+3)d} \tan \left(\frac{\pi}{2} + \theta_m \right), \frac{k}{(4N+3)d} \right), -2N - 1 \leq k \leq 2N + 1, \quad (5)$$

$$-2N - 1 \leq m \leq 2N + 1$$

2. Windowing— At this stage we may suppress those frequencies which we suspect to be noise-dominated by multiplying with a *window function*.

3. Separating into two functions— The sampled Fourier transform F of the object to be reconstructed is written as the sum of two functions, G and H . G has the same values as F at all the points specified in Eq. (4) except at the origin and it is zero at all other points. H has the same values as F at all the points specified in Eq. (5) except at the origin and is zero at all other points. Thus by first taking the two-dimensional inverse Fourier transforms of G and H separately and then adding the results, we get an estimate of f .

4. Chirp z-transformation in the second variable— we know that the value of G is zero outside the sampled region. Hence, for each fixed k , $0 < |k| \leq 2N+1$, we can use the chirp z -transform to estimate the inverse DFT in the second variable at points

$$\left(\frac{k}{(4N+3)d}, jd \right), -2N - 1 \leq k \leq 2N + 1, -N \leq j \leq N \quad (6)$$

The chirp z -transform can be implemented using three FFTs as reported by Edholm et. al (1988).

5. Inverse transformation in the first variable— The inverse Fourier transform of G can now be estimated at the required points by taking, for every fixed j , the inverse DFT in the first variable of the values at the points of Eq. (6).

Based on “Projection Slice Theorem” another method known as Convolution Back Projection (CBP) algorithm was developed by Bracewell and Riddle (1967), the discrete implementation of CBP algorithm was given by Ramchandran and Lakshminarayanan (1971) in astronomy and electron microscopy, Hermen and Rowland (1973) in x-ray tomography, Shepp and Logon (1974) in medical application. Lewitt et al (1978) modified the CBP method with implementation and comparison. Here this method is given for reference only as shown in Lewitt (1983).

In this algorithm, first, for fixed values of θ , convolutions defined by

$$[p * y q](l', \theta) = \int_{-\infty}^{\infty} p(l, \theta) q(l' - l, \theta) dl \quad (7)$$

are carried out, using a *convolving function* q . Second, estimate f^* of f is obtained by *backprojection* as follows:

$$f^*(r, \theta) = \int_0^\pi [p * y q](r \cos(\theta - \phi), \theta) d\theta \quad (8)$$

To make explicit the implementation of this for a given measurement vector, assume that the data function p is known at points $(nd, m\Delta)$, $-N \leq n \leq N$, $0 \leq m \leq M-1$, and $M\Delta = \Pi$. Further assume that the function f is to be estimated at points (r_j, Φ_j) , $1 \leq j \leq J$. The computer algorithm operates as follows.

A sequence f_0, \dots, f_{M-1}, f_M of estimates is produced; the last of these is the output of the algorithm. First define

$$f_0(r_j, \phi_j) = 0, \quad (9)$$

for $1 \leq j \leq J$. Then, for each value of m , $0 \leq m \leq M-1$, produce the $(m+1)$ estimate from the m th estimate by a two-step process:

1. For $-N \leq n' \leq N$, calculate

$$p_c(n'd, m\Delta) = d \sum_{n=-N}^N p(nd, m\Delta) q((n' - n)d) \quad (10)$$

using the measured values of $p(nd, m\Delta)$ and precalculated values (same for all m) of $q((n' - n)d)$. This is a discretization of Eq. (7).

2. For $1 \leq j \leq J$, set

$$f_{m+1}(r_j, \phi_j) = f_m(r_j, \phi_j) \Delta p_c(r_j \cos(m\Delta - \phi_j), m\Delta) \quad (11)$$

This is a discretization of Eq. (8). To do it, interpolate in the first variable of p_c from the values calculated in Eq. (10) to obtain the values needed in Eq. (11). In practice, once $f_{m+1}(r_j, \phi_j)$ has been calculated, $f_m(r_j, \phi_j)$ is no longer needed and the computer can reuse the same memory location for $f_0(r_j, \phi_j), \dots, f_{M-1}(r_j, \phi_j), f_M(r_j, \phi_j)$.

In a complete execution of the algorithm, the uses of Eq. (10) require $M(2N+1)$ multiplications and additions, while all the uses of Eq. (11) require MJ interpolations and additions.

Wei, Wang and Hsieh (2005) reported a new fan-beam CT formula, based on which, the relation between the filtered backprojection (FBP) algorithm and the backprojection (BP) algorithm is described. Specifically, the FBP algorithm can be expressed in a series with its first-order approximation being the BP algorithm.

Method of paired transforms for reconstruction of images from projections: Discrete model by Grigoryan (2003), an effective method of the discrete image reconstruction from their projections was introduced. The method is based on the vector and paired representations of the two-dimensional (2-D) image with respect to the 2-D discrete Fourier transform. Such representations yield algorithms of image reconstruction by minimal number of attenuation measurements in certain projections. The proposed algorithms are described in detail for an $N \times N$ image. The inverse formulas for image reconstruction are given. The efficiency of algorithms is expressed in the fact that they require a minimal number of multiplications.

Statistically optimal convolving function (filter) is derived for discrete implementation of the convolution backprojection method by Srivastava (1994). The method of derivation simultaneously takes the following steps into account (i) "the process" generating the object images, (ii) the data collection geometry, (iii) the discretization scheme used, (iv) various interpolation used, and (v) the data noise. The proposed filter minimizes the expected weighted sum of squared errors in pixel reconstructions.

The Error analysis for CBP algorithm is done by Natterer (1980), Munshi (1988) Lautsch (1989) gave an error analysis for spline inversion of Radon transform in the set-up of Sobolev spaces used by Natterer. These error analyses are for continuous CBP for discrete CBP by Rathore (1994), has used tomographic spaces for error analysis. But the nature of projection data and image function is statistical, thus statistical error analysis is done by Srivastava et al (1992), Srivastava (2003, 2004). Srivastava (2006).

2.3 Finite series expansion reconstruction methods

The finite series expansion methods are fundamentally different from transform methods. They differ basically in formulation of problem itself. In this method the problem is digitized first, which says that the image function f and projection data $p(s, \theta)$ both are considered in discrete form as the measurements (projection data) is practically available in discrete form. So these methods also take the image function to be discrete and find the reconstruction in discrete form than the image is produced. This approach leads to the system of linear or nonlinear equations. Thus the problem of image reconstruction from projections reduces to solving the system of linear equations $\mathbf{Af} = \mathbf{p}$, with $f_{n \times 1} = (f_1, f_2 \dots, f_n)'$ as image vector, $\mathbf{P}_{m \times 1} = (p_1, p_2 \dots, p_n)'$ as measurement vector both in discrete form and $\mathbf{A}_{m \times n} = ((a_{ij}))_{m \times n}$ as the coefficient (projection) matrix. Some of major work in this area is reported here.

This approach was introduced by Gordon et al (1970), where the problem of image reconstruction was formulated as system of linear equations and the solution is

provided by an iterative method, because of large size and sparsity of the system of linear equations. But it is shown that in general ART produces erroneous reconstructions. An alternative iterative method is proposed which will give correct reconstructions under certain conditions. One of the potential applications of this method is in determining the three-dimensional structure of objects from electron micrographs Gilbert (1971). But firstly this approach was practically used by Hounsefield (1972). Later it was observed that this iterative method is similar to the method provided by Kackmarz (1983) for solution of system of linear equations. Further many modifications in methods of solution of linear system of nonlinear system of equations (both referred as algebraic approach) are provided by many researchers such as Gordon and Herman (1971), Herman (1974), Gordon (1974), Elfving (1980), Eggermont et al (1981), Censor (1983).

Later for this discrete model other approaches were also given, such as in place of system of linear equations the system of linear inequalities $\mathbf{Af} \leq \mathbf{p}$ was considered, which is practically more accurate but mathematically the solution is more difficult. This approach and some solution is given by Robb et al (1974) and Herman (1975). Widely-used iterative method for solving sparse systems of linear equations proposed by Gordon (2006). The main advantages of ART are its robustness, its cyclic convergence on inconsistent systems, and its relatively good initial convergence. ART is widely used as an iterative solution to the problem of image reconstruction from projections in computerized tomography (CT), where its implementation with a small relaxation parameter produces excellent results. It is shown that for this particular problem, ART can be implemented in parallel on a

linear processor array. The parallel technique can be applied to various geometric models of image reconstruction.

All algebraic approaches provided are iterative thus convergence is an important property to check. The convergence of algebraic reconstruction algorithm technique (ART) is proved by Tanabe (1971), the concergence for SIRT is proved by Censor and Elfving (2002) and convergence proof of SART is given by Jiang and Wang (2003). The computational intensive nature of the problem and design and development of a Parallel ART (PART) algorithm and study its performance on a network of workstations using the Message Passing Interface (MPI) was done by Melvin, Thulasiraman and Gordon (1995). A comparison study under practical situations presented by Guan and Gordon (1996) and ART technique with the projections arranged and accessed in a multilevel scheme (MLS) for efficient algebraic image reconstruction in Computed tomography using algebraic reconstruction techniques (ARTs) with different projection access schemes. Test results demonstrate that one-iteration MLS produces the best reconstruction in many situations. It outperforms one-iteration RPS when the noise level is low. SAS in many cases can never attain the image quality of one-iteration MLS, even with many more iterations. A convergence test using different initial guesses also demonstrates that MLS has less initial dependence. The algebraic reconstruction technique for low-contrast detection in computed tomography applied three different projection access orders (the multilevel scheme (MLS), the sequence access scheme (SAS) and the random permutation scheme (RPS)) to the algebraic reconstruction technique (ART) in an attempt to improve low-contrast object detection in computed tomography (CT)

proposed by Guanyz, Gordon and Zhu (1998). Another approaches to solve the quadratic optimization are given by Herman and Lent (1978), Lent and Censor (1980), Censor (1981), Censor and Lent (1981).

Some more discussion on this category is done in chapter III

2.4 Statistical Methods

Based on statistical nature of data and image, certain statistical reconstruction methods are also proposed in this literature. The projection data is considered as weighted integrals of the image function f . Thus the problem of image reconstruction from projection is again reduced to that of solution of system of linear equations except that the system turns to be of the form $\mathbf{Af} = \mathbf{p} + \mathbf{n}$, where $\mathbf{A}, \mathbf{f}, \mathbf{p}$ are same as before and \mathbf{n} is the noise added in measurements (projection data). So the new system of equation is $\mathbf{Af} = \mathbf{g}$. Here \mathbf{f} and \mathbf{g} both are assumed to be random vectors. Thus problem of finding the solution the system of equations $\mathbf{Af} = \mathbf{g}$ is changed to find the estimates of \mathbf{f} with the help of projections \mathbf{g} . The Distribution of image variable is assumed to be the distribution of projection variable \mathbf{g} is considered as normal distribution. Some iterative methods to solve this problem provided by Herman and Lent (1976), Herman et al (1979) and Hanson (1987).

Using Poisson distribution assumption the ML estimate is given by Shepp and Vardi (1982). Lewitt and Muehllehner (1986) gave accelerated version of EM algorithm, Wood and More (1981) gave a minimum variance estimator. Nawak and Kolaczyk (2000) and Hasio et al (2002) gave generalized Bayes estimate. In statistical methods Wavelet technique is used by Frese et al (2002). A more comprehensive

Bayesian approach is suggested for these methods in which the ensemble mean and covariance specifications are adjusted on the basis of the measurements. Wang, Snyder, Sullivan, Vannier (1996) gave Iterative deblurring methods using the expectation maximization (EM) formulation and the algebraic reconstruction technique (ART), respectively, are adapted for metal artifact reduction in medical computed tomography (CT).

In experiments with synthetic noise-free and additive noisy projection data of dental phantoms, it was observed that simultaneous iterative algorithms produce superior image quality as compared to filtered backprojection after linearly fitting projection gaps. Also, for a given iteration number, the EM-type deblurring method produces better image clarity but stronger noise than the ART-type reconstruction. The computational complexity of EM- and ART-based iterative deblurring is essentially the same.

2.5 Limited View Methods

Image Reconstruction with limited angle projection data, a new image reconstruction technique for computed tomography discussed by Inouye (1999). Projection data obtained by a smaller angle rotation less than 180 degrees around the object used to make the image. The main feature of the method is the estimation of missing region in the Fourier transformed domain by extrapolation employing analytic continuity. Numerical simulations were carried out using computer generated pattern data. The results show strong effects of the content of noisy component on the reconstructed image. The method might be, however, practically applied to some real

fields for medical diagnosis. High speed array processing method described by Dorner (1979) applied to 2-D and 3-D image processing.

Tom Kwok C discussed the fidelity of limited-angle x-ray computerized tomography imaging is improved by taking multiple scans using x-ray beams at different energies. The projection data of the composite object is decomposed into the projections of the individual component substances. Reconstruction of a single substance is done more accurately than reconstructing the composite object because a priori information about the object, such as upper and lower bounds of the densities of the substances, is available.

The challenge facing CT is to reduce the radiation exposure while maintaining a quality of image that yields good diagnostic information. The problem and some solutions discussed as early as 1976 discussed by Gordan (1976). The standard algorithms perform poorly at 3-D reconstruction and at limited view reconstruction, so the iterative algorithms are used.

Devarey (1989) has discussed the problem of reconstructing the complex index of refraction of a weakly scattering object from a limited data set. This problem is defined into a form that includes the well studied limited-view problem of conventional computed tomography (CT). The theory is developed in detail for the case of plane-wave probes (parallel-beam case) in a manner completely parallel to that usually employed in studies of the limited-view problem in CT. The paper includes a discussion of invisible objects in DT and the CT case. A derivation of the filtered backpropagation algorithm is used when the data corresponds to a continuum of view angles over a limited angular range.

Galegekere, Wiesent, Mertelmier, Holdsoworth, (2000) have discussed that in many applications in computed tomography, practical limitations in data acquisition restrict the number of projections (views). The use of the standard convolution backprojection algorithm for reconstruction from an inadequate number of projections results in view aliasing artifacts. One approach to alleviating the effects of such artifacts consists of artificially increasing the number of views, by estimating a set of intermediate views. Two possible methods of estimating the intermediate views are interpolation and reprojection. Based on the merits and demerits of the two methods, a combination of the two methods is investigated. Specifically, a reconstruction from the available projections by intermediate view, and the projections interpolated from the original views, provide an additional improvement with respect to view aliasing artifacts. The advantage of computing reprojections over smaller regions of interest is also discussed in this paper. When the number of available projections is reasonably high but not adequate to produce an artifact-free reconstruction, estimating the intermediate views by interpolation that provides an improvement without much additional conditions, at minimal computational cost.

Boyd and James (1994) discussed ambiguity in the solution of inverse problems arises when data are insufficient to define a unique solution (i.e., the problem is ill-posed). This paper examines the application of data fusion to limited-angle computed tomography (CT) to resolve ambiguity. While CT in its conventional form is ill-posed with a small null space, limited-angle CT has a much larger null space. They described a novel constraint-based data fusion system that fuses spatial support and

ultrasound measurements with x-ray data. The ensuing problem is less ambiguous and reduced null space, and permits accurate reconstruction structure.

Dhawan, Rangayyan and Gordon (1984) have presented that in many applications of computed tomography, it is not possible to acquire the projection data at all angles evenly spaced over 360 deg. In such cases, the computed tomography images reconstructed using a limited number of projections. In this paper, it is shown that such geometric distortion and other artifacts introduced in the reconstruction process can be reduced substantially by using a priori knowledge derived from the given projections. Zhu, Zhuang and Chen (1992) discussed a Virtual Symmetry Reconstruction (VSR) algorithm for limited-view image reconstruction. The algorithm can be applied to such cases where the missing view angle up to $(\pi)/2$ is allowed for some nondestructive evaluation applications. Another image with property symmetrical about y-axis is reconstructed. With these two virtually symmetrical images, the desired image reflecting the real object is finally obtained by some sort of operations.

Oskoui and Stark (1989) discussed three novel methods that are used to reconstruct a simulated image from a set of incomplete data spanning a 160° angular range. These methods are the squashing affine transformation of Reeds and Shepp (1987), the circular interpolation method derived from the theory of Clark, Plamer and Lawrence (1985), and the geometry-free reconstruction using the theory of convex projections. Davison (1983) discussed the instability of inverting the limited angle Radon transform by constructing the singular value decomposition of this

operator. Connections are established with previously known series expansions and with the discrete prolate spheroidal wave functions.

A survey discussed by Rangayyan, Dhawan and Gordon (1984) in many applications of computed tomography it may not be possible to acquire projection data at all angles as required by the most commonly used method of convolution backprojection. They face an ill-posed problem in attempting to reconstruct an image from an incomplete set of projection. Rangayyan, Dhawan and Gordon (1985) discussed in many applications that many techniques have been proposed to tackle the situation, employing diverse theories such as signal recovery, image restoration, constrained deconvolution, and constrained optimization, as well as novel schemes such as iterative object-dependent algorithms incorporating *a priori* knowledge and use of multi-spectral radiation.

Salina, Mascarenhas and Cruvinel (2002) in a comparison of POCS algorithms for tomographic reconstruction under noise and limited view discussed a comparison among four algorithms for transmission tomography. The algorithms are based on the formalism of POCS (Projection onto Convex Sets): ART (Algebraic Reconstruction Technique), SIRT (Simultaneous Iterative Reconstruction Technique), sequential POCS and parallel POCS. They found that the use of adequate *a priori* knowledge about the solutions, expressed by convex sets restrictions, particularly in the case of the last algorithm, is an efficient way to reduce the variations on the solutions due to the ill-conditioning of the reconstruction problem, not only due to the noise in the projections, but also due to limited view reconstruction.

Delaney, Bresler and Sunnyvale (1998) they introduced a generalization of a deterministic relaxation algorithm for edge-preserving regularization in linear inverse problems. This algorithm transforms the original optimization problem into a sequence of quadratic optimization problems, and has been shown to converge under certain conditions when the original cost functional being minimized is strictly convex. They proved their general algorithm is globally convergent under less restrictive conditions. They applied this algorithm to tomographic reconstruction from limited-angle data by formulating the problem as one of regularized least-squares optimization. Yau and Wong (1996) in A linear sinogram extrapolator for limited angle tomography discussed the problem of limited angle tomography in which a complete sinogram is not available and proposes a linear extrapolator to the missing part of the sinogram. Once the complete sinogram is obtained via extrapolation, standard reconstruction techniques can be used to generate artifact free reconstructions. Once the extrapolator is designed, it can be used to extrapolate any incomplete sinogram. Since the sinogram is non-iterative, it is much more efficient than other iterative algorithms.

Delaney and Bresler (1995), discussed that the constraint of piecewise smoothness, applied through the use of edge-preserving regularization, can provide excellent tomographic reconstructions from limited-angle data. The tomography problem is formulated as a regularized least-squares optimization problem, and is then solved using a generalization of a recently proposed deterministic relaxation algorithm. They have proven that their algorithm is globally convergent under less restrictive conditions.

Laroque, Sidky and Pan (2008) present a method for obtaining accurate image reconstruction from highly sparse data in diffraction tomography (DT). A practical need exists for reconstruction from few-view and limited-angle data. Their method does this by minimizing the total variation (TV) of the estimated image. Using simulation studies, they shown that the TV-minimization algorithm allows accurate reconstruction in a variety of few-view and limited-angle situations in DT. Accurate image reconstruction is obtained from far fewer data samples than are required by common algorithms such as the filtered-backpropagation algorithm.

Sidky, Kao and Pan (2006) discussed that in accurate image reconstruction from few-views and limited-angle data, there are often challenges for image reconstruction due to under-sampling and insufficient data. In computed tomography (CT), for example, image reconstruction from few views would enable rapid scanning with a reduced x-ray dose delivered to the patient. Limited-angle problems are also of practical significance in CT. In this work, they developed and investigated an iterative image reconstruction algorithm based on the minimization of the image total variation (TV) that applies to divergent-beam CT. Andersen (1989) in Algebraic reconstruction in CT from limited views, presented an algebraic reconstruction technique (ART) as a viable alternative in computerized tomography (CT) from limited views. Recently, algorithms of iterative reconstruction-reprojection (IRR) based on the method of convolution-backprojection have been proposed for application in limited-view CT.

Paul, Rangayyan and Gordon (1985) in Quantitative and Qualitative Evaluation of Geometric Deconvolution of Distortion in Limited-View discussed that Computed Tomography Images reconstructed using a set of a few projections calculated from

the initial reconstruction. A second reconstruction is computed from the union of both sets of projections. Two-dimensional (2-D) filtering of the second reconstruction is performed to reduce the noise, while preserving the reduction in geometric distortion. Results obtained using several 2-D filters were compared visually and by point noise content, distortion, and projection error measures.

Prince and Willsky (1990) in Constrained sinogram restoration for limited-angle tomography discussed the Tomographic reconstruction from incomplete data is required in many fields, including medical imaging, sonar, and radar. They presented a new reconstruction algorithm for limited-angle tomography, a problem that occurs when projections are missing over a range of angles. They presented results of simulations that illustrate the performance of the algorithm and discuss directions for further research.

Krimmel, Baumann, Kiss, Kuba, Nagy, and Stephan (2005) in Discrete tomography for reconstruction from limited view angles in non-destructive testing described that discrete tomography (DT) is suitable to increase the possible inspection size of single material objects compared to filtered back projection (FBP) in non-destructive testing (NDT) with 2D X-ray computed tomography (CT). For such objects which are in one dimension larger than the maximum detectable material thickness limited view angles occur and FBP is not suitable for reconstruction. Nassi, Menahem, William, Medoff and Macovski (1982) in Iterative Reconstruction a Reprojection: An Algorithm for Limited Data Cardiac-Computed Tomography Cardiac X-ray computed tomography (CT) has described that convolution-backprojection algorithm is not suited for CT image reconstruction from

measurements comprising an incomplete set of projection data. In this present paper, they proposed an iterative reconstruction-reprojection (IRR) algorithm for limited projection data CT image reconstruction. At each iteration, the missing views are estimated based on reprojection, which is a software substitute for the scanning process. The standard fan-beam convolution-backprojection algorithm is then used for image reconstruction. For incomplete projection data (limited view availability of projection data in certain applications) problem in this method of solution using algebraic approach are also given. These methods are given by Anderson (1989), Inouye (1979), Zhong Qu et al (2005).

As transform methods are theoretical methods, so for practical application they need to be discretized, thus increase the discretization errors. Also, statistical methods requires some projection distribution for image function as prior information, which practice is taken to be Gaussian, but this is approximation, thus again increased approximation error with discretization error (since here again functions are assumed to be continuous). The Fourier transformation are band limited so are given as filtered inverse Fourier transforms. While in finite series expansion methods the problem is modeled in discrete set up. Thus we get the solution directly in discrete setup, which minimizes the discretization error as well these methods do not require separate application approach.

Thus, from these methods studied, we chose the finite series expansion reconstruction methods as they are directly applicable to different practical problems of real world. In next chapter this method is discussed in more details.

CHAPTER III: FINITE SERIES EXPANSION RECONSTRUCTION METHODS: A REVIEW

3.1 INTRODUCTION

Finite series expansion reconstruction methods have been applied in the Computed Tomography industry since 1970. These methods known as algebraic methods, iterative algorithms or optimization theory techniques. These methods are different than the Image Reconstruction Transform methods. The image space in case of Finite Series Expansion Reconstruction Method is discretized prior to the mathematical analysis while in case of Transform Methods the mathematical analysis is carried out without discretization then the result is discretized for computational implementation. The discretization gives Image Reconstruction in discrete form and, the discrete mathematical methods are employed for computational implementation to provide the required Image Reconstruction. The formulation of the discretized model for image reconstruction, methodology of the series expansion approach, basic approaches and methods of finite series expansion, the algebraic approaches, the feasibility approach, the optimization and least square regularization approach are discussed in the section 3.2, 3.3, 3.4, 3.5, 3.6, 3.7 and section 3.8 respectively.

3.2 THE FORMULATION OF DISCRETIZED MODEL FOR IMAGE RECONSTRUCTION

The image to be reconstructed in a plane is divided into large number of pixels (square elements) numbered from 1 to n. The total loss (absorption & reflection) of the radiation (X-rays etc.) is assumed to be constant for a pixel x_j which may vary

from pixel to pixel in the image. The intersection of an i th ray (a line between a source and a detector) with j th pixel, a_{ij} represents the weight of the contribution of the j th pixel to the total loss of the energy along the ray denoted by y_i (the data/measurement). Thus, y_i represents the line integral of the unknown attenuation function along the ray. It means that the line integral is a finite sum of losses resulted by all the pixels in a line and the whole image can be described by a system of linear equations,

$$y_i = \sum_{j=1}^n a_{ij}x_j, \quad i = 1, 2, \dots, m \quad (3.2.1)$$

In matrix form the above equation (3.2.1) can be written as

$$y = Ax \text{ or } A_{mxn}f_{nx1} = b_{mx1} \quad (3.2.2)$$

Where

$f_{nx1} = (f_1, f_2, \dots, f_n)$ is image vector,

$b_{mx1} = (b_1, b_2, \dots, b_m)$ is measurement vector and

$A_{mxn} = ((a_{ij}))_{mxn}$ is the projection matrix.

So the problem of image reconstruction from projection is now to get the value of f from the system (3.2.2)

Parallel beam and Fan beam scanning have been used in practice to sample the line integral of the losses. Here in this thesis work parallel beam scanning is used. In parallel beam scanning parallel line integrals are determined for a fixed direction and the process is repeated for a number of different directions. As mentioned above the complete region of interest is taken to be rectangular; which is divided into a cartesian

grid of square pixels (fig. 3.1). The size of a pixel is chosen according to the resolution required for the measurement called Projection data. The number of data in one angular direction (initially at x-axis) should be almost equal to the number of pixels on that axis Herman (1980) and Gordan (1974). Thus, the complete domain of the image function is descretized into nxn cartesian grid of number of pixels (n²). The value of the attenuation at the centre of a pixel is taken as the value of the function for that pixel and is assumed to be the same throughout the pixel, say f_j for jth pixel. The pixels are numbered from top left corner to bottom right corner as 1, 2, 3, ..., n-1, n. The total loss of energy along a line say ith line denoted by b_i is the sum of absorptions in all the pixels intersected by the ray (line) for i=1, 2, ..., m-1, m. Thus the model of the physical measurement is

$$\sum_{j=1}^n a_{ij}f_j = b_i, \quad i = 1, 2, \dots, m \quad (3.2.3)$$

Where f_j is value of image functions for jth pixel while b_i is the measurement of total attenuation along ith ray and a_{ij} is coefficient of intersection of ith ray and jth pixel. All these details are shown in figure 3.1. In figure 3.1, source is used to transmit the energy through the object and detector is on another side to receive the transmitted energy, discretization of the object in the form of pixels through which the energy is transmitted shown. Figure 3.2 shows a line strip for projection element P_j giving the measurement data (summation of a line strip passing through the object) to find the image value.

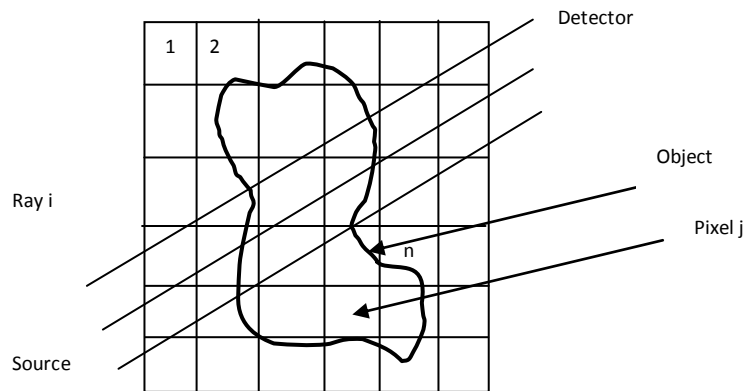


Figure 3.1: Digitization of image and projection data

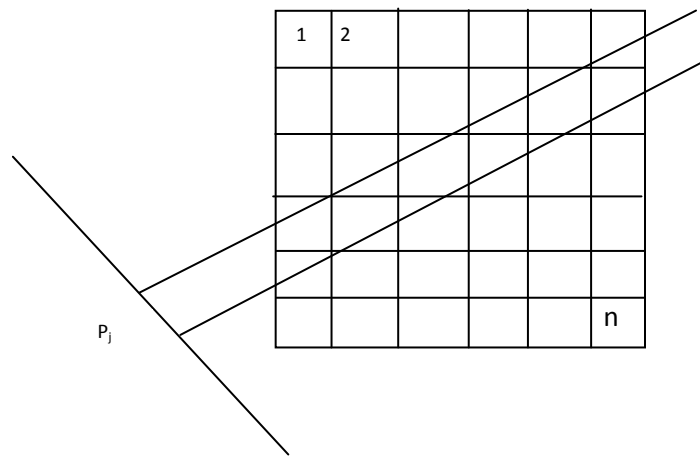


Figure 3.2: Projection as sum of intersected pixels

3.3 METHODOLOGY OF THE SERIES EXPANSION APPROACH

In previous section we formulated the problem of image reconstruction from projections as system of equation (3.2.2). Now a solution concept of the system of linear equations is to be chosen. The next step is to develop an algorithm, which can handle the problem in the mathematical environment of huge dimensions and sparseness and implemented on a computer.

The solution of image reconstruction problem means to get a solution of linear system of algebraic equations given in 3.2.2., various methods of solving (3.2.2) under various assumptions to get the value of co-efficient matrix A (projection matrix) have been given by [Gordon et al (1970), Herman (1980), Kak and Slaney (2001), Srivastava (1994)]. We choose the method which is most suitable for solving the problem. For this purpose we have to find out the characteristics of projection matrix A , image vector f and the measurement vector b .

In order to get fine resolution and good estimate of image function the discretization is done as fine as possible, which makes the size of image vector f to be very large. Also to get good resolution the measurements taken at very fine (small) difference both at angular distance and perpendicular distance, which makes the size of measurement vector b also very large. Since f and b are very large, so the size of co-efficient or projection matrix is very large, f and b are approximately varying from 2500(for small models) up to 10^6 or 10^9 in the applications in various field. [Kak and Slaney (2001), Gordon and Herman (1971)]. The size of projection matrix will be somewhere between 2.6×10^7 and 10^{16} for these sizes of image and measurement vector.

Further the projection or co-efficient matrix is too much sparse, it has very small number of non-zero entries. Since every ray will have intersection with only a few number of pixels. It has approximately less than 1% non-zero element [Censor (1983), Herman (1980)].

The system is ordinarily highly under determined i.e. $m \ll n$, as measurements taken are less, the system becomes inconsistent [Gordon (1974), Herman (1980),

Censor (1983), Kak and Slaney (2001)]. The rank of projection (co-efficient) matrix is unknown as it depends on that particular test application.

The error or noise in measurement data may make the system to be inconsistent and the approximations taken for the discretization process may cause errors. The image reconstruction a large image has large dimensions of projection matrix, image vector and measurement vector, scarcity of co-efficient matrix, inconsistency, ill-conditioning of the system. Since the rank of the sparse matrix A is unknown and the system is ill-conditioned as well as very large. The solution of the system of the linear equation (3.2.2) becomes very difficult and the normal procedures or any direct mathematical methods are not applicable. Most often some optimization criteria are set as concept of solution. Let us first consider the reasons responsible for selection of optimization criterion. First we try to get a set of feasible solutions according to the constraints imposed on the actual image reconstruction problem. These constraints are decided by the assumptions assumed during the formulation of problem. They are as

- I. The coefficient of projection matrix is positive i.e. projection element $a_{ij} \geq 0$.
- II. The measurements b_i (the elements of measurement vector \mathbf{b}), are ordinarily positive ($b_i \geq 0$).
- III. The unknown function, to be reconstructed, (f_j) the element of image vector \mathbf{f} is assumed to be positive ($f_j \geq 0$).
- IV. The measurements may be affected by noise, either due to instruments or due to measurement methods or due to basic scattering problems.

The equalities in system of equations may change to inequalities. We may have system of equations where f_j can have values negative (-ive) to positive (+ive) through zero.

$$\sum_{j=1}^n a_{ij}f_j \leq b_i \text{ for some values of } i$$

$$\sum_{j=1}^n a_{ij}f_j \geq b_i \text{ for some other values of } i$$

$$\text{And } \sum_{j=1}^n a_{ij}f_j = b_i \text{ for rest values of } i$$

In view of above observations, it can be concluded that the problem of image reconstruction is an optimization problem rather than simply solution of algebraic equations (even in case of linear system). The decision taken about “concept of solution” will affect the solution. Thus choosing the criterion according to actual image reconstruction problem is very important, which will lead to many kinds of approaches and solution.

Thus an optimization criterion is setup with the system of equations for some system of inequalities derived from it as the set of constraints over which the optimization is to be performed. Generally different roots are possible, each leading to a variety of solution concepts but the decision of which one to choose in any particular application rests with the reference with the specific reconstruction problem. The basic approaches are the following:

1. Feasibility approach (described in section 3.6)
2. Optimization approach (described in section 3.7)

After finding the method to get a solution, its computer implementation is made, which says that “the solution” should also possess one more characteristic, which is

computer applicability. In other words, we can say that the solution must have the quality of its being convertible to mathematical algorithm, which can be easily converted to computer implementation. Thus the next step is the development of an image reconstruction algorithm. The algorithm should be capable of handling the problem within the special mathematical environment of huge dimensions and sparseness. It should also be efficiently implementable on a computer. The results of the computer implementation are then evaluated not only in the light of the mathematical problem but chiefly with respect to the original reconstruction problem. The last step is to test the solution on computer for some real world original image reconstruction problem. The flow chart of the methodology of finite series expansion approach is given in figure 3.3. In the first step we have the original image for which the algorithm for image reconstruction has to develop, then the image is discretized to find the set of linear or nonlinear equations then select the criteria to solve these linear or nonlinear set of equations, after choosing the criteria to solve the set of equations a reconstruction algorithm is developed that can be implemented on computer to solve the problem of image reconstruction than at last the results are evaluated with the original problem. The line square, numbered 9 in that figure, represents the mathematical efforts involved. The tools for these investigations come from linear algebra, optimization theory, and numerical analysis Censor (1983).

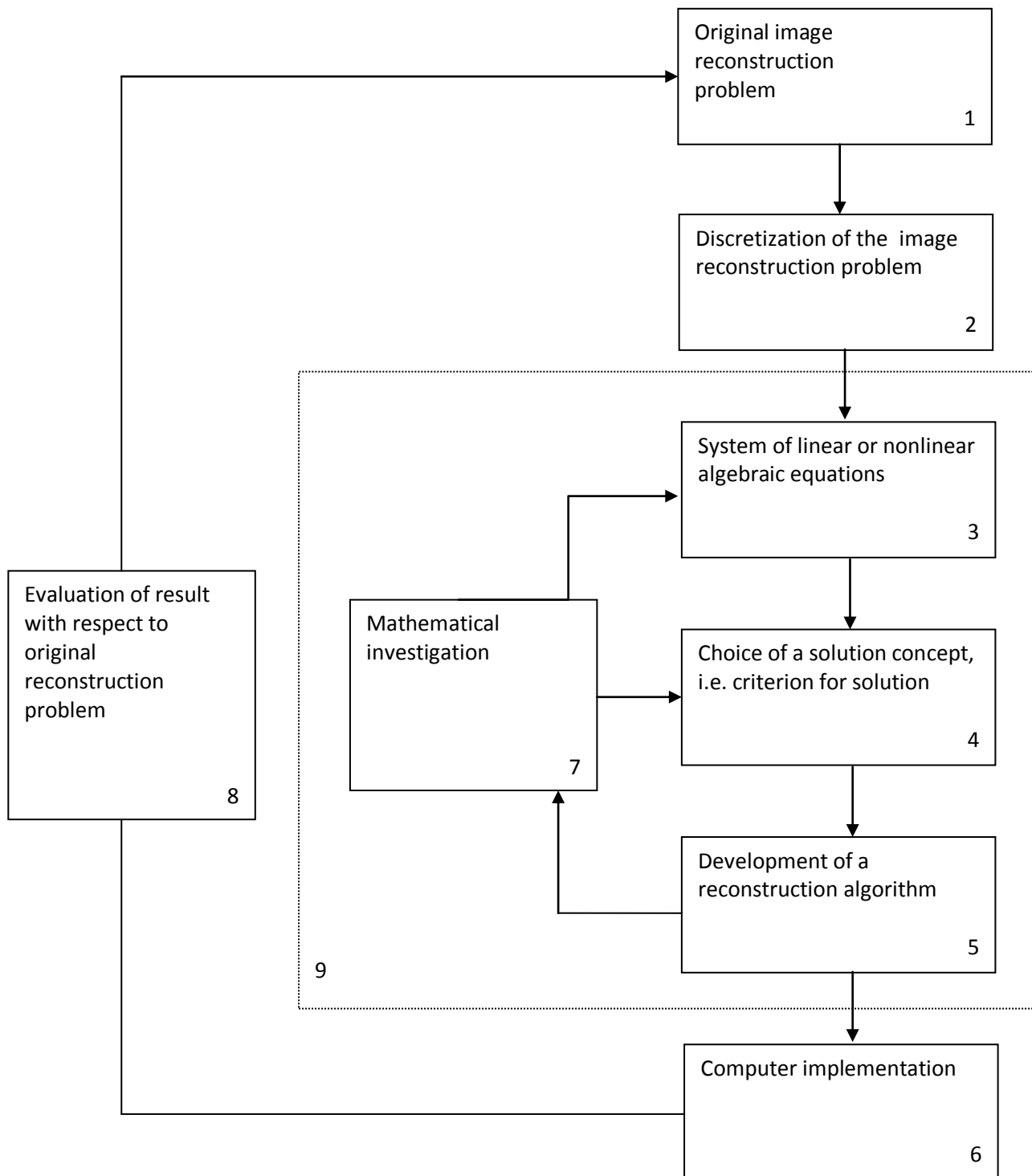


Figure 3.3: Methodology of series expansion approach [Censor (1983)]

3.4 BASIC APPROACHES AND METHODS OF FINITE SERIES EXPANSION

The solution concepts and the solution for real world image reconstruction differ from one problem to another. A particular image reconstruction problem involves different assumptions for unknown functions and their measurements, which in turn leads to the choice of solution concepts. In general different approaches and methods exist [Herman (1970), Gordon (1974), Tanabe (1971), Cencer et al (1983), Herman (1973), Agmon (1954) etc...]. Each method and approach leads to variety of solution concepts; one has to choose a suitable concept depending upon the nature of problem, instruments and methodology available to user. One important point to be considered in choosing a particular solution concept and a method is its ability to be converted into a suitable algorithm which can be applied on computer. Moreover the solutions obtained should be compatible with mathematical analysis as well as with actual application.

3.5 THE ALGEBRAIC APPROACH

In this approach the measurement obtained by machines are directly assumed as ray sum and the projections are taken as

$$\sum_{j=1}^n a_{ij}f_j = b_i, i = 1, 2, \dots, m \quad (3.2.3)$$

Thus the problem of image reconstruction through projection of transmission becomes solving the above (3.2.3) system of linear algebraic equations i.e. $A\mathbf{f} = \mathbf{b}$. As mentioned earlier in section 3.3, the system of equation is ill-conditioned and the coefficient matrix or projection matrix is sparse, the direct methods of solution for this

system of algebraic linear equation become in-efficient and most of the time inapplicable. Therefore some iterative methods summarized in the following sections were discovered to solve the above system of equation (3.2.3).

3.5.1 ALGEBRAIC RECONSTRUCTION TECHNIQUE

A finite number of photographs (projections) taken at different angles in 2-Ds are used to reconstruct the original 3-D image. The basic idea behind this technique is that each projection in 2-Ds is thrown back across 3-Ds space from where it was taken with repeated corrections to bring the each estimated projection into agreement with the measurement.. The Algebraic Reconstruction Technique was first published as a Reconstruction Algorithm in 1970 by Gordon, Bender and Herman. The ART algorithm begins with some initial estimate of the image to be reconstructed (usually taken as a uniformly gray image). It modifies this estimate repeatedly until the pixel values appear to converge by some criterion. ART decides how to modify the image by summing the pixels along some straight path and comparing this sum to the measured ray sum. The difference between projections calculated from the image estimate, and the measured ray is calculated, and the adjustment is divided among the pixels in the ray sum.

This is identical with Kackmarz's algorithm for solving system of linear equation (3.2.3). They proposed an iterative method in which the values of the function f_j 's for each pixel intersected by a ray, say 'i' in k^{th} iteration step are modified in $(k + 1)^{\text{st}}$ step by redistributing the difference (error) between the actual measurement (projection) value for the i^{th} ray of k^{th} iteration image $\sum_{j=1}^n a_{ij} f_j^k$ among the pixels of the i^{th} ray

proportional to their weight a_{ij} . The i^{th} ray is chosen cyclically for each iteration. So if we assume $\mathbf{f}^k = (f_1^k, f_2^k, \dots, f_j^k, \dots, f_n^k)$, as k^{th} iteration image, then $\mathbf{f}^0 \in \mathbb{R}^n$ is chosen arbitrarily, thus an iterative step is

$$f_j^{k+1} = f_j^k + a_{ij} \frac{b_i - \sum_{j=1}^n a_{ij} f_j^k}{\sum_{j=1}^n a_{ij}^2},$$

$$\forall j \ni a_{ij} \neq 0, \text{ and } i = k(\text{mod } m) + 1 \quad (3.5.1)$$

The geometrical interpretation of this method is that the initial guess $\mathbf{f}^0 \in \mathbb{R}^n$ is projected on all hyper planes. In ART for solving the system of linear algebraic equations, in each iteration only those f_j 's are modified which intersect with i^{th} ray and in one iteration only one ray is considered, thus it makes to do a large number of iterations for getting some significant results and making the rate of convergence very slow. Also it gives noise as measurements are computed and give inconsistency in the system as well. These are the limitations of ART approaches. Since the iterative step (3.5.1) is additive, hence technique is referred as additive ART. There are several ART's (additive ART, multiplicative ART, Simultaneous ART etc...) which are used to solve the system of linear equation. These techniques are described along with their merits, demerits, limitations etc in the following sections of this chapter.

3.5.2 MULTIPLICATIVE ART

This method of image reconstruction was suggested by Gordon, Bender and Herman (1970). This method is similar to earlier iterative method and starts with the

initial arbitrary guess $\mathbf{f}^0 = (f_1^0, f_2^0, \dots, f_j^0, \dots, f_n^0)'$ and $(k+1)^n$ iterative steps are given as

$$f_j^{k+1} = \left(\frac{b_i}{\sum_{j=1}^n a_{ij} f_j^k} \right) f_j^k$$

$$\forall j \ni a_{ij} \neq 0, \text{ and } i = k \pmod{m} + 1 \quad (3.5.2)$$

The image vector is modified iteratively as given in (3.5.1), where i^{th} is chosen cyclically in similar way. The difference in 3.5.1 and 3.5.2 is in iterative step. In 3.5.1 iterative step modifies the image elements f_j by addition, while in 3.5.2 it is modified through multiplication. Moreover the modifications are also different in 3.5.1 and 3.5.2. In 3.5.1 the difference in actual measurement and ray sum of k^{th} iteration's image is distributed on elements intersection i^{th} ray in proportion to a_{ij} . In 3.5.2 the ratio of actual measurement with ray sum of k^{th} iteration image is equally weighted to all elements intersecting i^{th} ray. In this method initial guess f_j^0 should not be zero for any $j = 1, 2, \dots, n$. Badea and Gordon (2004) developed the multiplicative algebraic reconstruction technique (MART) with two advantages that make it superior to other algorithms: for nonlinear and chaotic behavior of equations it confines the image to the convex hull of the object, and it maximizes entropy. They have undertaken a series of experiments to determine the importance of MART nonlinearity to image quality. Variants of MART (the Power MART, Boxcar Averaging MART and Bouncing MART) were implemented aiming to exploit and exaggerate the nonlinear properties of the algorithms.

3.5.3 GENERALIZED ART

In previous two methods we saw that they differ only in their iterative steps additive or multiplicative modification. Gordon (1974) developed a generalized method for iterative steps. This method also starts with initial guess $\mathbf{f}^0 = (f_1^0, f_2^0, \dots, f_j^0, \dots, f_n^0)'$ and the $(k+1)^{\text{st}}$ modification is defined as

$$f_j^{k+1} = A(f_j^k, b_i, j \ni a_{ij} \neq 0) \quad (3.5.3)$$

With condition that

$$\left| \sum_{j=1}^n a_{ij} f_j^{k+1} - b_i \right| < \left| \sum_{j=1}^n a_{ij} f_j^k - b_i \right|$$

Where $i = k(\text{mod } m) + 1$

In general A of 3.5.3 is explicitly depend upon f_j^k . They suggested a series as

$$f_j^{k+1} = \max \left\{ 0, \sum_{l=0}^0 A_l (f_j^k)^l \right\}$$

Where co-efficient A_l 's are constrained by relation

$$\sum_{j=1}^n a_{ij} f_j^{k+1} \leq A_0 \sum_{j=1}^n a_{ij}^2 + A_1 \sum_{j=1}^n a_{ij} f_j^k + \sum_{l=2}^{\infty} A_l \sum_{j \ni a_{ij} \neq 0} (f_j^k)^l = b_i$$

For additive ART in 3.5.1 the choice of coefficients A_l are

$$A_l = a_{ij} \frac{b_j - \sum_{j=1}^n a_{ij} f_j^k}{\sum_{j=1}^n a_{ij}^2}, i = 0, 1, 2 \dots$$

And for multiplicative ART in 3.5.2, the choices of coefficient are

$$A_0 = 0, A_i = \frac{b_j}{\sum_{j=1}^{\infty} a_{ij} f_j^k}, i = 0, 1, 2, \dots$$

Censor (1987), Darroch (1972) and Schmidlin (1972) proposed another version of MART known as simultaneous MART (SMART). Which starts with a positive vector having calculated, f^{k+1} calculated using

$$\log f_j^{k+1} = \log f_j^k + s_j^{-1} \sum_{i=1}^I A_{ij} \log \frac{b_i}{(Af^k)_i},$$

where $s_j = \sum_{i=1}^I A_{ij} > 0$.

when $Af = b$ has no positive solutions, the SMART converges to an approximate solution in the sense of cross-entropy, or Kullback-Leibler distance Byrne (1993, 2005). For positive numbers u and v, the Kullback-Leibler distance Kullback et. al (1951) from u to v is

$$KL(u, v) = u \log \frac{u}{v} + v - u.$$

They also defined $KL(0, 0) = 0$, $KL(0, v) = v$ and $KL(u, 0) = +\infty$. The KL distance is extended to nonnegative vectors component-wise, so that for nonnegative vectors f and z is

$$KL(f, z) = \sum_{j=1}^J f_j \log f_j - f_j.$$

Clearly, $KL(f, z) \geq 0$ and $KL(f, z) = 0$ if and only if $f = z$.

One advantage of SMART has over MART is that, if the nonnegative system $Af = b$ has no nonnegative solutions, the SMART converges to the nonnegative minimize of

the function $\text{KL}(\mathbf{Af}, \mathbf{b})$ for which $\text{KL}(\mathbf{f}, \mathbf{f}^0)$ is minimized. One disadvantage of SMART, compared to MART, is that it is slow.

3.5.4 KACKMARZ'S RELAXATION METHOD

All above methods talk of a solution in iterative manner. [Tanabe (1971)] pointed out that these methods converge to a reasonable solution only when the system $\mathbf{Af} = \mathbf{b}$ is consistent otherwise not. But there can be many image reconstruction problems where the system may be inconsistent. In such cases using Kackmarz (1937), [Eggermont et al (1981), Cencer et al (1983)] reported that Kackmarz's Relaxation iterative method with relaxation parameter introduced helps to get a solution.

In this method starting with initial guess \mathbf{f}^0 the iterative step modifies the image vector as

$$f_j^{k+1} = f_j^k + \lambda_k a_{ij} \frac{b_j - \sum_{j=1}^n a_{ij} f_j^k}{\sum_{j=1}^n a_{ij}^2},$$

$$\forall j \ni a_{ij} \neq 0, \text{ and } i = k(\text{mod } m) + 1 \quad (3.5.4)$$

Where coefficient $\{\lambda_k\}_{k=0}^{\infty}$, called relaxation parameters are a sequence of real numbers, confined to the interval

$$\epsilon_1 \leq \lambda_k \leq 2 - \epsilon_2, \quad \epsilon_1, \epsilon_2 > 0$$

These relaxation parameters makes less or more orthogonal projections and so give satisfactory results in practical applications [Herman (1980), Kak and Slaney

(2001)]. But it increases the number of iterations and requires more memory to store the value after each iteration.

3.5.5 ALGEBRAIC RECONSTRUCTION WITH ONE INTERMEDIATE STEP (ART2)

Herman, Lent and Rowland (1973) introduced one more step in the ART method described in 3.5.1, which is an extra estimate at k^{th} modification. Starting with initial guess \mathbf{f}^0

$$\tilde{f}_{j}^{k+1} = \tilde{f}_j^k + \lambda_{ij}^k \frac{b_j - \sum_{j=1}^n a_{ij} f_j^k}{\sum_{j=1}^n a_{ij}^2} a_{ij}, \quad \forall j \exists a_{ij} \neq 0,$$

$$\text{and } f_j^{k+1} = \max \{0, \tilde{f}_j^{k+1}\}, \quad i=k(\text{mod } m)+1 \quad (3.5.5)$$

In (3.5.5) λ_{ij}^k are similar to relaxation parameter λ_k in (3.5.4) but the image function values were modified in different manner. The difference is in calculating ray sum for i^{th} ray of k^{th} iteration image, it includes actual iteration value, and the image value is modified using the practical assumption i.e. $f_j \geq 0$.

3.6 THE FEASIBILITY APPROACH

In this approach the constraints are set, according to the problem of image reconstruction at hand, and then methods are sought to get the solution of constrained problem. The work of this thesis is confined to transmission method of measurement data collection, where the constraints could be of two kinds; one on measurement (projection element) and other on the image function. First we will discuss the method in which the measurements are affected by noise. Thus linear equation (3.2.1) of

series expansion method for image reconstruction problem will have some inequalities as reported by [Herman (1975), Herman and Lent (1978)] and the system of linear equations (3.2.3) is changed into system of linear inequalities

$$b_i - \epsilon_i \leq \sum_{j=1}^n a_{ij} f_j \leq b_i + \epsilon_i, \quad \forall i = 1, 2, \dots, m \quad (3.6.1)$$

Where $\epsilon_i, i = 1, 2, \dots, m$ are predefined non negative “tolerances”, is feasible for computing the values of f_j in equation (3.6.1). Some methods are briefly described in following subsections for different constraints.

3.6.1 ALGEBRAIC RECONSTRUCTION FOR INEQUALITIES

In this method the inequalities (3.6.1)

$$b_i - \epsilon_i \leq \sum_{j=1}^n a_{ij} f_j \leq b_i + \epsilon_i, \quad \forall i = 1, 2, \dots, m$$

are in pairs, one with +ive inequality and another with -ive inequality written as

$$\sum_{j=1}^n a_{ij} f_j \leq b_i + \epsilon_i \quad \text{and} \quad \sum_{j=1}^n a_{ij} f_j \leq b_i - \epsilon_i \quad (3.6.2)$$

Thus the system of inequalities is twice the system of algebraic equations (3.6.2)

$$\sum_{j=1}^n c_{ij} f_j \leq d_i, \quad i = 1, 2, \dots, 2m.$$

Where d_i is the projection elements after including the inequalities.

This system of one sided inequalities is solved using relaxation methods given by Agmon (1954) and Motzkin and Schoenberg (1954). The resulting method is an

iterative method, as follows, in which an initial guess $\mathbf{f}^0 = (f_1^0, f_2^0, \dots, f_j^0, \dots, f_n^0)'$ and

$(k+1)^{st}$ iterative step are

$$f_j^{k+1} = f_j^k + \sum_{j=1}^n c_{ij} s_j^k$$

where,

$$s_j^k = \min \left\{ 0, \lambda_k \frac{d_i - \sum_{j=1}^n c_{ij} f_j^k}{\sum_{j=1}^n c_{ij}^2} \right\} \quad \forall j \ni c_{ij} \neq 0 \text{ and}$$

$i = k(\bmod 2m) + 1$, with relaxation parameters $\{\lambda_k\}_{k=0}^\infty$ as defined in (3.5.4).

3.6.2 ALGEBRAIC RECONSTRUCTION TECHNIQUE – 3 (ART3)

This method which is applicable in finding solution of the linear interval feasibility problem was given by Herman (1975), where the inequalities in (3.6.1), defining hyper slabs are enveloped by bigger hyper slabs. To find the solution underlying methods are used where we get $(k+1)^{st}$ estimate of image vector.

(i) If f_j^k is such that

$$b_i - \epsilon_i \leq \sum_{j=1}^n a_{ij} f_j^k \leq b_i + \epsilon_i \quad (3.6.3)$$

$$\forall j \ni a_{ij} \neq 0, i = k(\bmod m) + 1$$

$$\text{Then } f_j^{k+1} = f_j^k \quad \forall j \ni a_{ij} \neq 0, i = k(\bmod m) + 1$$

(ii) If (3.6.3) does not hold true for f_j^k that is $\forall j \ni a_{ij} \neq 0, i = k(\bmod m) + 1$, f_j^k do not satisfy equation (3.6.3) but satisfy within large hyper slab which is

$$b_i - \epsilon_i^* \leq \sum_{j=1}^n a_{ij} f_j \leq b_i + \epsilon_i^* \quad (3.6.4)$$

$$\forall j \exists a_{ij} \neq 0, i = k(\text{mod } m) + 1 \text{ and } \epsilon_i^* < \epsilon_i$$

Then \mathbf{f}^{k+1} should be taken as orthogonal reflection of \mathbf{f}^k with respect to (3.6.4)

- (iii) If f_j^k does not satisfy (3.6.4) even for any other ϵ_i^* also, then \mathbf{f}^{k+1} is taken as orthogonal projection of \mathbf{f}^k onto i^{th} hyper plane that is on $\sum_{j=1}^n a_{ij} f_j^k = b_i$

Using this methodology Herman (1975) gave following algorithm: starting with arbitrary initial guess $\mathbf{f}^0 = (f_1^0, f_2^0, \dots, f_n^0)'$ then $(k+1)^{\text{st}}$ modification of f as

$$f_j^{k+1} = f_j^k + s_k \frac{a_{ij}}{\sum a_{ij}^2}, \quad \forall j \exists a_{ij} \neq 0, i = k(\text{mod } m) + 1,$$

where

$$s_k = \begin{cases} 0, & \text{if } \left| b_i - \sum_{j=1}^n a_{ij} f_j^k \right| \leq \epsilon_i \\ b_i - \sum_{j=1}^n a_{ij} f_j^k & \text{if } \left| b_i - \sum_{j=1}^n a_{ij} f_j^k \right| \geq 2 \epsilon_i \\ 2(b_i + \epsilon_i - \sum_{j=1}^n a_{ij} f_j^k), & \text{if } b_i + \epsilon_i < \sum_{j=1}^n a_{ij} f_j^k < b_i + 2 \epsilon_i \\ 2(-b_i + \epsilon_i + \sum_{j=1}^n a_{ij} f_j^k), & \text{if } b_i - 2 \epsilon_i < \sum_{j=1}^n a_{ij} f_j^k < b_i - \epsilon_i \end{cases},$$

Robb et al (1974), Herman (1975).

This method increases the execution time and number of iterations. One more method to find the solution of linear interval feasibility problem was given by Sweeny and Vest (1973), described as follows.

3.6.3 ART WITH A DAMPING FACTOR

This method introduces a damping factor in iterative step similar to relaxation parameter, except that while relaxation parameters are in sequence of any real number, the damping factor (say δ) is a constant and lies in the interval $(0, 1)$ that is $0 < \delta < 1$. We start with an arbitrary initial guess $f_j^0, \forall j = 1, 2, \dots, n$ and the iterative step is

$$f_j^{k+1} = f_j^k + \delta \frac{b_j - \sum_{j=1}^n a_{ij} f_j^k}{\sum_{j=1}^n a_{ij}^2} a_{ij} \quad (3.6.5)$$

For $\delta \leq \frac{1}{2}$ better reconstructions were obtained.

Next we will look when constraints were put on image function i.e. measurement are assumed to be equations, $\sum_{j=1}^n a_{ij} f_j = b_i, \forall i = 1, 2, \dots, m$.

But constraints are introduced on unknown vector $f_j, \forall j = 1, 2, \dots, n$. If constraints are partial such that image function is non-negative i.e. $f_j > 0, \forall j = 1, 2, \dots, n$, then all method of algebraic approach can be applied with modification in iterative step. For example in additive ART given in section 3.6.1, start with an arbitrary non negative initial guess as

$$f_j^0, \forall j = 1, 2, \dots, n$$

and modify the iterative step as

$$f_j^{k+1} = \max \left\{ 0, f_j^k + \frac{b_j - \sum_{j=1}^n a_{ij} f_j^k}{\sum_{j=1}^n a_{ij}^2} \right\}$$

$$\forall j \exists a_{ij} \neq 0, i = k(\text{mod } m) + 1 \quad (3.6.6)$$

But if constraints are double sided, i.e. $0 < f_j < F, \forall j = 1, 2, \dots, n$, for that some other more methods were reported by [Rowland (1973), Herman (1973), Gilbert (1972),], out of which only two methods are briefly described in the following subsections 3.6.4 and 3.6.5 respectively.

3.6.4 CONSTRAINED ART

The equation (3.6.6) is modified starting with initial guess

$$0 < f_j^0 < F, \forall j = 1, 2, \dots, n \text{ and}$$

$$f_j^{k+1} = \min \left\{ F, \max \left\{ 0, f_j^k + \frac{b_j - \sum_{j=1}^n a_{ij} f_j^k}{\sum_{j=1}^n a_{ij}^2} \right\} \right\}$$

$$\forall j \exists a_{ij} \neq 0, i = k(\text{mod } m) + 1$$

on inconsistent data, constraint ART is used to converge cyclically reported by Herman et al (1973).

3.6.5 ART WITH BINARY CONSTRAINT

If we assume the image function takes binary values 0 and 1 only implying that f_j either 0 or 1, then solution of image reconstruction problem can be obtained by using method of (3.5.5). If constraints are introduced in measurement (projection) as well, then method described in section (3.6.2) is applicable. Both solutions should be modified according the method described in (3.6.4) [Herman (1973)]. But another

method which can separate zero's and one's with some a priori knowledge would make the iteration faster [Gilbert (1972)].

3.7 THE OPTIMIZATION APPROACH

This approach is one step ahead of feasibility approach described in (3.6). In feasibility approach we try to get a solution that satisfies the constraints defined in the problem. An objective function is pre-designated according to which a particular element will be singled out from the feasible region. The feasible region may be composed from inequalities. These inequalities describing a priori information about the optimal solution. Two optimization methods in image reconstruction are briefly described in the following two sub sections 3.7.1 and 3.7.2 respectively.

3.7.1 ENTROPY OPTIMIZATION

Entropy optimization is used when projection data for several angular distances are not available. The optimality criterion, or better known as “objective function” in optimization problem, is set here as

$$o(\mathbf{f}) = - \sum_{j=1}^n f_j \ln f_j$$

This objective function is obtained as a measure of information contained. Thus optimization problem is mathematically formulated as: maximize the above objective function

Subject to

$$\sum_{j=1}^n a_{ij} f_j = b_i, i = 1, 2, \dots, m; \quad x_j \geq 0, j = 1, 2, \dots, n. \quad (3.7.1)$$

a modification of the method described in section (3.5.2), (the multiplicative ART), with some conditions gives the solution as maximum entropy problem (3.7.1), which is redefined as follows. Start with initial guess $f_j^0 = \frac{1}{e}, \forall j = 1, 2, \dots, n$, and the iterative step is

$$f_j^{k+1} = \left(\frac{b_i}{\sum_{j=1}^n a_{ij} f_j^k} \right)^{\lambda_1 a_{ij}} \cdot f_j^k \quad \forall j \ni a_{ij} \neq 0, i = k(\text{mod } m) + 1 \quad (3.7.2)$$

the necessary condition for (3.7.2) to give the solution of (3.7.1) is that the feasible set should be non empty, which states that the system $Af = b$ must have a non-negative solution [Lent (1977)].

3.7.2 QUADRATIC OPTIMIZATION

This approach is used in finite series expansion methods of image reconstruction. In this approach the objective function chosen for optimality criterion are quadratic. Thus the image reconstruction problem in series expansion method could be modeled as following mathematical optimization problem.

Minimize

$$o(\mathbf{f}) = \left(\sum_{j=1}^n f_j^2 \right)^{1/2}$$

Subject to

$$\sum_{j=1}^n a_{ij} f_j = b_i, i = 1, 2, \dots, m; f_j \geq 0, j = 1, 2, \dots, n \quad (3.7.3)$$

Here one method based on Hildreth's algorithm Lent and Censor (1980) is described. This is again an iterative procedure which is supposed to give a solution of equation (3.7.3). The method is as follows:

Start with arbitrary positive initial guess of measurement as $d_i^0 > 0, i = 1, 2, \dots, m$.

Then take the initial estimate of image vector as $f^0 = -\mathbf{A}^T \mathbf{d}^0$, where \mathbf{A}^T is transpose of matrix \mathbf{A} .

The iterative step is

$$f_j^{k+1} = f_j^k + c_{ki} a_{ij} \quad \forall j \ni a_{ij} \neq 0,$$

$$d_i^{k+1} = d_i^k - c_{ki} \quad i = k(\text{mod } m) + 1$$

Where,

$$c_{ik} = \min \left\{ d_i^k, \lambda_k \frac{b_j - \sum_{j=1}^n a_{ij} f_j^k}{\sum_{j=1}^n a_{ij}^2} \right\}$$

With $\{\lambda_k\}_{k=0}^\infty$ as sequence of relaxation parameters satisfying

$$\epsilon_1 \leq \lambda_k \leq 2 - \epsilon_2, \quad \epsilon_1, \epsilon_2 > 0$$

Since more modification in methods are also suggested [Bregman (1967), Herman et al (1973), Herman and Lent (1978)]. Belgacem, Kaber (2008) in Quadratic optimization in ill-posed problems, Ill-posed quadratic optimization frequently occurs in control and inverse problems and is not covered in these methods. Typically, small changes in the input data can produce very large oscillations on the output. They investigated the conditions under which the minimum value of the cost function is finite and they explored the 'hidden connection' between the optimization problem and the least-squares method.

3.8 LEAST SQUARE REGULARIZATION APPROACH

In least square regularization approach the objective function is taken to be quadratic as in quadratic approach, but the objective function and constraints are combined with some coefficients or weights and then with this new objective function, the optimization problem is solved. Thus the image reconstruction problem is to solve $\mathbf{Af} = \mathbf{b}$ such that \mathbf{f} satisfies some constraints, say $\mathbf{f} \in \mathbf{Q}$ where \mathbf{Q} is some set of constraints, for example we may have $f_j > 0, \forall j = 1, 2, \dots, n$, then in this approach the formulation will be

$$\sum_{j=1}^n f_j^2 + \alpha^2 \sum_{i=1}^m \left(\sum_{j=1}^n a_{ij} f_j - b_i \right)^2 \quad (3.8.1)$$

Such that $f_j > 0, \forall j = 1, 2, \dots, n$.

This image reconstruction problem (3.8.1) has unique solution, this solution is referred as least square regularized solution.

However, for non-Cartesian sampling, the matrix \mathbf{A} is often ill-conditioned or even singular, so the Least Square solution leads to undesirable noise amplification.

Thus in finite series expansion methods the problem of image reconstruction can be formulated using many approaches depending on the particular application problem and the method of measurement data acquisition system, which result in different kind of data measurement (projection).

These geometries lead to different kind of measurement problem, from where we can start to formulate the assumption, so that the problem can be solved. In finding the solution, it is most important that the solution can be implemented in actual

problem. The solution should be mathematically valid and at the same time should be able to give solution to actual real world problem with concrete interpretation and results.

The method developed by us for finding out the value of f_j the image vector in the system of linear equation (3.2.3) is explained in chapter IV by taking examples of 2×2 and 3×3 matrices. The solution of 2×2 matrix has been explained mathematically as well as computationally. The mathematically solution of 3×3 matrix is too lengthy and complicated therefore only computationally solution has been explained. This developed method is reliable and fast.

CHAPTER IV: MODIFIED SIMULTANEOUS ALGEBRAIC RECONSTRUCTION TECHNIQUE (MSART)

4.1 INTRODUCTION

The image reconstruction algorithms can be grouped in four major categories: Transformation Methods, Statistical Methods, Limited View Methods and Finite Series Expansion Reconstruction Methods discussed in chapter II. The algebraic reconstruction techniques algorithms belong to the Finite Series Expansion Reconstruction Methods. The original Algebraic Reconstruction Techniques algorithms and various variations in the original ART algorithms such as; Generalized ART, ART2, ART3, MART, SMART, ART with dumping factor etc, all have been discussed discerning the fundamental difference between the finite series methods and the others methods haves been discussed in chapter III. ART governs to modify the image by summing the pixels along some straight path and comparing this sum to the measured ray sum. The difference between estimated image projections, and the measured ray is calculated. The difference is then distributed over all the pixels in the ray sum.

The property of iterative methods is used to find the sum of appropriate image data in all ART algorithms. The algebraic approach is one of many approaches for formulating image reconstruction problem. In this approach the unknown image function is assumed to be an unknown vector. The algebraic equations in terms of unknown image function are set up to find the value of unknown vector. The finite series method is simple as compare to others methods as far as formulation of the

image reconstruction problem is concerned. The determination of solution of the formulated problem mathematically as well as computationally is simple in case of algebraic approach as compared to other approaches. For the purpose of this thesis we will follow the algebraic approach.

In this chapter, first we explain the mathematical principle behind the algebraic reconstruction technique given by Gordon, Herman and Bender (1970). Then we discuss the convergence of the algorithm. After that we explain our Modified Simultaneous Algebraic Reconstruction Technique (MSART) along with its merits in terms of convergence.

4.2 MATHEMATICAL PRINCIPLE OF ART

The image function f is assumed to be constant for a pixel, say f_j for j^{th} pixel, and total number of pixels varies from pixel to pixel are n , i.e. $j = 1, 2, \dots, n$. The line joining the source and detector is called a ray or a line. The physical measurement of total energy loss along the fixed ray is sum of energy loss in each pixel intersecting the line as explained earlier. The projection for the i^{th} ray for m no. of projection,

$$P_i = \sum_{j=1}^n a_{ij} f_j, \quad i = 1, 2, \dots, m \quad (4.2.1)$$

$$\text{Where, } a_{ij} = \begin{cases} 1 & j^{\text{th}} \text{pixel is intersected by } i^{\text{th}} \text{line} \\ 0 & \text{otherwise} \end{cases}$$

For the transmission method the noise which is negligible is included in the problem of image reconstruction is a linear algebraic system and can be written as

$$\mathbf{Af} = \mathbf{p} \quad (4.2.2)$$

where

$\mathbf{A}_{m \times n}$ is the projection matrix,

$\mathbf{f}_{n \times 1}$ is the image vector and

$\mathbf{P}_{m \times 1}$ is the measurement vector.

The problem is ill conditioned, either overdetermined $m >> n$ or underdetermined $m << n$ and \mathbf{A} is very sparse matrix. Thus usual methods of solving system of linear equations are not suitable, so iterative methods are applied. The principle of method of projection to solve the linear equations is explained in subsection 4.2.1. The determination of f_j from the above equation (4.2.2) is also explained in general in subsection 4.2.1. The image problem of 2×2 matrix and 3×3 are illustrated in subsection 4.2.2 to explain the method of projection using MSART [Srivastava, Nirvikar and Singh (2010, 2011)] which has been explained in section 4.3.

4.2.1 PRINCIPLE OF METHOD OF PROJECTION

Let us write the system explicitly, as (4.2.1)

$$a_{11}f_1 + a_{12}f_2 + \dots + a_{1j}f_j + \dots + a_{1n}f_n = P_1$$

$$a_{21}f_1 + a_{22}f_2 + \dots + a_{2j}f_j + \dots + a_{2n}f_n = P_2$$

$$a_{31}f_1 + a_{32}f_2 + \dots + a_{3j}f_j + \dots + a_{3n}f_n = P_3$$

.....

$$a_{i1}f_1 + a_{i2}f_2 + \dots + a_{ij}f_j + \dots + a_{in}f_n = P_i \quad (4.2.3)$$

.....

$$a_{m1}f_1 + a_{m2}f_2 + \dots + a_{mj}f_j + \dots + a_{mn}f_n = P_m$$

The left side of first equation in system (4.2.3) is scalar product of first row of coefficient matrix \mathbf{A} with column vector \mathbf{f} (=the unknown image function). Thus measurement p_1 is equated to this scalar product, which is actually a hyper plane in \mathbb{R}^{n-1} , while $\mathbf{f} \in \mathbb{R}^n$. Thus the equations in (4.2.3) are hyper planes in \mathbb{R}^{n-1} . The projection method starts from an arbitrary solution $\mathbf{f}^* \in \mathbb{R}^n$ of system (4.2.3), means that there is an arbitrary point \mathbf{f}^0 in \mathbb{R}^n , then drop a perpendicular from this arbitrary point \mathbf{f}^0 to the first hyper plane

$$H_1 = a_{11}f_1 + a_{12}f_2 + \cdots + a_{1j}f_j + \cdots + a_{1n}f_n = P_1,$$

Let us say it meets the hyper plane H_1 on point $\mathbf{f}^{(1)}$, now from this point $\mathbf{f}^{(1)} \in \mathbb{R}^n$ again drop a perpendicular on second hyper plane

$$H_2 = a_{21}f_1 + a_{22}f_2 + \cdots + a_{2j}f_j + \cdots + a_{2n}f_n = P_2$$

This perpendicular meets the hyper plane H_2 say at the point $\mathbf{f}^{(2)} \in \mathbb{R}^n$. In this way we will reach the point $\mathbf{f}^{(m)} \in \mathbb{R}^n$, which is point on m^{th} hyper plane:

$$H_m = a_{m1}f_1 + a_{m2}f_2 + \cdots + a_{mj}f_j + \cdots + a_{mn}f_n = P_m$$

In this manner one set of m iterations is completed. Now again start from first hyper plane H_1 , which says again drop the perpendicular from $\mathbf{f}^{(m)}$ to H_1 say that point of intersection as $\mathbf{f}^{(m+1)}$. This way we will repeat the iterations until we reach the solution. Now what we described as intersection of perpendicular from a point $\mathbf{f}^{(k)}$ in \mathbb{R}^{n-1} , is actually the projection of point $\mathbf{f}^{(k)}$ on hyper plane H_{K+1} .

Hence again using linear algebra, we get the formulation of this iterative process as follows:

Initial point in \mathbb{R}^n is \mathbf{f}^0 now its projection on

$$H_1 = a_{11}f_1 + a_{12}f_2 + \cdots + a_{1j}f_j + \cdots + a_{1n}f_n = P_1$$

or $H_1 : \langle \mathbf{a}^1, \mathbf{f} \rangle = p_1$, where, $\mathbf{a}^1 = (a_{11}, a_{12}, \dots, a_{1n})'$ is

$$\mathbf{f}^{(0)} + \frac{p_1 - \langle \mathbf{a}^1, \mathbf{f}^0 \rangle}{\langle \mathbf{a}^1, \mathbf{a}^1 \rangle} \mathbf{a}^1 \quad (4.2.4)$$

So in general we can write that the projection of point $\mathbf{f}^{(k)}$ on $(K+1)^{\text{st}}$ hyper plane

$$H_{k+1} : a_{k+11}f_1 + a_{k+12}f_2 + \cdots + a_{k+1n}f_n = P_{k+1}$$

or $H_{k+1} : \langle \mathbf{a}^{k+1}, \mathbf{f} \rangle = P_{k+1}$ is

$$\mathbf{f}^{(k)} + \frac{p_{k+1} - \langle \mathbf{a}^{k+1}, \mathbf{f}^{(k)} \rangle}{\langle \mathbf{a}^{k+1}, \mathbf{a}^{k+1} \rangle} \mathbf{a}^{k+1}$$

or in other words:

$$\mathbf{f}^{(k+1)} = \mathbf{f}^{(k)} + \frac{p_{k+1} - \langle \mathbf{a}^{k+1}, \mathbf{f}^{(k)} \rangle}{\langle \mathbf{a}^{k+1}, \mathbf{a}^{k+1} \rangle} \mathbf{a}^{k+1}$$

As described above this projection method is repeated after first m estimates $\mathbf{f}^{(M)}$ of \mathbf{f} have been obtained again starting from first hyper plane H_1 . Thus we can write in general the typical iterative step as:

$$\mathbf{f}^{(k+1)} = \mathbf{f}^{(k)} + \frac{p_{k+1} - \langle \mathbf{a}^{k+1}, \mathbf{f}^{(k)} \rangle}{\langle \mathbf{a}^{k+1}, \mathbf{a}^{k+1} \rangle} \mathbf{a}^{k+1} \quad (4.2.5)$$

where, i is advanced in cyclic manner $i = k(\text{mod } m) + 1$

Again using the explicit expression for inner products from linear algebra, we can write $\langle \mathbf{a}^i, \mathbf{a}^i \rangle = \|\mathbf{a}^i\|^2 = \sum_{j=1}^n a_{ij}^2$, where, $\|\cdot\|$ is Euclidean norm, and $\langle \mathbf{a}^i, \mathbf{f}^{(k)} \rangle = \sum_{j=1}^n a_{ij} f_j^{(k)}$.

It is clear that \mathbf{a}^i is i^{th} row of matrix \mathbf{A} of system (4.2.2), thus (4.2.5) can be written in explicit form as:

$$f_j^{k+1} = f_j^{(k)} + a_{ij} \frac{P_j - \sum_{j=1}^n a_{ij} f_j^{(k)}}{\sum_{j=1}^n a_{ij}^2} \quad (4.2.6)$$

$$j = 1, 2, \dots, n, \quad i = k(\text{mod } m) + 1$$

Since we are projecting the points in \mathbb{R}^n on hyper planes in \mathbb{R}^{n+1} in cyclic manner, and assuming that unique solution of system (4.2.3) exists, which says a; hyper planes meet at a single point \mathbf{f}^* in \mathbb{R}^n . So when we start from arbitrary point in \mathbb{R}^n and project on given hyper planes in cyclic manner this new point will be nearer to actual intersection point and cyclic manner ensures that we do proceed towards the intersection consistently. This complete principle is explained by a small example here.

4.2.2 EXAMPLE EXPLAINING PROJECTION METHOD:

This is explained for a small set up for an image of 2X2, shown in figure 4.1(a)

In this model, each pixel ' j ' is assumed to have an attenuation f_j , an unknown value to be determined. The measured projection data b_i is the weighted sum of the attenuations of pixels along a given ray, also known as a ray integral or raysum

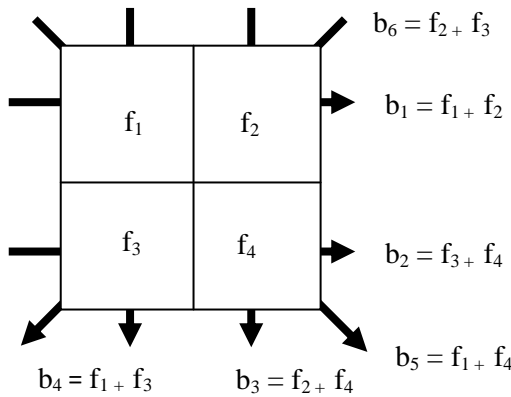


Figure. 4.1(a): The reconstruction problem as a system of linear equation (2X2).

Different variations of the model can be used to determine the weight w_{ij} contribution of each pixel ‘ j ’ to the total i^{th} weighted attenuation ‘ P_i ’. Let us use a model where each weight w_{ij} is the product of the pixel’s attenuation f_j and the length of the ray’s intersection with the pixel (expressed in pixel length). The weights can then be determined geometrically from the angle and position of the ray and the chosen pixel dimensions.

The Figure. 4.1(a) shows four pixels f_1, f_2, f_3 and f_4 , ($n = 4$) and their projections. There are 4 detectors in the detector array, and the array is rotated through 4 views (horizontal, vertical, diagonal and anti-diagonal) to produce raysums ($m = 6$), Srivastava, Nirvikar and Singh (2010). In the following model we have four unknown variables (image pixels) and assume the raysums ($m=6$) for these image pixels. In step one we start with the initial guess of pixel as value zero then we proceed to step 2 to step 4 to calculate the image value from different angels:

$$\begin{matrix} w & x \\ y & z \end{matrix} \begin{matrix} 11 \\ 7 \end{matrix}$$

6 10 8 12

then

1. Initial guess and projections

$$\begin{bmatrix} 0 & 0 \\ 0 & 0 \\ 0 & 0 \end{bmatrix}^0$$

2. Refine projection I, view 1

$$\begin{bmatrix} w \\ x \\ y \\ z \end{bmatrix} = \begin{bmatrix} 0 + \frac{11-0}{2} \\ 0 + \frac{11-0}{2} \\ 0 + \frac{7-0}{2} \\ 0 + \frac{7-0}{2} \end{bmatrix} = \begin{bmatrix} 5.5 \\ 5.5 \\ 3.5 \\ 3.5 \end{bmatrix}$$

3. Refine projection II, view 2

$$\begin{bmatrix} w \\ x \\ y \\ z \end{bmatrix} = \begin{bmatrix} 5.5 + \frac{10-9}{2} \\ 5.5 + \frac{8-9}{2} \\ 3.5 + \frac{10-9}{2} \\ 3.5 + \frac{8-9}{2} \end{bmatrix} = \begin{bmatrix} 6 \\ 5 \\ 4 \\ 3 \end{bmatrix}$$

4. Refine projection III, view 3

$$\begin{bmatrix} w \\ x \\ y \\ z \end{bmatrix} = \begin{bmatrix} 6 + \frac{12-9}{2} \\ 5 + \frac{6-9}{2} \\ 4 + \frac{12-9}{2} \\ 3 + \frac{6-9}{2} \end{bmatrix} = \begin{bmatrix} 7.5 \\ 3.5 \\ 2.5 \\ 4.5 \end{bmatrix}$$

$$\begin{bmatrix} 7.5 & 3.5 \\ 2.5 & 4.5 \end{bmatrix} \begin{matrix} 11 \\ 7 \end{matrix}$$

6	10	8	12
---	----	---	----

After the step for as calculate we got the solution that shows the distribution of projection value in image pixels and for authentication we can check the sum of

image value that is equal to the projection value in that direction, these four steps are calculate in just one iteration its mean that by using this method we are getting the image value in one iteration. But this is not working for large image as shown in next example because here in this image we have the limited views (four views).

The ray traverses the width of pixel 1, so the weight of contribution of pixel 1 to the raysum is $a_{11} = 1$. Likewise, $a_{12} = 1$. ray 1 does not intersect Pixels 3 and 4, so $a_{13} = a_{14} = 0$. Similarly for the other rays in this example, all weights are 0 or 1, and the raysum equations are as follows:

$$\begin{aligned} b_1 &= f_1 a_{11} + f_2 a_{12} + f_3 a_{13} + f_4 a_{14} = f_1 + f_2 \\ b_2 &= f_1 a_{21} + f_2 a_{22} + f_3 a_{23} + f_4 a_{24} = f_3 + f_4 \\ b_3 &= f_1 a_{31} + f_2 a_{32} + f_3 a_{33} + f_4 a_{34} = f_2 + f_4 \\ b_4 &= f_1 a_{41} + f_2 a_{42} + f_3 a_{43} + f_4 a_{44} = f_1 + f_3 \\ b_5 &= f_1 a_{51} + f_2 a_{52} + f_3 a_{53} + f_4 a_{54} = f_1 + f_4 \\ b_6 &= f_1 a_{61} + f_2 a_{62} + f_3 a_{63} + f_4 a_{64} = f_2 + f_3 \end{aligned}$$

In general, for each ray b_i can be written as:

$$b_i = \sum_{j=0}^n a_{ij} f_j, i = 1, 2, \dots, m$$

Where half of the nm weights a_{ij} are zero. Another example having an image of 3 X 3, In figure 4.1(b), an image of 9 pixels with 4 detectors. The array is rotated through 4 views (horizontal, vertical, diagonal and anti diagonal) to produce $m = 16$ ray sums Srivastava and Nirvikar (2010).

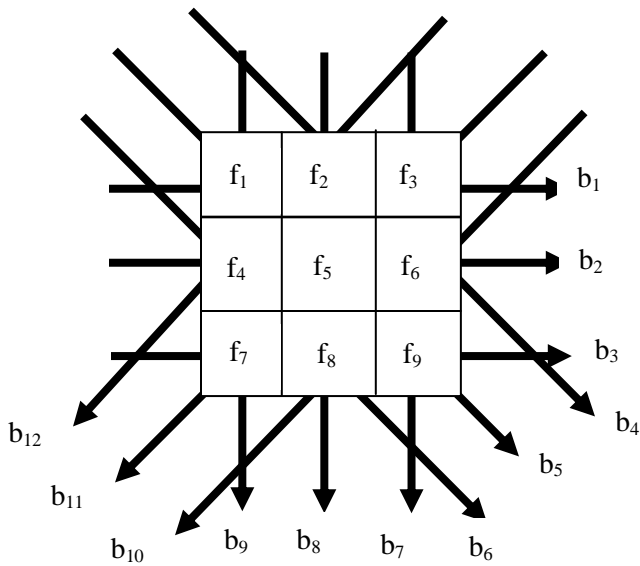


Figure. 4.1(b): The reconstruction problem as a system of linear equation (3X3).

Starting with initial guess (image value) at $f^{(0)} = (0, 0, 0, 0, 0, 0, 0, 0, 0)$ with projections that is calculate from the test image of 9x9 using the algorithm

$$p = (3, 7, 9, 8, 6, 4, 4, 9, 7, 4, 9, 4, 2, 6, 4, 1),$$

after 4 iterations we found the image data and projection match.

$$f = (2.78, 0.00, 3.04, 3.67, 2.33, 0.67, 8.22, 3.67, 1.78) \text{ (image value)}$$

$$p = (5.81, 6.67, 13.67, 14.67, 6.00, 5.48, 8.22, 7.34, 6.89, 0.67, 3.04, 1.78, 4.54, 13.59, 3.67, 2.78)$$

Here in this example we see that the initial projection value is not matched after the 4th iteration because the limited number of views, In general, for large images, a substantial portion of the weights are zero, because many of the pixels make no contribution to a particular raysum. One approach to solve large systems of equations is iterative approximations which is the basis of the *iterative* or *algebraic* methods. Successive adjustments are made to the attenuation values until a solution is reached that is consistent with the projection values by some criterion. Iterative methods compare the computed ray sums of an estimated image with the original projection

measurements and use the error obtained from this comparison to correct the estimated image.

In general, m and n are quite large. For example, when reconstructing an image size of 256×256 pixels, from 256 detector measurements in each of 256 views, n and m are both 65,536. Here we consider the 256 detectors to improve the pictorial quality and to reduce the number of iterations because we have seen in previous example that the limited view is not useful for the large image. In such cases the weight matrix size is $65,536 \times 65,536 = 4,294,967,296$. We require algorithms that are efficient in terms of both time and memory requirement to solve this system of liners equations on a computer without increasing the execution time.

Again by using an example of 3×3 image whose projection data is given in four directions i.e. $\theta=0^\circ, 45^\circ, 90^\circ$ and 135° are given in Table 4.2.1. Starting with initial guess f^0 given in Table 4.2.2. Its four iterations are given in Table 4.2.3 and in Table 4.2.4 the projection at each iteration in all four directions are given. From Table 4.2.5 it is evident that errors in successive iterations are reducing very fast. [Srivastava, Nirvikar and Singh (2011)]. Starting with initial guess $f^{(0)}$ and projections p .

2	6	8	7
9	7	2	1
3	9	2	6
8	7	9	7

Table 4.2.1. Projection Value (p)

0	0	0
0	0	0
0	0	0

Table 4.2.2. Initial Image Data ($f^{(0)}$)

Image after 1 iteration		
2.22	5.78	2.22
3.11	3.00	6.11
3.56	4.11	3.89
Image after 2 iteration		
2.99	5.69	1.99
2.56	2.65	5.44
4.68	3.32	4.01
Image after 3 iteration		
2.63	6.01	1.66
2.59	2.70	5.85
4.60	3.40	3.97
Image after 4 iteration		
2.74	5.97	1.65
2.47	2.59	5.68
4.71	3.25	3.96

Table 4.2.3. Reconstructed Image

Projection after 1 iteration			
10.22	12.22	11.06	8.89
12.89	12.22	3.56	7.22
9.11	11.89	2.22	2.22
8.89	8.78	10.22	3.89
Projection after 2 iteration			
10.67	10.65	12.01	10.23
11.66	11.44	4.68	5.88
9.65	11.13	1.99	2.99
8.25	9.32	8.76	4.01
Projection after 3 iteration			
10.30	11.14	11.97	9.82
12.11	11.48	4.60	5.99
9.65	11.13	1.99	2.99
8.25	9.32	8.76	4.01
Projection after 4 iteration			
10.36	10.74	11.92	9.92
11.81	11.29	4.71	5.72
9.29	11.65	1.65	2.74
8.44	8.95	8.93	3.96

Table 4.2.4. Projection data at each iteration

Iteration	$ f_{i+1} - f_i $	$(f_{i+1} - f_i)^2$
1	33.9999	143.9506
2	4.6913	3.4226
3	1.6872	0.5149
4	0.8254	0.1038

Table 4.2.5. Error calculated in Image pixel values for every iteration

The mathematical implementation of 3X3 or higher matrices is very complicated and lengthy therefore we are taking the example of only 2X2 to demonstrate the method to explain the calculations explicitly, consider a system of linear equations having solutions in \mathbb{R}^2 , thus hyper planes will be lines. For making the unique solution we will consider only two hyper planes. Thus we have

$$\begin{aligned} H_1 : 2f_1 + f_2 &= 10 \\ H_1 : f_1 + 3f_2 &= 15 \end{aligned} \quad (4.2.7)$$

The system (4.2.7) has a unique solution $\mathbf{f} = \begin{bmatrix} 3 \\ 4 \end{bmatrix} \in \mathbb{R}^2$. For applying the projection method to find the solution of this system let us first write the vectors, matrices and points in last section's terminology. Hence n=2, m=2,

$$\begin{aligned} \mathbf{f} &= \begin{bmatrix} f_1 \\ f_2 \end{bmatrix}, \mathbf{A} = \begin{bmatrix} 2 & 1 \\ 1 & 3 \end{bmatrix}, \mathbf{p} = \begin{bmatrix} 10 \\ 15 \end{bmatrix} \\ \Rightarrow \mathbf{a}^1 &= \begin{bmatrix} 2 \\ 1 \end{bmatrix}, \mathbf{a}^2 = \begin{bmatrix} 1 \\ 3 \end{bmatrix}, p_1 = 10, p_2 = 15 \end{aligned}$$

Now

$$\|\mathbf{a}^1\| = \langle \mathbf{a}^1, \mathbf{a}^1 \rangle = \sum_{j=1}^2 a_{1j}^2 = 4 + 1 = 5$$

$$\|\mathbf{a}^2\| = \langle \mathbf{a}^2 \cdot \mathbf{a}^2 \rangle = \sum_{j=1}^2 a_{2j}^2 = 1 + 9 = 10$$

Start with initial guess $\mathbf{f}^0 = \begin{bmatrix} 1 \\ 1 \end{bmatrix} \Rightarrow f_1^0 = 1, f_2^0 = 1,$

Using the explicit formula (4.2.6), we get

$$f_1^{(1)} = f_1^{(0)} + a_{11} \frac{p_1 - \sum_{j=1}^2 a_{1j} f_j^{(0)}}{\sum_{j=1}^2 a_{1j}^2}, \text{ since } k=0, \text{ so } I=1,$$

$$= 1 + 2 \frac{10 - 3}{5} = \frac{19}{5} = 3.8$$

$$f_2^{(1)} = f_2^{(0)} + a_{12} \frac{p_1 - \sum_{j=1}^2 a_{1j} f_j^{(0)}}{\sum_{j=1}^2 a_{1j}^2}$$

$$= 1 + 1 \frac{10 - 3}{5} = \frac{12}{5} = 2.4$$

Thus, $\mathbf{f}^1 = \begin{bmatrix} 3.8 \\ 2.4 \end{bmatrix}$ is first projection of \mathbf{f}^0 on H_1 . Now next iteration will be projection

of $\mathbf{f}^{(1)}$ on H_2 , since the formula (4.2.5) which is vector (composite) form of formula (4.2.6), we get,

$$\mathbf{f}^2 = \mathbf{f}^1 + \frac{p_2 - \langle \mathbf{a}^2 \cdot \mathbf{f}^{(1)} \rangle}{\langle \mathbf{a}^2 \cdot \mathbf{a}^2 \rangle} \mathbf{a}^2$$

$$= \begin{bmatrix} 3.8 \\ 2.4 \end{bmatrix} + \frac{15 - 11}{10} \begin{bmatrix} 1 \\ 3 \end{bmatrix}$$

$$= \begin{bmatrix} 3.8 \\ 2.4 \end{bmatrix} + 0.4 \begin{bmatrix} 1 \\ 3 \end{bmatrix} = \begin{bmatrix} 4.2 \\ 3.6 \end{bmatrix}$$

Thus projection of $\mathbf{f}^1 = \begin{bmatrix} 3.8 \\ 2.4 \end{bmatrix}$ on H_2 is $\mathbf{f}^2 = \begin{bmatrix} 4.2 \\ 3.6 \end{bmatrix}$. Now moving in cyclic manner for next iterations again we will project $\mathbf{f}^{(2)}$ on H_1 and so on. Here we will provide few iterations, k=2 iteration number 3

$$\mathbf{f}^3 = \mathbf{f}^{(1)} + \frac{p_1 - \langle \mathbf{a}^1 \cdot \mathbf{f}^{(2)} \rangle}{\langle \mathbf{a}^1 \cdot \mathbf{a}^1 \rangle} \mathbf{a}^1$$

$$= \begin{bmatrix} 4.2 \\ 3.6 \end{bmatrix} + \frac{10 - 12}{5} \begin{bmatrix} 2 \\ 1 \end{bmatrix}$$

$$= \begin{bmatrix} 4.2 \\ 2.4 \end{bmatrix} - 0.4 \begin{bmatrix} 2 \\ 1 \end{bmatrix}$$

$$= \begin{bmatrix} 3.4 \\ 3.2 \end{bmatrix}$$

Iteration number 4, k=3

$$\mathbf{f}^{(4)} = \mathbf{f}^{(3)} + \frac{p_2 - \langle \mathbf{a}^2 \cdot \mathbf{f}^{(3)} \rangle}{\langle \mathbf{a}^2 \cdot \mathbf{a}^2 \rangle} \mathbf{a}^2$$

$$= \begin{bmatrix} 3.4 \\ 3.2 \end{bmatrix} + \frac{15 - 13}{10} \begin{bmatrix} 1 \\ 3 \end{bmatrix}$$

$$= \begin{bmatrix} 3.4 \\ 3.2 \end{bmatrix} - 0.2 \begin{bmatrix} 1 \\ 3 \end{bmatrix}$$

$$= \begin{bmatrix} 3.6 \\ 3.8 \end{bmatrix}$$

Iteration number 5, k=4

$$\mathbf{f}^{(5)} = \mathbf{f}^{(4)} + \frac{p_1 - \langle \mathbf{a}^1 \cdot \mathbf{f}^{(2)} \rangle}{\langle \mathbf{a}^1 \cdot \mathbf{a}^1 \rangle} \mathbf{a}^1$$

$$= \begin{bmatrix} 3.6 \\ 3.8 \end{bmatrix} + \frac{10 - 11}{4} \begin{bmatrix} 2 \\ 1 \end{bmatrix}$$

$$= \begin{bmatrix} 3.6 \\ 3.8 \end{bmatrix} - 0.2 \begin{bmatrix} 2 \\ 1 \end{bmatrix}$$

$$= \begin{bmatrix} 3.2 \\ 3.6 \end{bmatrix}$$

Iteration number 6, k=5

$$\mathbf{f}^{(6)} = \mathbf{f}^{(5)} + \frac{p_2 - \langle \mathbf{a}^2 \cdot \mathbf{f}^{(5)} \rangle}{\langle \mathbf{a}^2 \cdot \mathbf{a}^2 \rangle} \mathbf{a}^2$$

$$= \begin{bmatrix} 3.2 \\ 3.6 \end{bmatrix} + \frac{15 - 14}{10} \begin{bmatrix} 1 \\ 3 \end{bmatrix}$$

$$= \begin{bmatrix} 3.2 \\ 3.6 \end{bmatrix} - 0.1 \begin{bmatrix} 1 \\ 3 \end{bmatrix}$$

$$= \begin{bmatrix} 3.3 \\ 3.9 \end{bmatrix}$$

Iteration number 7, k=6

$$\mathbf{f}^{(7)} = \mathbf{f}^{(6)} + \frac{p_1 - \langle \mathbf{a}^1 \cdot \mathbf{f}^{(6)} \rangle}{\langle \mathbf{a}^1 \cdot \mathbf{a}^1 \rangle} \mathbf{a}^1$$

$$= \begin{bmatrix} 3.3 \\ 3.9 \end{bmatrix} + \frac{10 - 10.5}{5} \begin{bmatrix} 2 \\ 1 \end{bmatrix}$$

$$= \begin{bmatrix} 3.3 \\ 3.9 \end{bmatrix} - 0.1 \begin{bmatrix} 2 \\ 1 \end{bmatrix}$$

$$= \begin{bmatrix} 3.1 \\ 3.8 \end{bmatrix}$$

Iteration number 8, k=7

$$\mathbf{f}^{(8)} = \mathbf{f}^{(7)} + \frac{p_2 - \langle \mathbf{a}^2 \cdot \mathbf{f}^{(7)} \rangle}{\langle \mathbf{a}^2 \cdot \mathbf{a}^2 \rangle} \mathbf{a}^2$$

$$= \begin{bmatrix} 3.1 \\ 3.8 \end{bmatrix} + \frac{15 - 14.5}{10} \begin{bmatrix} 1 \\ 3 \end{bmatrix}$$

$$= \begin{bmatrix} 3.1 \\ 3.8 \end{bmatrix} + 0.05 \begin{bmatrix} 1 \\ 3 \end{bmatrix}$$

$$= \begin{bmatrix} 3.15 \\ 3.95 \end{bmatrix}$$

Iteration number 9, k=8

$$\begin{aligned}\mathbf{f}^{(10)} &= \begin{bmatrix} 3.05 \\ 3.9 \end{bmatrix} + \frac{15 - 14.75}{10} \begin{bmatrix} 1 \\ 3 \end{bmatrix} \\ &= \begin{bmatrix} 3.05 \\ 3.9 \end{bmatrix} - 0.025 \begin{bmatrix} 1 \\ 3 \end{bmatrix} \\ &= \begin{bmatrix} 3.075 \\ 3.975 \end{bmatrix}\end{aligned}$$

It is evident from this example that starting from any arbitrary value \mathbf{f}^0 one reaches towards the unique solution by substituting the value of iteration in the subsequent iteration in cyclic manner on next hyper plane.

One more thing we observe from this example that the method is reaching towards the actual solution step by step consistently. Each iteration say, (k^{th}) gives a point on one of the hyper planes say H_i , thus the solution, $\mathbf{f}^{(k)}$ satisfies the i^{th} equation. The only requirement to get the image value is that at least one nonzero element should be in every row of the matrix A, which can be represented mathematically as $\|\mathbf{a}^i\| \neq 0$. Practically it says that, we are not considering the measurements which are not intercepted from any pixel, which is quite a natural restriction and also will not add to noises.

The merit of an iterative method is convergence which means that how fast the convergence, if at all it is there, is approaching towards the correct solution. In other words how many iterations steps are taken to achieve the solution. The geometric interpretation and efficiency of projection method has been described as follows.

4.2.3 GEOMETRIC INTERPRETATION

We will discuss this with the help of second example described in section 4.2, we had system in two dimension planes thus getting hyper planes in one dimension that means they are lines, thus we get the system

$$\begin{aligned} H_1 : a_{11}f_1 + a_{12}f_2 &= p_1 \\ H_2 : a_{21}f_1 + a_{22}f_2 &= p_2 \end{aligned} \quad (4.2.8)$$

Geometrically this system and solution \mathbf{f}^* , the intersection of hyper planes H_1 and H_2 is shown in fig. 4.2 (This interpretation is applicable in higher dimension as well).

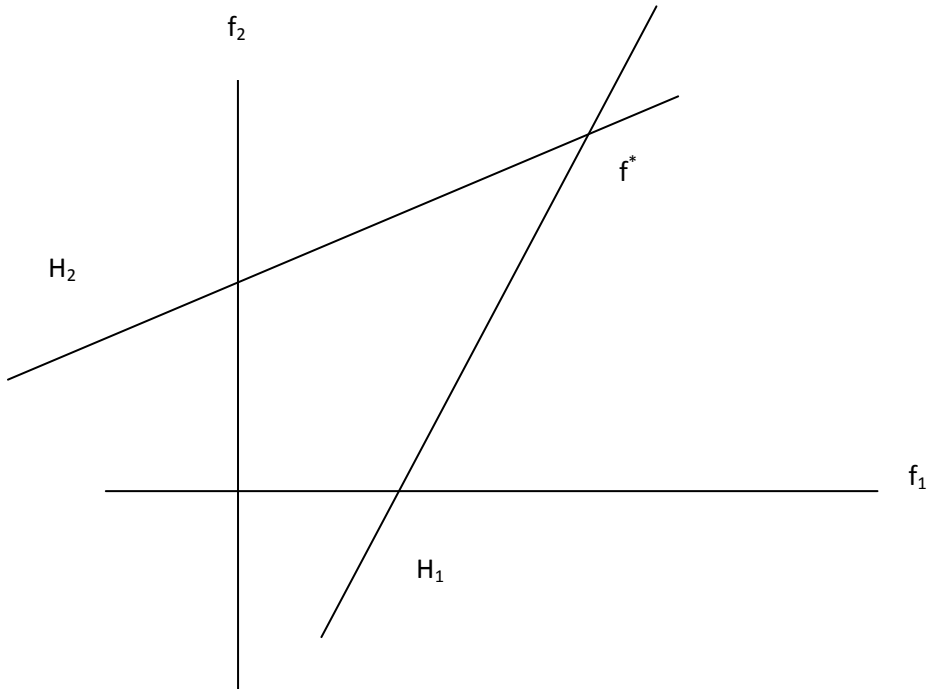


Figure 4.2: Showing two hyper planes H_1 and H_2 Equation (4.3.1) and their intersection \mathbf{f}^*

Now let us consider the arbitrary point \mathbf{f}^0 in \mathbb{R}^2 and project this on H_1 , which says drop a perpendicular from \mathbf{f}^0 to H_1 as shown in figure 4.3.

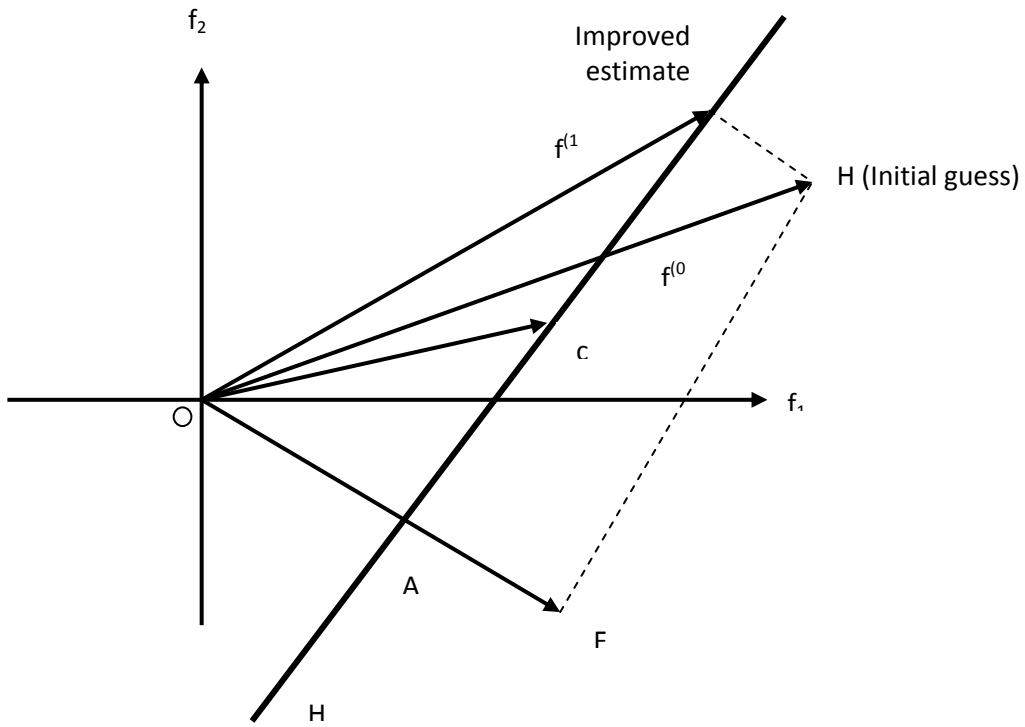


Figure 4.3: Showing plane H_1 , point f^0 and its projection on H_1

$\mathbf{a}^1 = \begin{bmatrix} a_{11} \\ a_{12} \end{bmatrix}$ is normal to hyper plane H_1 of (4.2.8) and if we take any point C on H_1 , its position vector \overrightarrow{OC} will have constant inner product with \mathbf{a}^1 , $\therefore \mathbf{a}^1 \cdot \overrightarrow{OC} = p_1$ by first equation of (4.2.8) which is also visible from Fig. 4.3.

If $B = f^0 = \begin{bmatrix} f_1^0 \\ f_2^0 \end{bmatrix}$ is any arbitrary point in \mathbb{R}^2 then $f^{(1)}$, the projection of f^0 on H_1 is a point on H_1 say G and $f^{(1)} = f^{(0)} + \overrightarrow{BG}$ [clear from Figure 4.3] and \overrightarrow{BG} is parallel to \mathbf{a}^1 thus

$$f^{(1)} = f^{(0)} + \frac{p_1 - \mathbf{a}^1 \cdot f^0}{\mathbf{a}^1 \cdot \mathbf{a}^1} \mathbf{a}^1$$

since C is on H_1 $\overrightarrow{OC} \cdot \mathbf{a}^1 = p_1$ and $|\overrightarrow{BG}| = |\overrightarrow{OA}| - |\overrightarrow{OF}|$, where

$$|\overrightarrow{OA}| = \overrightarrow{OC} \cdot \frac{\mathbf{a}^1}{(\mathbf{a}^1 \cdot \mathbf{a}^1)^{1/2}}, |\overrightarrow{OF}| = \overrightarrow{OC} \cdot \frac{\mathbf{f}^0 \cdot \mathbf{a}^1}{(\mathbf{a}^1 \cdot \mathbf{a}^1)^{1/2}}$$

$$\Rightarrow |\overrightarrow{BG}| = \frac{p_1}{(\mathbf{a}^1 \cdot \mathbf{a}^1)^{1/2}} - \frac{\mathbf{f}^0 \cdot \mathbf{a}^1}{(\mathbf{a}^1 \cdot \mathbf{a}^1)^{1/2}} \therefore \overrightarrow{BG} = \frac{p_1 - \mathbf{f}^0 \cdot \mathbf{a}^1}{(\mathbf{a}^1 \cdot \mathbf{a}^1)^{1/2}} \frac{\mathbf{a}^1}{(\mathbf{a}^1 \cdot \mathbf{a}^1)^{1/2}}$$

Similarly we can draw H_2 also in this, see figure (4.4) and from $\mathbf{f}^{(1)}$ draw a perpendicular on H_2 say $\mathbf{f}^{(2)}$ again as explained in case of $\mathbf{f}^{(1)}$, we will get

$$\mathbf{f}^{(2)} = \mathbf{f}^{(1)} + \frac{p_2 - \mathbf{a}^2 \cdot \mathbf{f}^{(1)}}{\mathbf{a}^2 \cdot \mathbf{a}^2} \mathbf{a}^2.$$

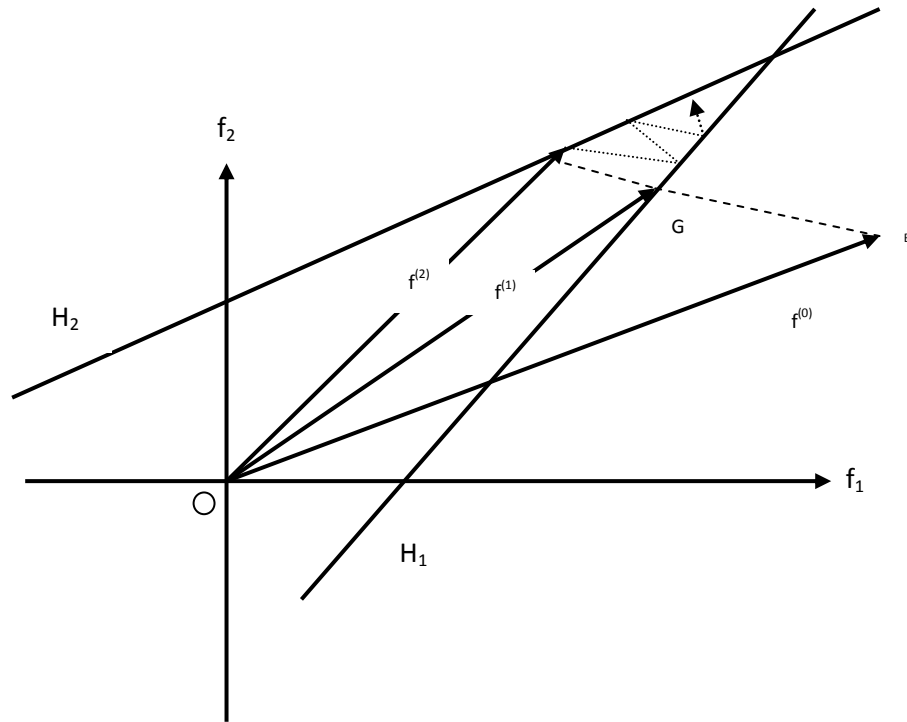


Figure 4.4: Showing plane H_1 , H_2 and point \mathbf{f}^0 with the projections

Repeating the same process we find that each iteration when moved in cyclic manner is reaching near point of inter-section \mathbf{f}^* of hyper planes H_1 and H_2 which is the solution.

Thus geometrically it is clear that if unique solution exists then this method of projections to solve linear algebraic equations converges to actual solution.

The rigorous mathematical proof using linear algebra to show that as $k \rightarrow \infty, \mathbf{f}^{(Km)} \rightarrow \mathbf{f}^*$ is given by Tanabe (1971).

Now we are interested in the efficiency of this method, which in other words is rate of convergence of this method. Moreover in actual problem of image reconstruction from projections how fast this method converges to the solution, when actually we do not know whether such a unique solution does exist or not, then what should be the stopping criterion of the iterative process of this method.

4.2.4 EFFICIENCY

As shown with example in section 4.2 that the iterative process is approaching towards the solution consistently, but as it reaches near to actual solution the speed of rate of convergence becomes very slow. Describing this in mathematical terms says that the difference between consecutive iterative terms is very small. Thus we would stop the iterative process when the difference between consecutive estimates of \mathbf{f} is very small (which can be prefixed according to the requirement in image reconstruction problem). So we may stop the iteration when

$$\|\mathbf{f}^{(k+1)} - \mathbf{f}^{(k)}\| \leq \epsilon_1 \quad (4.2.9)$$

where $\epsilon_1 > 0$, is some prefixed small number say for example may be 10^{-5} when dealing with image reconstruction problem in non-destructive testing.

If we use Euclidean norm then (4.2.9) is translated as: stop the iterative process when $[\sum_{j=1}^n (f_j^{(k+1)} - f_j^{(k)})^2]^{1/2} \leq \epsilon_1$ and then solution of system (4.2.2) or (4.2.3) is $\mathbf{f}^{(k+1)}$ or $f_j^{(k+1)}, j = 1, 2, \dots, N$.

But practically this criterion is not the only stopping rule for this projection method. Various other rules were also used in literature, thus giving many other algorithms and approaches as described in Chapter III. Here we will give some more convergence criterion and their stopping rules, which are applicable in algebraic reconstruction techniques.

First we introduce certain parameters on which convergence is decided.

The discrepancy measure between projections

$$\mathbf{P}_d^{(k)} = \|\mathbf{P}^k - \mathbf{P}^q\| = \left(\sum_{i=1}^m (p_i - p_i^{(k)})^2 \right)^{1/2}$$

where, $p_i^{(k)} = i^{th}$ ray sum of k^{th} iteration estimate

$$\Rightarrow p_i^{(k)} = \sum_{j=1}^n a_{ij} f_j^{(k)}, \quad i = 1, 2, \dots, m$$

and p_i = the original i^{th} ray projection data.

The discrepancy in consecutive estimates of image

$$\mathbf{f}_d^{(k)} = \left[\sum_{j=1}^n (f_j^{(k+1)} - f_j^{(k)})^2 \right]^{1/2}$$

where $\mathbf{f}^{(k)} = (f_1^{(k)} \dots f_n^{(k)})'$ is the k^{th} iteration estimate of the image.

The variance of k^{th} estimate of image

First estimate the mean value of image function along i^{th} ray as: $\bar{f}_i = \frac{\sum_{j=1}^n a_{ij} f_j}{\sum_{j=1}^n a_{ij}} = \frac{p_i}{\sum_{j=1}^n a_{ij}}$, then again take average over all rays thus $\bar{f} = \frac{1}{m} \sum_{i=1}^m \bar{f}_i = \frac{1}{m} \sum_{i=1}^m \frac{p_i}{\sum_{j=1}^n a_{ij}}$, thus variation in k^{th} estimate is defined as $V^{(k)} = \sum_{j=1}^n (f_j^{(k)} - \bar{f})^2$

The Discrepancy in Test Patterns

For some test images the projection data is calculated mathematically as ray sum, and then using that data reconstruction is done by this iterative method, then difference between k^{th} iteration estimate and test image is defined with $\mathbf{f}^t = (f_1^t \dots f_N^t)'$ is test image as

$$\delta^{(k)} = \|\mathbf{f}^{(k)} - \mathbf{f}^t\|$$

$$= \left[\sum_{j=1}^n (f_j^{(k)} - f_j^t)^2 \right]^{1/2}$$

This had been shown that $\delta^{(k)} / \sqrt{V^{(k)}}$ for test images was converging for k, then it started to diverge [Gilbert (1972)].

Thus it is advisable to stop the iterations before they start diverging for this some criterion based on $V^{(k)}$ has been suggested in literature such as $|V^{(k+1)} - V^k| < V^{(k)}/100$ by Herman, Lent and Rowland (1973). With all these characteristics of algebraic approach, we proposed an alternative method named Modified Simultaneous Algebraic Reconstruction Technique (MSART) for computed tomography using parallel beam projection data for image reconstruction. The thesis claimed that this method produced superior image quality when compared to Conventional backprojection, especially for limited view (few projections), discussed in the next section.

4.3 MODIFIED SIMULTANEOUS ALGEBRAIC RECONSTRUCTION TECHNIQUE (MSART)

This method is modification of the method of projection. We have discussed some modification as relaxation method, SIRT or SART described in Chapter III. Our modification is to improve convergence rate to reach to solution in spite of noise present in the projection data. This method is combination of SART with other modifications. In ART given by (3.6.1) in Chapter III as

$$f_j^{k+1} = f_j^k + a_{ij} \frac{p_i - \sum_{j=1}^n a_{ij} f_j^k}{\sum_{j=1}^n a_{ij}^2},$$

$$\forall j \exists a_{ij} \neq 0, \text{ and } i = k(\text{mod } m) + 1$$

for solving the system of linear algebraic equations

$$\mathbf{A}\mathbf{f} = \mathbf{p} \text{ with } \mathbf{A} = ((a_{ij}))_{m \times n}, \mathbf{f} = (f_j)_{n \times 1}, \mathbf{p} = (p_i)_{m \times 1}.$$

Using ART, in each iteration only those f_j 's are modified which intersect with i^{th} ray and in one iteration only one ray is considered. It makes a large number of iterations for getting some significant results and making the rate of convergence very slow. Also it gives noise as measurements are computed by noise and give inconsistency in the system as well. To improve upon these difficulties simultaneous algebraic reconstruction technique (SART) was introduced by Anderson (1984).

In this method to reduce noise, the f_j 's are not modified in each ray at one iteration but the modification only is stored separately for all rays of projection measurements and then in one iteration the modification of all rays for j^{th} value is been incorporated at the end. Thus give the formula as

$$f_j^{(k+1)} = f_j^{(k)} + \frac{1}{\sum_{i=1}^m a_{ij}} \sum_{i=1}^m \frac{p_i - \sum_{j=1}^n a_{ij} f_j^{(k)}}{\sum_{i=1}^m a_{ij}^2} a_{ij} \quad \forall j = 1, 2, \dots, n$$

This formulation actually makes a single iteration more time and cost consuming, but reduces noises. Thus in applications where accurate estimates are required on the cost of expensive iteration, this is suitable, its convergence was also proved by Ming (2003). Now we introduced our method, Modified Simultaneous Algebraic Reconstruction Technique (MSART) as described follows.

The basic principle behind this is first the reconstruction space is taken to be square, thus if it is of any shape we cover it by square, if it is of any shape we cover it

by square grid and pixels were also taken to be square as shown in Figure 4.5 and measurements taken as lines or strips across the reconstruction region. The strips are first approximated as lines, or the strip width is neglected.

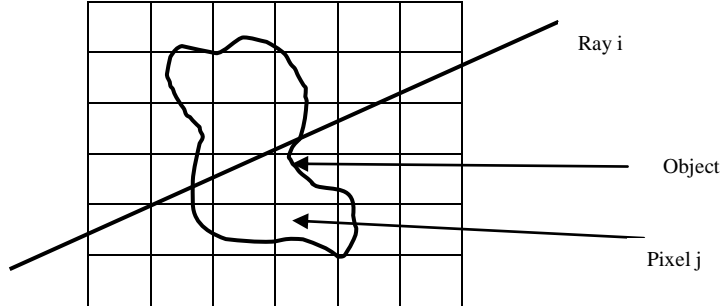


Figure 4.5: Digitization with square grid

Unlike ART where measurements p_i are numbered in a manner and then iterations were moving in cyclic manner over these numbered rays, in this method we do not require to number the measurements in any particular manner. Here we require to have a_{ij} 's as guiding force for modification of image values. First we start with each ray and modify all f_j 's which are intersecting that ray, when we move to next ray we modify all pixel elements of this ray, which may result that some modified f_j in previous iteration are again modified. The modification which we are introducing at each ray is similar to constrained ART, at first we introduce only partial constraints that are all image values and measurements are non negative. The modification in each ray is given for all f_i 's which intersect that ray so a typical i^{th} ray modification is

$$\frac{p_i - \sum_{j=1}^n a_{ij} f_j^{*(k)}}{\sum_{j=1}^n a_{ij}^2} a_{ij} \quad (4.4.1)$$

which is added to all f_j 's such that $a_{ij} \neq 0$ here $f_j^{*(k)}$ is used instead of $f_j^{(k)}$ which is either $f_j^{(k)}$ if f_j was not modified in any of previous rays or it is modified $f_j^{(k)}$, if it has been modified previously. Then the elements f_j of i^{th} ray are modified as

$$\max \left\{ 0, f_j^{*(k)} + a_{ij} \frac{p_i \sum_{j=1}^n a_{ij} f_j^{*(k)}}{\sum_{j=1}^n a_{ij}^2} \right\}$$

This modification keeps for each ray the non-negative constraint.

Once this process is completed for all rays $i = 1, 2, \dots, m$, the final outcome $f_j^{(k+1)}, j = 1, 2, \dots, n$ is said to be $(k+1)^{\text{st}}$ estimate obtained for k^{th} estimate.

This modification actually makes the convergence process fast and computationally also requires less storage capacity. In the next section we will discuss mathematical explanation of this method converting the image reconstruction problem in the form of linear equations as shown in hyper planes than the convergence of the MSART is described and finally the algorithm and the implementation of MSART on some tested images for which the projection data is available is described in chapter V.

4.3.1 MATHEMATICAL EXPLANATION AND CONVERGENCE OF MSART

Let us reconsider our problem which is system (4.2.3)

$$H_1 = a_{11}f_1 + a_{12}f_2 + \cdots + a_{1j}f_j + \cdots + a_{1n}f_n = P_1$$

$$H_2 = a_{21}f_1 + a_{22}f_2 + \cdots + a_{2j}f_j + \cdots + a_{2n}f_n = P_2$$

$$H_3 = a_{31}f_1 + a_{32}f_2 + \cdots + a_{3j}f_j + \cdots + a_{3n}f_n = P_3$$

.....

.....

$$H_i = a_{i1}f_1 + a_{i2}f_2 + \cdots + a_{ij}f_j + \cdots + a_{in}f_n = P_i \quad (4.3.1)$$

.....

.....

$$H_m = a_{m1}f_1 + a_{m2}f_2 + \cdots + a_{mj}f_j + \cdots + a_{mn}f_n = P_m$$

where i^{th} equation is hyper plane in \mathbb{R}^{n-1} , while $\mathbf{f} \in \mathbb{R}^n$.

In MSART, we start with an initial guess $\mathbf{f}^0 \in \mathbb{R}^n$, as in one iteration order is not mattering but in any order we can have these equations, so without loss of generality assume the same order, then the modification on first ray is

$$\mathbf{f}^{*(1)} = \mathbf{f}^0 + \frac{p_i - \sum_{j=1}^n a_{ij}f_j^{(0)}}{\sum a_{ij}^2} \mathbf{a}_1 \quad (4.3.2)$$

Or the modification for i^{th} ray is

$$\mathbf{f}^{*(1)} = \mathbf{f}^{*(0)} + \frac{p_i - \mathbf{a}^i \cdot \mathbf{f}^{*(0)}}{\mathbf{a}^i \cdot \mathbf{a}^i} \mathbf{a}^i \quad i = 1, 2, \dots, m \quad (4.3.3)$$

which is projection of \mathbf{f}^0 on H_1 in (4.3.2) then systematically we are taking successive projections of \mathbf{f}^0 on all hyper planes. Stating in other words, in one iteration we start with an arbitrary point $\mathbf{f}^0 \in \mathbb{R}^n$ and project it on hyper plane H_1 , the projection of \mathbf{f}^0 on H_1 say \mathbf{f}^{01} is then projected on H_2 and so on we get projection on H_M (say) \mathbf{f}^{0m} .

Thus we have combined m steps of ART into one iteration, and then we proceed further and modify the estimate of image in next iteration again.

Thus this method has expensive single iteration, but this does not slow down the convergence process as it modifies all entries within iteration, and projection on next hyper plane is with modified $\mathbf{f}^{*(k)}$.

In this if hyper plane are organized in pair wise orthogonal manner the convergence will be faster towards actual solution as reported by Ramkrishna et al (1985). Thus we get a better method. Pair wise orthogonal hyper plane will lead to faster convergence; this can be explained geometrically in \mathbb{R}^2 as follows: Let H_1 and H_2 are two orthogonal hyper planes such that H_1 is orthogonal to H_2

$$H_1 : \mathbf{a}^1 \cdot \mathbf{f} = p_1, \quad H_2 : \mathbf{a}^2 \cdot \mathbf{f} = p_2$$

which says, $\mathbf{a}^1 \cdot \mathbf{a}^2 = 0$ or $\mathbf{a}^1 \perp \mathbf{a}^2$ (being normal to planes). Then projection of \mathbf{f}^0 on H_1 (see Fig. 4.6) is a point on H_1 denoted by \mathbf{f}^{01} and vector $\mathbf{f}^0 - \mathbf{f}^{01}$ is in direction of \mathbf{a}^1 . Thus now projection of \mathbf{f}^{01} on H_2 will be in direction of \mathbf{a}^2 which is orthogonal to \mathbf{a}^1 , thus it will reach to point of intersection A. thus the solution is obtained in only two projections. Thus in this manner in one iteration only solution is obtained which gives accelerated convergence speed.

CHAPTER V: IMPLEMENTATION OF MODIFIED SIMULTANEOUS ALGEBRAIC RECONSTRUCTION TECHNIQUE

5.1 INTRODUCTION

In Chapter IV we introduced the Modified Simultaneous Algebraic Reconstruction Technique (MSART). The reconstruction of the image starts from the first iteration step itself and minimizes the noise. Further the algorithm developed for this technique seems to be faster than the algorithms developed in other techniques. Heuristically it is shown in last chapter that it will converge to actual solution in few iterations steps because number of rays in projection data (m) are combined in a single iteration while for simple ART one has to perform m iterations for m number of rays in the projection data. In case of simple ART, every iteration calculation of projection data requires storage space with extra calculations, while in this modified method, where we are combining the iterations, the extra large storage space is not required. Moreover we are modifying the projection data for each ray simultaneously, thus making the convergence faster with no storage space required to store the projection data for every iteration. So far these properties specially the convergence have been shown heuristically, and not proved computationally. In this chapter, the algorithm is implemented on some images for which discretized data were available and the convergence with respect to errors based on discrepancy measures mentioned in chapter IV are shown (section 4.2).

The test patterns for which the images were reconstructed are shown in subsection 5.2.1. The calculated projection data of these patterns are shown in subsection 5.2.2. The formulas used for determining discrepancy measure between the projections and

discrepancy in consecutive estimation of image are given in subsection 5.2.3. Two MSART algorithms developed for the image reconstructions of the test patterns which include the errors considered for stopping rule and for convergence are reported in section 5.3. Finally the computationally output and the results are reported in section 5.4.

5.2 TEST OBJECTS

5.2.1 TEST IMAGES

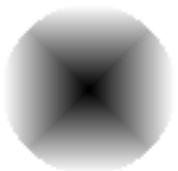
For the purpose of computational implementation of the developed algorithm for the MSART, four test image patterns have been considered. The first test image named PIC1 is Chromosomes, Gonzalez (1977), second test image named here as PIC2 is Saturn, third test image named here as PIC3 is Smooth and PIC4 is Thorax. The images are 64X64 digitized models. All these test images are shown in Figure 5.2.1.



PIC1: Chromosomes



PIC2: Saturn



PIC3: Smooth



PIC4: Thorax

Figure 5.2.1: Digitized test images are 64X64 digitized images.

5.2.2. PROJECTION DATA

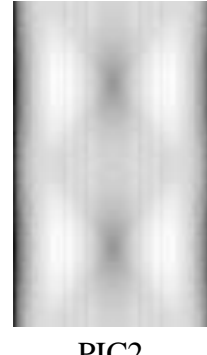
The projection data for the above mentioned test images have been calculated as line integral on unit circle. The expression for determining the line integrals for each line (s, θ) is

$$p(s, \theta) = \int_{-L}^L f(s \cos \theta - t \sin \theta, s \sin \theta + t \cos \theta) dt$$

This integral is numerically calculated using Simpson's method. For image PIC1 to PIC4 the size of projection data is 100X64 that is 100 views (θ) and 64 lines (s) for each view. The digitized images of the calculated projection data are shown in Figure 5.2.2.



PIC1



PIC2



PIC3



PIC4

Figure 5.2.2: 100X64 digitized image of projection data for test image PIC1-PIC4.

5.2.3 ERRORS

There are two types of errors which occur in the image reconstructions one is Discrepancy Measure between the Projections and another is Discrepancy in Consecutive Estimation of image. The Discrepancy Measure between the Projections means the difference between the two consecutive calculated projection values while the Discrepancy in Consecutive Estimation of image means the difference between the two consecutive calculated pixel values of the image. The expressions used respectively for determining the discrepancy measure between projections and the discrepancy in consecutive estimation of the image are as follows:

Discrepancy Measure between the Projections

$$EP1 = \sum_{i=1}^m |p_i - p_i^k|$$

$$EP2 = \left(\sum_{i=1}^m (p_i - p_i^k)^2 \right)^{1/2}$$

Where, $p_i^k = i^{th}$ ray sum of k^{th} iteration estimate

$$\Rightarrow p_i^k = \sum_{j=1}^n a_{ij} f_j^{(k)}, \quad i = 1, 2, \dots, m$$

and p_i = the original i^{th} ray projection data

Discrepancy in Consecutive Estimation of image

$$EF1 = \sum_{j=1}^n |f_j^{(k+1)} - f_j^{(k)}|$$

$$EF2 = \left(\sum_{j=1}^n (f_j^{(k+1)} - f_j^{(k)})^2 \right)^{1/2}$$

5.3 MSART ALGORITHM

The two schemes of the algorithms developed for the MSART described in chapter IV have been presented here in this section. In the first scheme (Algorithm 5.1) the number of iterations are predefined and the stopping rule is based on iterations. In the second scheme (Algorithm 5.2) stopping rule has been taken on the basic of errors in projection and image estimates as described in sub section 5.3.2.

Algorithm 5.1

1. Begin
2. Get the projection data with m
3. Prefix number of iteration (NIT)
4. Start with iteration (k)=0
5. Get initial Guess with c as constant, $\mathbf{f}^0 = (c, \dots, c)^T$,
6. i=0
7. $f_j^{1(k+1)} = f_j^{*(k)} + a_{ij} \frac{p_i - \sum_{j=1}^n a_{ij} f_j^{*(k)}}{\sum_{j=1}^n a_{ij}^2}$
8. $f_j^{(k+1)} = \max \{0, f_j^{1(k+1)}\}, \quad \forall j \exists a_{ij} \neq 0$

9. $i=i+1$, check ($i < m$) if yes repeat step 7, 8
10. Else $k=K+1$, check ($k < NIT$) If yes repeat steps 6 to 9
11. Else stop
12. END

Algorithm 5.2

1. Begin
2. Get the projection data with m
3. Get stopping criterion as ϵ
4. Start with iteration ($k=0$)
5. Get initial Guess with c as constant, $\mathbf{f}^0 = (c, \dots, c)$,
6. $i=0$

$$7. \quad f_j^{1(k+1)} = f_j^{*(k)} + a_{ij} \frac{p_i - \sum_{j=1}^n a_{ij} f_j^{*(k)}}{\sum_{j=1}^n a_{ij}^2}$$

$$8. \quad f_j^{(k+1)} = \max \left\{ 0, f_j^{1(k+1)} \right\}, \quad \forall j \ni a_{ij} \neq 0$$

9. $i=i+1$, check ($i < m$) if yes repeat step 7, 8

10. Else $k=K+1$,

11. Calculate

$$EP2 = \left(\sum_{i=1}^m (p_i - p_i^k)^2 \right)^{1/2}$$

or

$$EF2 = \left[\sum_{j=1}^n (f_j^{(k)} - f_j^t)^2 \right]^{1/2}$$

12. Check ($EP_2 > e$) or ($EF_2 > e$) If yes repeat steps 6 to 11

13. Else stop

14. END

5.4 RESULTS OF NUMERICAL IMPLEMENTATION

The implementation of the two algorithms 5.1 and 5.2 given in section 5.3 has been carried on test image patterns shown in section 5.2.1 with projection data given in section 5.2.2. The results at different iteration steps and convergence table for discrepancy measure between projections (EP_1 and EP_2) and discrepancy measure between successive reconstructions (EF_1 and EF_2) of the test pattern images for the two algorithms are reported here in this section.

PIC1: Reconstruction results at different iterations is shown in figure 5.4.1 and convergence table for the discrepancy measures between projections EP_1 and EP_2 are given in table 5.4.2, and for the discrepancy measures between successive reconstruction of test image EF_1 and EF_2 are given in table 5.4.3.

PIC2: Reconstruction results at different iterations is shown in figure 5.4.4 and convergence table for the discrepancy measures between projections EP_1 and EP_2 are given in table 5.4.5, and for the discrepancy measures between successive reconstruction of test image EF_1 and EF_2 are given in table 5.4.6.

PIC3: Reconstruction results at different iterations is shown in figure 5.4.7 and convergence table for the discrepancy measures between projections EP_1 and EP_2 are given in table 5.4.8, and for the discrepancy measures between successive reconstruction of test image EF_1 and EF_2 are given in table 5.4.9.

PIC4: Reconstruction results at different iterations is shown in figure 5.4.10 and convergence table for the discrepancy measures between projections EP1 and EP2 are given in table 5.4.11, and for the discrepancy measures between successive reconstruction of test image EF1 and EF2 are given in table 5.4.12.

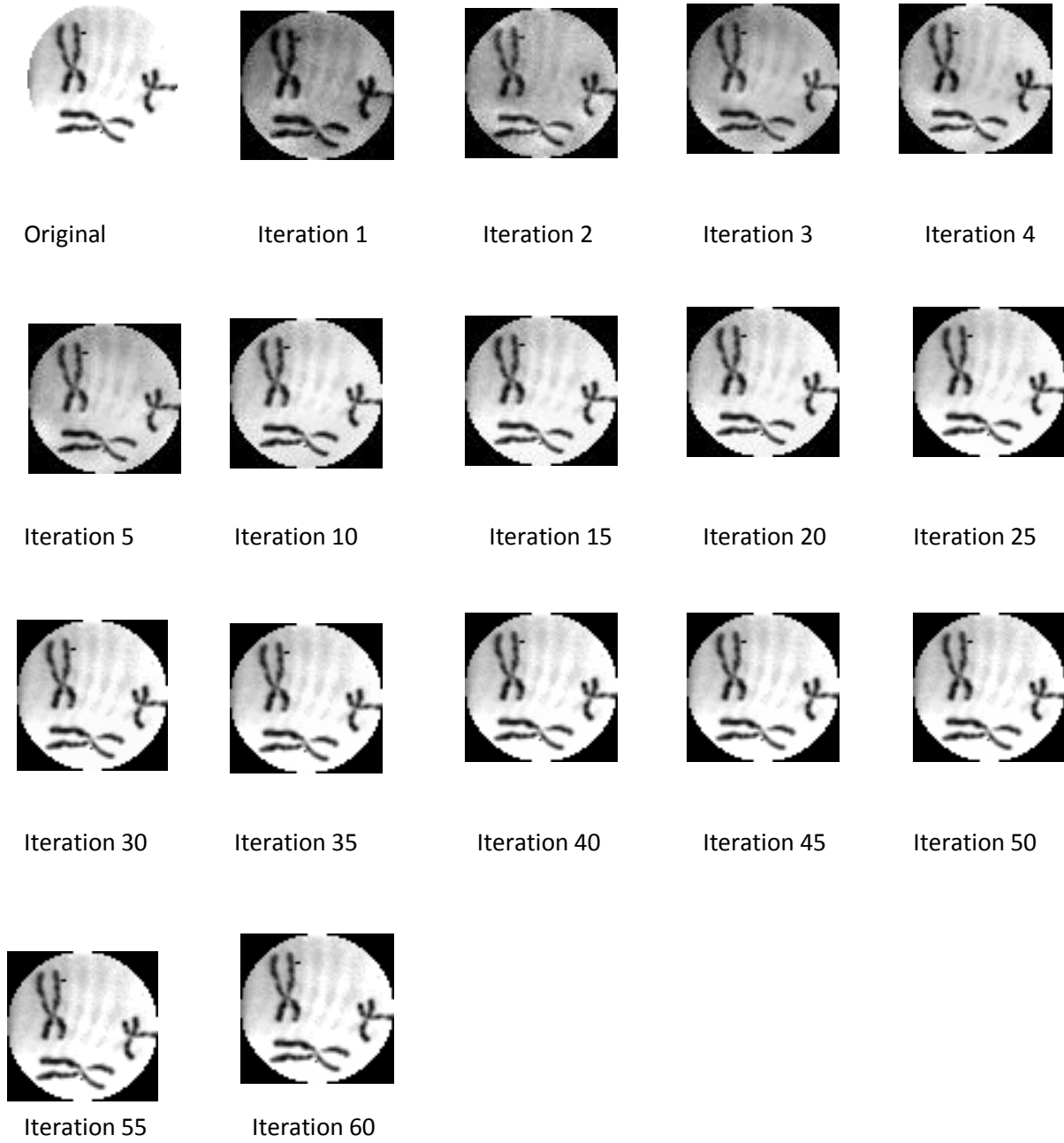


Figure 5.4.1 Reconstruction of PIC1 at different iterations

Iteration	EP1	EP2
0	53.196	67.3669
1	43.1115	55.4668
2	36.879	48.2259
3	32.449	42.886
4	28.91	38.5274
5	26.9159	34.5353
6	24.9413	30.8511
7	22.4283	27.7436
8	19.4887	25.0868
9	16.965	22.708
10	15.1023	20.5217
11	13.9283	18.5119
12	12.9636	16.7403
13	11.8174	15.1144
14	10.5534	13.7145
15	9.33713	12.4737
16	8.51624	11.3895
17	7.92575	10.3951
18	7.45858	9.48666
19	6.90801	8.7025
20	6.27047	8.02701
21	5.71457	7.46724
22	5.33701	6.95304
23	5.09651	6.48393
24	4.84586	6.04023
25	4.54899	5.62789
26	4.22622	5.25198
27	3.93288	4.90712
28	3.69875	4.59964
29	3.49369	4.31122
30	3.30243	4.04393

Table 5.4.2: Convergence with projection data in PIC1

Iteration	EP1	EP2
31	3.10229	3.79034
32	2.89788	3.55203
33	2.70057	3.33061
34	2.52318	3.12244
35	2.36965	2.92904
36	2.23369	2.74814
37	2.10045	2.57953
38	1.97066	2.42363
39	1.84463	2.27717
40	1.73017	2.14082
41	1.62735	2.01147
42	1.53417	1.89003
43	1.44538	1.77588
44	1.35985	1.66918
45	1.27838	1.57041
46	1.20246	1.47786
47	1.13278	1.39157
48	1.06798	1.30987
49	1.00649	1.23275
50	0.947976	1.16016
51	0.891903	1.09164
52	0.839649	1.02777
53	0.790533	0.967496
54	0.745092	0.911227
55	0.701915	0.858028
56	0.66121	0.808042
57	0.622416	0.760891
58	0.585972	0.716439
59	0.551754	0.67462

Table 5.4.2(contd): Convergence with projection data in PIC1

Iteration	EF1	EF2
0	16.4988	20.1765
1	3.63744	5.35146
2	2.85782	4.12235
3	2.40685	3.39949
4	2.08071	2.90069
5	1.80304	2.51624
6	1.52958	2.20123
7	1.34761	1.93817
8	1.21679	1.71799
9	1.09387	1.536
10	0.98149	1.38174
11	0.880131	1.24644
12	0.783837	1.12348
13	0.677509	1.01116
14	0.59348	0.910194
15	0.543827	0.822007
16	0.504645	0.744513
17	0.462289	0.675489
18	0.414369	0.61241
19	0.361715	0.555227
20	0.328393	0.504515
21	0.309035	0.460579
22	0.288196	0.422725
23	0.269161	0.389165
24	0.245893	0.358782
25	0.224426	0.330962
26	0.211809	0.305962
27	0.202318	0.283827
28	0.192484	0.264152
29	0.179937	0.246353

Table 5.4.3: Convergence in consecutive estimates in PIC1

Iteration	EF1	EF2
30	0.164462	0.229859
31	0.149207	0.214532
32	0.140754	0.200319
33	0.13568	0.187303
34	0.129509	0.175389
35	0.121691	0.164366
36	0.112563	0.154062
37	0.103401	0.14434
38	0.0963788	0.135238
39	0.0919199	0.12677
40	0.0877562	0.118917
41	0.0829085	0.111617
42	0.0774739	0.104768
43	0.0719842	0.098347
44	0.0672492	0.0923161
45	0.0635266	0.0866924
46	0.0602778	0.0814535
47	0.0569689	0.0765677
48	0.0535597	0.0719984
49	0.0501791	0.0677008
50	0.0471105	0.0636675
51	0.0444051	0.0598799
52	0.0419411	0.0563322
53	0.0395528	0.0530073
54	0.0371968	0.0498825
55	0.0349546	0.0469475
56	0.0328701	0.0441836
57	0.0309907	0.0415881
58	0.0292435	0.0391486
59	0.0275623	0.0368571

Table 5.4.3(contd.): Convergence in consecutive estimates in PIC1

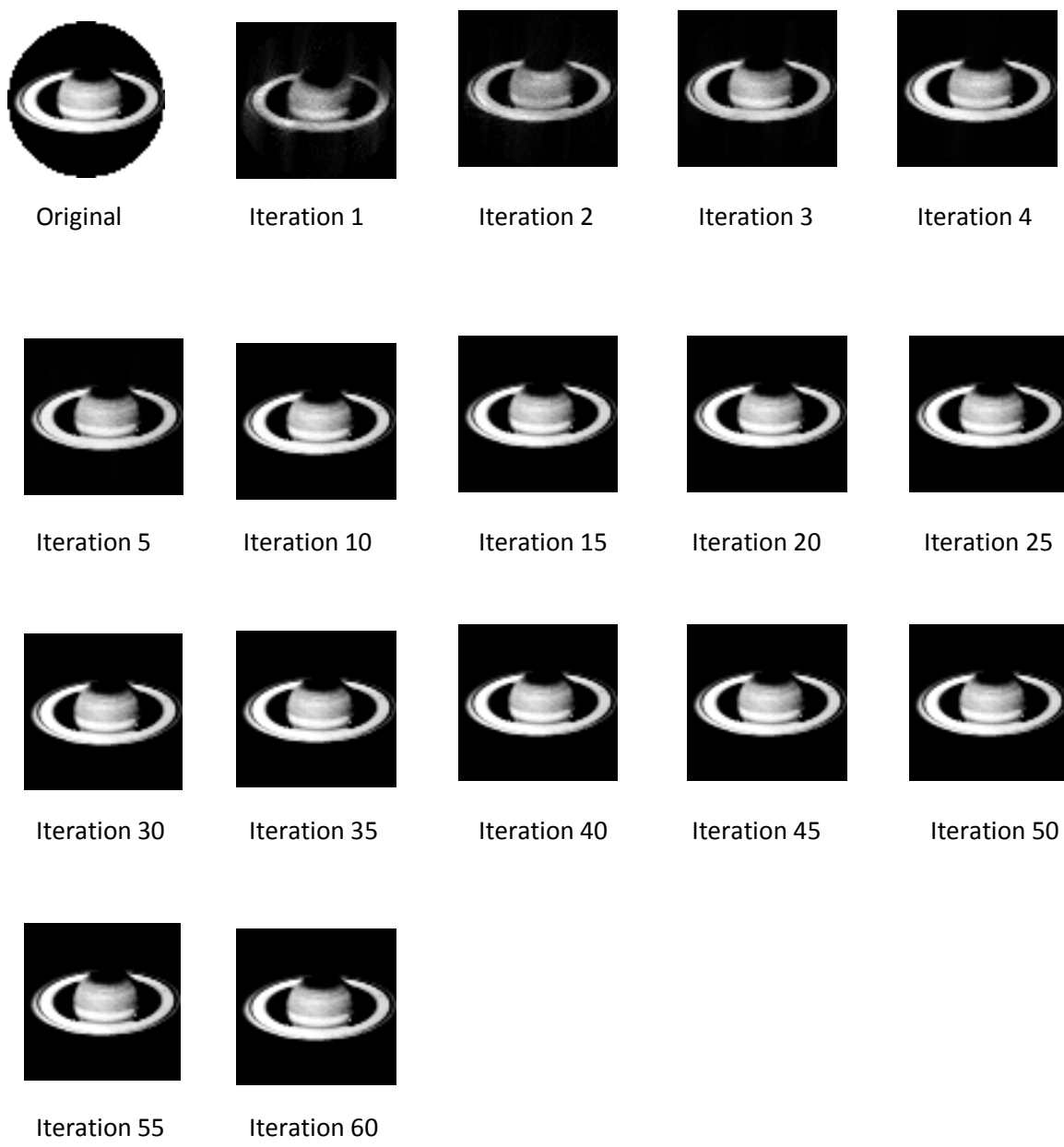


Figure 5.4.4 Reconstruction of PIC2 at different iterations

Iteration	EP1	EP2
0	43.9125	59.0426
1	21.0601	29.7678
2	12.0144	16.4641
3	7.03292	9.87284
4	4.15056	5.76799
5	2.54759	3.5074
6	1.49086	2.09876
7	0.940231	1.30463
8	0.5699	0.822116
9	0.382508	0.534638
10	0.249777	0.360786
11	0.184643	0.253568
12	0.132249	0.186374
13	0.106972	0.14388
14	0.0833112	0.114204
15	0.0707222	0.0941535
16	0.0579411	0.0782178
17	0.04994	0.0665725
18	0.042172	0.0566718
19	0.0365174	0.0488971
20	0.0314083	0.0422164
21	0.0273442	0.0367379
22	0.0237922	0.0320221
23	0.0208314	0.0280494
24	0.018264	0.0246163
25	0.0160712	0.0216764
26	0.0141723	0.0191262
27	0.0125309	0.0169222
28	0.0111014	0.0149994
29	0.00985685	0.0133256

Table 5.4.5: Convergence with projection data in PIC2

Iteration	EP1	EP2
30	0.00876886	0.0118557
31	0.00780999	0.0105619
32	0.00697469	0.00943534
33	0.00623329	0.00843053
34	0.00557893	0.00754728
35	0.00499867	0.00676372
36	0.00448461	0.00606801
37	0.00404086	0.00546724
38	0.00363925	0.00492484
39	0.00328052	0.0044399
40	0.00296222	0.00400684
41	0.00267763	0.00362301
42	0.00241937	0.00327155
43	0.00218986	0.00296015
44	0.00198671	0.00268498
45	0.00180215	0.00243642
46	0.0016292	0.00220332
47	0.00148579	0.00200825
48	0.00134776	0.00181958
49	0.00123562	0.0016686
50	0.00112654	0.00152165
51	0.00102652	0.00138891
52	0.000936995	0.00126615
53	0.00085471	0.00115514
54	0.000784989	0.00106095
55	0.00071721	0.000969818
56	0.00065675	0.000887002
57	0.000593439	0.000801125
58	0.000549914	0.000741922
59	0.000506175	0.00068475

Table 5.4.5(contd): Convergence with projection data in PIC2

Iteration	EF1	EF2
0	5.75331	9.47434
1	2.05256	4.12229
2	1.07184	2.03827
3	0.602953	1.16185
4	0.348423	0.678427
5	0.197765	0.402597
6	0.116967	0.243449
7	0.0666715	0.146493
8	0.0397795	0.0900761
9	0.0236605	0.055464
10	0.0146121	0.0348321
11	0.00906307	0.0219422
12	0.00585506	0.0140709
13	0.00380199	0.00916936
14	0.00255118	0.00616489
15	0.00176236	0.00430666
16	0.00128093	0.00315864
17	0.000941797	0.00242262
18	0.000745802	0.00193767
19	0.000584982	0.00159048
20	0.000485494	0.0013344
21	0.00039955	0.00113225
22	0.000336577	0.000970581
23	0.000283481	0.00083668
24	0.000241295	0.000725269
25	0.000206021	0.000631143
26	0.000177328	0.000551379
27	0.000152711	0.000482992
28	0.00013226	0.000424253
29	0.000114814	0.000373696

Table 5.4.6: Convergence in consecutive estimates in PIC2

Iteration	EF1	EF2
30	0.000100002	0.000329782
31	0.000087508	0.000291751
32	0.000076558	0.000258502
33	0.000067367	0.000229583
34	0.000059397	0.000204237
35	0.000052567	0.000182008
36	0.000046460	0.000162372
37	0.000041091	0.000145061
38	0.000036551	0.000129876
39	0.000032690	0.00011652
40	0.000029100	0.000104572
41	0.000025991	0.000093975
42	0.000023306	0.000084533
43	0.000020963	0.000076263
44	0.000018768	0.000068808
45	0.000016853	0.000062094
46	0.000015400	0.000056242
47	0.000013693	0.000050895
48	0.000012574	0.000046189
49	0.000011192	0.000041831
50	0.000010254	0.000038081
51	0.000009406	0.000034640
52	0.000008509	0.000031493
53	0.000007847	0.000028623
54	0.000007030	0.000026094
55	0.000006457	0.000023763
56	0.000005980	0.000021774
57	0.000005507	0.000019851
58	0.000004929	0.000018137
59	0.000004661	0.000016617

Table 5.4.6(contd.): Convergence in consecutive estimates in PIC2

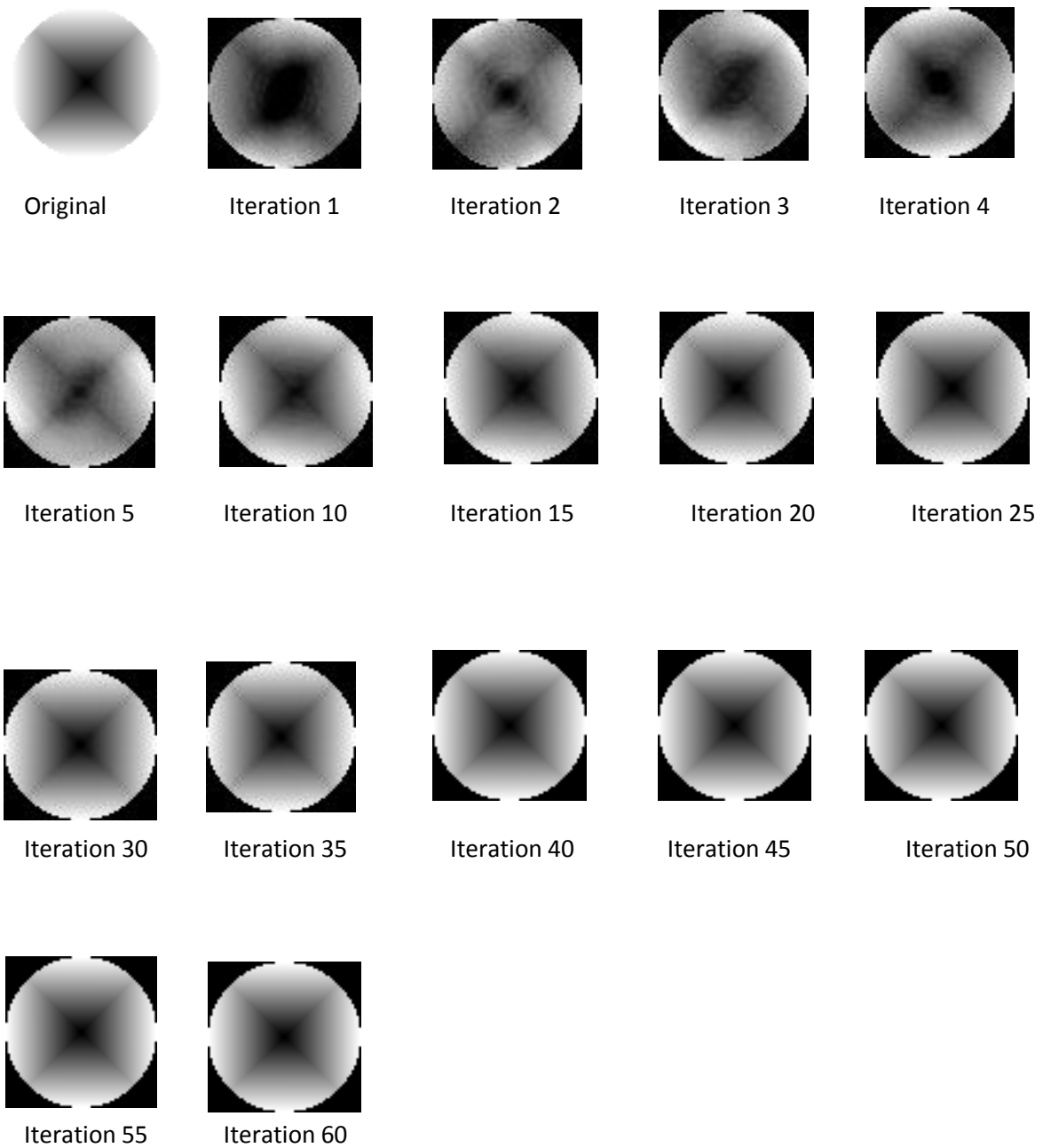


Figure 5.4.7 Reconstruction of PIC3 at different iterations

Iteration	EP1	EP2
0	89.546	112.465
1	80.9621	99.6894
2	75.1799	89.2195
3	66.0525	80.3833
4	54.9855	71.8462
5	47.3032	63.2845
6	41.5292	56.5343
7	36.351	50.1408
8	34.8041	44.6224
9	31.3333	38.8785
10	26.6101	34.0409
11	22.6817	30.1677
12	20.3612	26.9491
13	17.7096	24.157
14	16.647	21.3584
15	15.3784	19.0177
16	13.2306	16.9865
17	11.0601	15.1885
18	9.99061	13.6201
19	8.68749	12.1742
20	8.18641	10.9054
21	7.76123	9.69125
22	6.82631	8.55275
23	5.76396	7.58065
24	5.08301	6.76175
25	4.51637	6.07374
26	4.03445	5.40823
27	3.81763	4.78947
28	3.41546	4.24898
29	2.85661	3.78156

Table 5.4.8: Convergence with projection data in PIC3

Iteration	EP1	EP2
30	2.48519	3.39146
31	2.22862	3.03017
32	1.97375	2.71407
33	1.89409	2.41824
34	1.72648	2.14467
35	1.46671	1.90419
36	1.25024	1.69521
37	1.1333	1.52448
38	0.983709	1.36379
39	0.935278	1.21522
40	0.869234	1.07798
41	0.746614	0.957397
42	0.631311	0.857558
43	0.569915	0.767655
44	0.498738	0.68986
45	0.468134	0.615286
46	0.440361	0.546918
47	0.385491	0.485712
48	0.322921	0.431817
49	0.287785	0.387413
50	0.252984	0.346467
51	0.230109	0.309805
52	0.219254	0.274937
53	0.194943	0.243492
54	0.163745	0.216863
55	0.142621	0.193577
56	0.128416	0.174095
57	0.114187	0.155366
58	0.108995	0.138333
59	0.098855	0.122748

Table 5.4.8(contd): Convergence with projection data in PIC3

Iteration	EF1	EF2
0	11.3336	15.2706
1	5.00806	7.45474
2	4.50447	6.60098
3	4.0412	5.84101
4	3.75954	5.16217
5	3.4508	4.57687
6	3.08722	4.07226
7	2.70021	3.627
8	2.30451	3.20525
9	1.9713	2.82817
10	1.69516	2.48313
11	1.49685	2.18736
12	1.33785	1.9357
13	1.17801	1.7249
14	1.07041	1.53666
15	0.958649	1.36019
16	0.854556	1.20134
17	0.776855	1.06395
18	0.699137	0.94949
19	0.618168	0.851761
20	0.553795	0.762489
21	0.494376	0.679783
22	0.428542	0.603542
23	0.377063	0.53616
24	0.341861	0.478295
25	0.307269	0.428499
26	0.276112	0.384337
27	0.244991	0.342955
28	0.211384	0.30431
29	0.187926	0.269613

Table 5.4.9: Convergence in consecutive estimates in PIC3

Iteration	EF1	EF2
30	0.171964	0.239929
31	0.15455	0.214819
32	0.13683	0.19242
33	0.122888	0.171732
34	0.10748	0.152355
35	0.0946923	0.134929
36	0.0854257	0.119914
37	0.0770948	0.107171
38	0.0689348	0.0961353
39	0.062053	0.085975
40	0.0544795	0.0764994
41	0.0476694	0.0678245
42	0.0429606	0.0602781
43	0.0387542	0.0539108
44	0.0344764	0.0483927
45	0.0311454	0.0433938
46	0.0277572	0.0386694
47	0.0242545	0.0343203
48	0.0216707	0.0304835
49	0.019638	0.0272138
50	0.0175641	0.024417
51	0.0157525	0.0218823
52	0.0140346	0.0195235
53	0.012171	0.0173237
54	0.0107831	0.0153626
55	0.00978111	0.0136858
56	0.0087777	0.0122556
57	0.00783951	0.010995
58	0.007044	0.00981526
59	0.00615031	0.00871601

Table 5.4.9(contd.): Convergence in consecutive estimates in PIC3

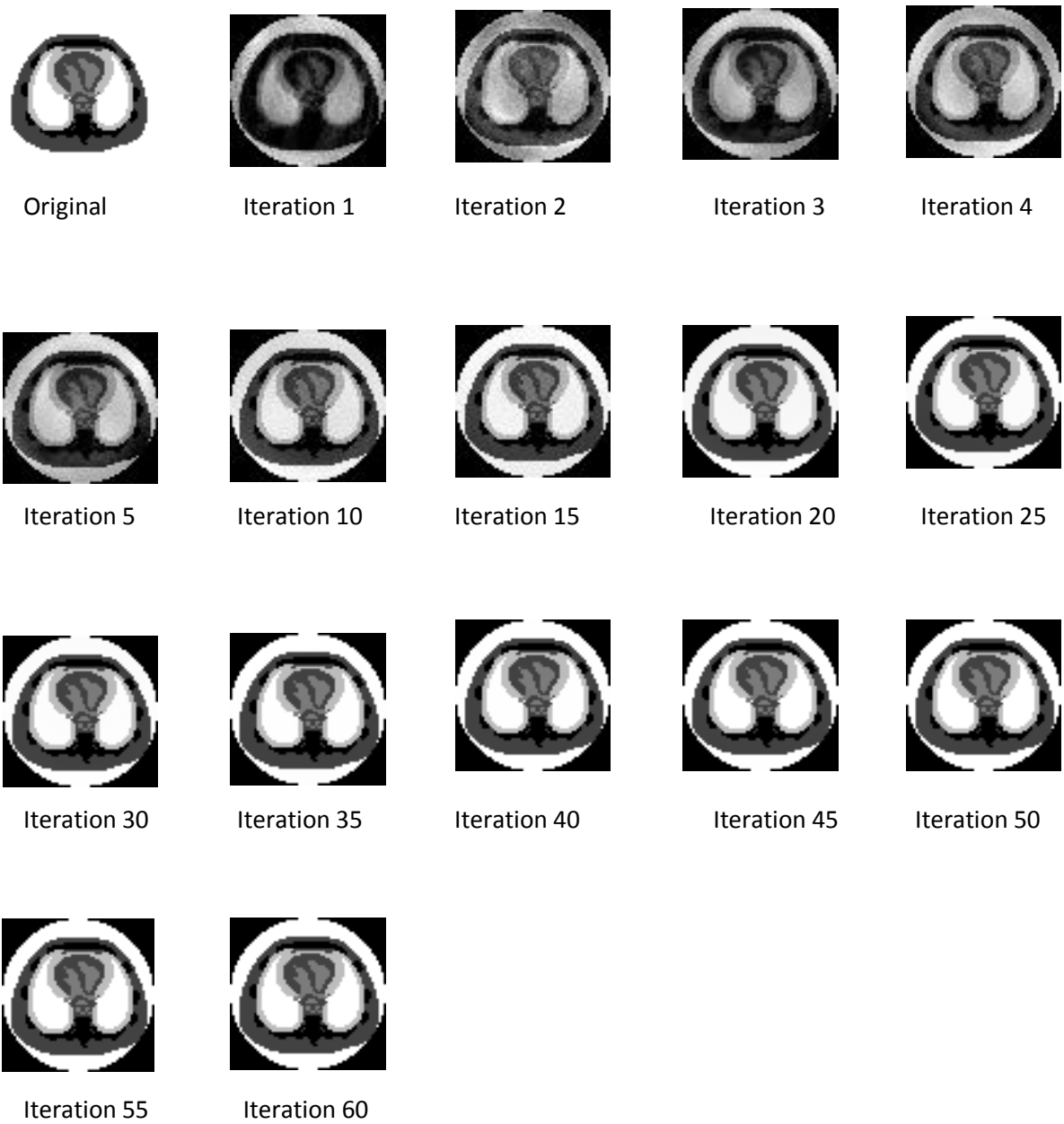


Figure 5.4.10 Reconstruction of PIC4 at different iterations

Iteration	EP1	EP2
0	80.1978	108.602
1	63.472	87.1056
2	49.6635	69.0656
3	42.6977	58.5293
4	36.0484	48.4947
5	31.2197	41.6876
6	26.8743	35.9542
7	23.053	30.9644
8	20.4774	27.3401
9	17.4734	22.9721
10	15.6531	20.4618
11	13.1208	17.4134
12	11.8322	15.7121
13	10.2481	13.7267
14	9.32895	12.3459
15	8.28639	10.7904
16	7.33969	9.58059
17	6.39805	8.40503
18	5.6327	7.52571
19	4.97807	6.63842
20	4.46913	5.99793
21	3.9793	5.29143
22	3.58885	4.80033
23	3.17935	4.2607
24	2.84983	3.85859
25	2.55139	3.44017
26	2.30535	3.10162
27	2.07401	2.76216
28	1.86132	2.4865
29	1.65847	2.21205

Table 5.4.11: Convergence with projection data in PIC4

Iteration	EP1	EP2
30	1.48711	1.99853
31	1.32292	1.77603
32	1.1982	1.60994
33	1.0689	1.4304
34	0.969095	1.29783
35	0.864163	1.15473
36	0.782695	1.04702
37	0.700054	0.932673
38	0.634201	0.844323
39	0.567283	0.751886
40	0.512134	0.679934
41	0.457116	0.605097
42	0.41202	0.54732
43	0.367447	0.486818
44	0.331686	0.440655
45	0.295864	0.39191
46	0.267376	0.354854
47	0.238568	0.315702
48	0.21562	0.285743
49	0.192432	0.254283
50	0.173843	0.230034
51	0.155107	0.204686
52	0.139996	0.185097
53	0.124811	0.164653
54	0.112626	0.148911
55	0.100368	0.132441
56	0.0906315	0.119831
57	0.0807627	0.106567
58	0.072958	0.0964286
59	0.0650164	0.0857579

Table 5.4.11(contd): Convergence with projection data in PIC4

Iteration	EF1	EF2
0	12.6175	18.6563
1	6.22376	8.94651
2	4.65964	6.86046
3	3.65819	5.46216
4	2.88243	4.41128
5	2.32665	3.60068
6	1.93434	2.974
7	1.62699	2.48417
8	1.38277	2.09427
9	1.16924	1.77412
10	0.994531	1.51244
11	0.8679	1.30225
12	0.755921	1.13362
13	0.656456	0.993114
14	0.576877	0.874255
15	0.50545	0.767722
16	0.436726	0.674186
17	0.379155	0.592251
18	0.332484	0.523109
19	0.292655	0.463502
20	0.256328	0.411879
21	0.223288	0.366719
22	0.196803	0.326685
23	0.178203	0.292064
24	0.162578	0.261314
25	0.147139	0.234165
26	0.131446	0.209817
27	0.116618	0.187815
28	0.103678	0.168021
29	0.0928248	0.150231

Table 5.4.12: Convergence in consecutive estimates in PIC4

Iteration	EF1	EF2
30	0.0835121	0.134418
31	0.0748719	0.120334
32	0.0669314	0.107788
33	0.0598939	0.096646
34	0.0537639	0.0866555
35	0.0485311	0.0777813
36	0.043759	0.0698074
37	0.0394531	0.0626745
38	0.0354033	0.0562526
39	0.0317662	0.0504717
40	0.0284473	0.0452705
41	0.0255324	0.0405949
42	0.0228979	0.0364013
43	0.0205492	0.0326452
44	0.0184225	0.029277
45	0.0165401	0.0262663
46	0.014844	0.0235617
47	0.0133427	0.0211444
48	0.0119812	0.0189705
49	0.0107642	0.0170236
50	0.00965468	0.0152726
51	0.00866449	0.0137015
52	0.00776488	0.0122892
53	0.00696701	0.0110226
54	0.00624475	0.00988535
55	0.00560408	0.00886652
56	0.00502448	0.00795195
57	0.00451006	0.00713346
58	0.00404521	0.0063983
59	0.00363187	0.00574006

Table 5.4.12(contd.): Convergence in consecutive estimates in PIC4

CHAPTER VI: DISCUSSION AND COMPARISON

6.1 INTRODUCTION

The Modified Simultaneous Algebraic Reconstruction Technique (MSART) was described in chapter IV, which has been implemented on certain test images in chapter V. In both chapters the quality of reconstruction and the speed of convergence have been shown. In chapter IV suitability of proposed method and its fast convergence have been shown with geometrical method and proved heuristically. In chapter V the algorithm proposed in chapter IV has been implemented computationally on four test images with projection data calculated numerically using computer. In this implementation the noise factor other than the numerical approximations has not been considered. In present chapter we will compare our computed results with the computed results of another algorithm Convolution Back Projection (CBP). The CBP algorithm is probably the most widely used for image reconstructions, as it is claimed to be fast, efficient, reasonably accurate, and easy to implement on computer. The section 6.2 provides the comparison of MSART with CBP with respect to both in terms of error (explained in sub section 6.2.1) and pictorial quality of reconstruction (explained in sub section 6.2.2). The results in terms of convergence using 46 projections for four views (horizontal, vertical, diagonal and anti diagonal) have been discussed in section 6.3 and the image is shown pictorially as well as using the line graph.

6.2 COMPARISON WITH CBP

For the purpose of comparison of MSART with CBP again we have the same four test images of chapter V section 5.2.1, the first test image named PIC1 is Chromosomes, Gonzalez (1977), second test image named here as PIC2 is Saturn, third one named PIC3 is Smooth and PIC4 is Thorax. The images are 64X64 digitized models. All these test images were shown in Figure 5.2.1 and their digitized projection data is shown in Figure 5.2.2.

6.2.1 ERROR ANALYSIS

The error considered for error analysis, L_1 and L_2 errors in reconstruction at different iterations and original test image. They are represented as EL1 and EL2 in result tables.

With $\mathbf{f}^{(k)} = (f_1^{(k)} \dots f_N^{(k)})'$ as k^{th} iteration estimate and $\mathbf{f}^{(k)} = (f_1^t \dots f_n^t)'$ as test image EL1 and EL2 are defined as

$$EL1 = \sum_{j=1}^n |f_j^{(k)} - f_i^t|$$

$$EL2 = \left[\sum_{j=1}^n (f_j^{(k)} - f_i^t)^2 \right]^{1/2}$$

The results are shown in table 6.1 to 6.4 for four test images PIC1 to PIC4 respectively.

Iteration	EL1	EL2
1	2.33103	3.49939
2	1.72138	2.51695
3	1.38785	1.99987
4	1.17987	1.67072
5	1.02291	1.42924
10	0.536603	0.756416
15	0.295645	0.446155
20	0.177427	0.27176
25	0.120526	0.176148
30	0.0872606	0.121181
35	0.0636797	0.0861953
40	0.0456586	0.0621995
45	0.0331949	0.0452698
50	0.0247011	0.0331949
55	0.0182843	0.0244628
60	0.0135654	0.0180711
CBP	1.25507	2.26749

Table 6.1: L₁ and L₂ errors for PIC1

Iteration	EL1	EL2
1	1.89727	3.76061
2	0.950297	1.69564
3	0.513121	0.95153
4	0.306638	0.567384
5	0.183577	0.346144
10	0.0249847	0.0571719
15	0.00759808	0.0210928
20	0.00329164	0.0102237
25	0.0016279	0.00547476
30	0.000877343	0.00309795
35	0.000500838	0.0018232
40	0.000297853	0.00110607
45	0.000183013	0.000686689
50	0.000115485	0.000433508
55	0.000073867	0.000276651
60	0.000047717	0.000177862
CBP	0.779714	1.38142

Table 6.2: L₁ and L₂ errors for PIC2

Iteration	EL1	EL2
1	2.7179	4.16445
2	2.45911	3.65291
3	2.20667	3.23095
4	2.01804	2.8447
5	1.88046	2.52515
10	0.938714	1.37091
15	0.525048	0.748465
20	0.30198	0.417207
25	0.167623	0.234078
30	0.0931359	0.131414
35	0.0523618	0.0742481
40	0.0303076	0.0421568
45	0.0169128	0.0239176
50	0.00966192	0.0135113
55	0.00538702	0.00764664
60	0.00311699	0.00436965
CBP	0.954538	2.03294

Table 6.3: L₁ and L₂ errors for PIC3

Iteration	EL1	EL2
1	3.95019	5.64227
2	2.83461	4.13309
3	2.22463	3.24428
4	1.73911	2.60017
5	1.41841	2.12046
10	0.600805	0.883162
15	0.296723	0.437528
20	0.153604	0.23248
25	0.0874064	0.13157
30	0.0501334	0.075642
35	0.0290743	0.0439299
40	0.0171987	0.0257098
45	0.0100348	0.0150765
50	0.00594936	0.00886423
55	0.0034847	0.00523985
60	0.00207362	0.00310904
CBP	1.83189	3.04238

Table 6.4: L₁ and L₂ errors for PIC4

6.2.2 PICTORIAL QUALITY OF RECONSTRUCTION

In this section the digitized images of reconstruction at various iteration with reconstruction by convolution back projection algorithm are compared the results are shown in figures 6.1 to 6.4 for four test images PIC1 to PIC4 respectively.

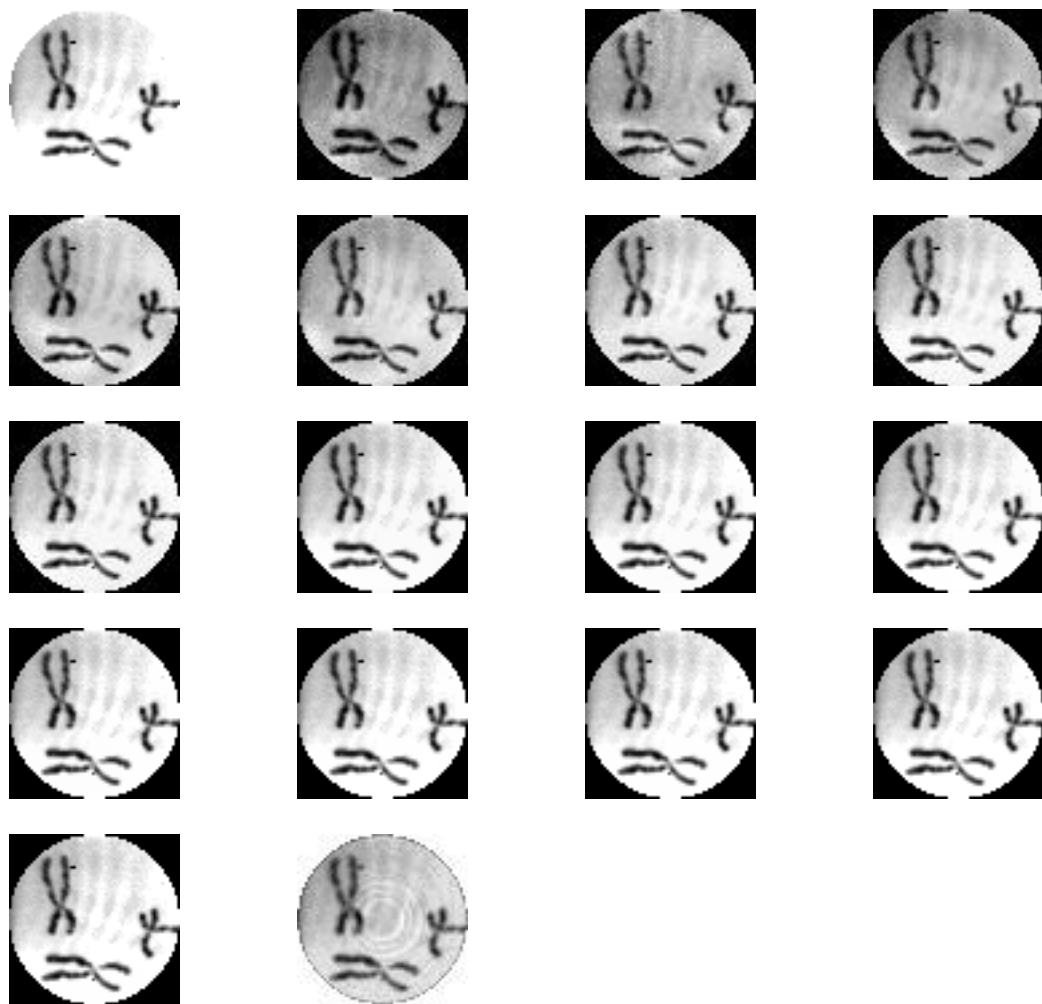


Figure 6.1: Comparison of reconstruction with CBP for PIC1

From Left to Right: Row1—Original image, Reconstruction by SMART in iteration 1, 2, 3 Row2—iteration 4, 5, 10, 15, Row3 – iteration 20, 25, 30, 35, Row4- 40, 45, 50, 55 Row5—iteration 60 and last image reconstructed by CBP.

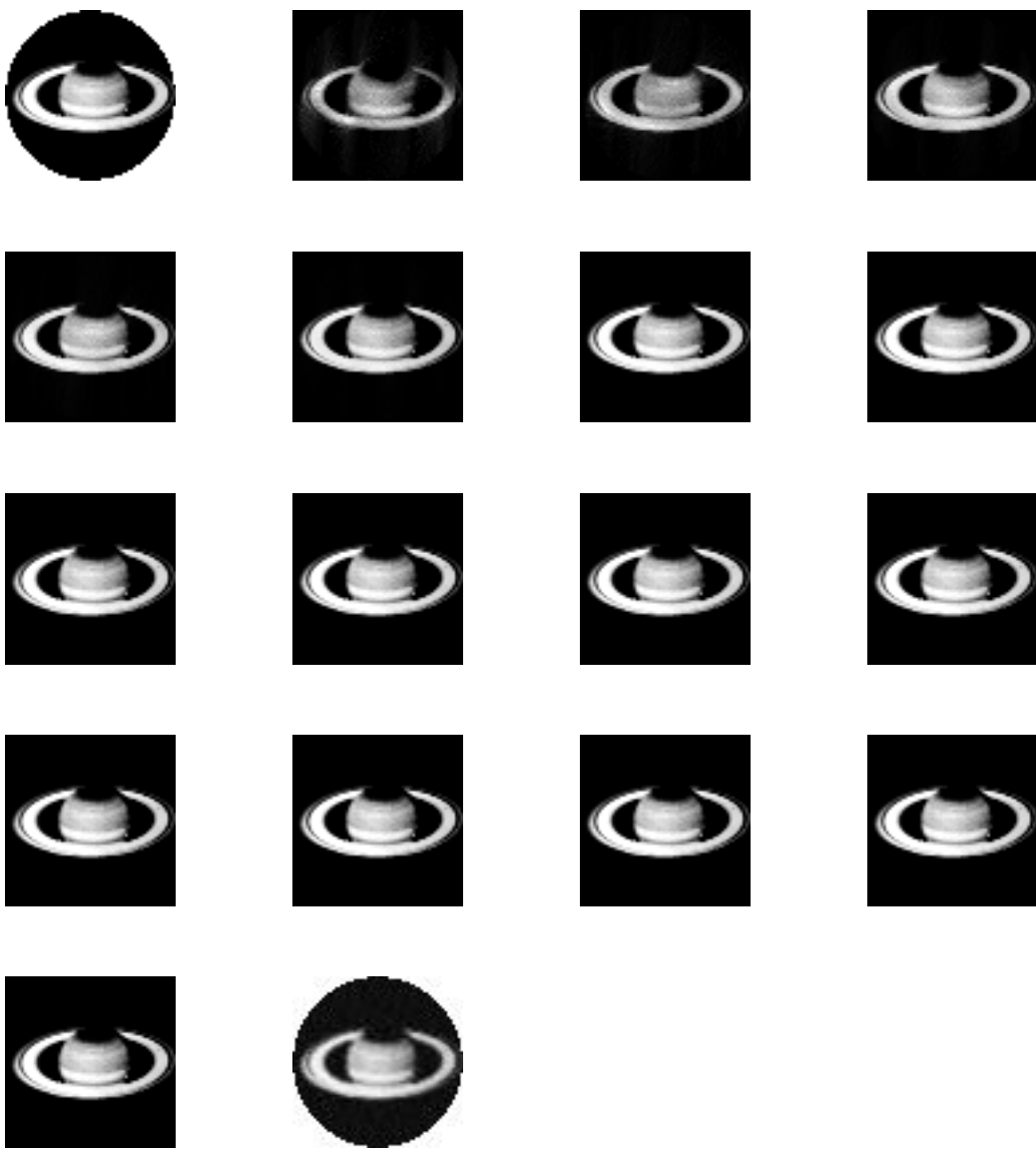


Figure 6.2: Comparison of reconstruction with CBP for PIC2

From Left to Right: Row1—Original image, Reconstruction by SMART in iteration 1, 2, 3 Row2—iteration 4, 5, 10, 15, Row3 – iteration 20, 25, 30, 35, Row4- 40, 45, 50, 55 Row5—iteration 60 and last image reconstructed by CBP.

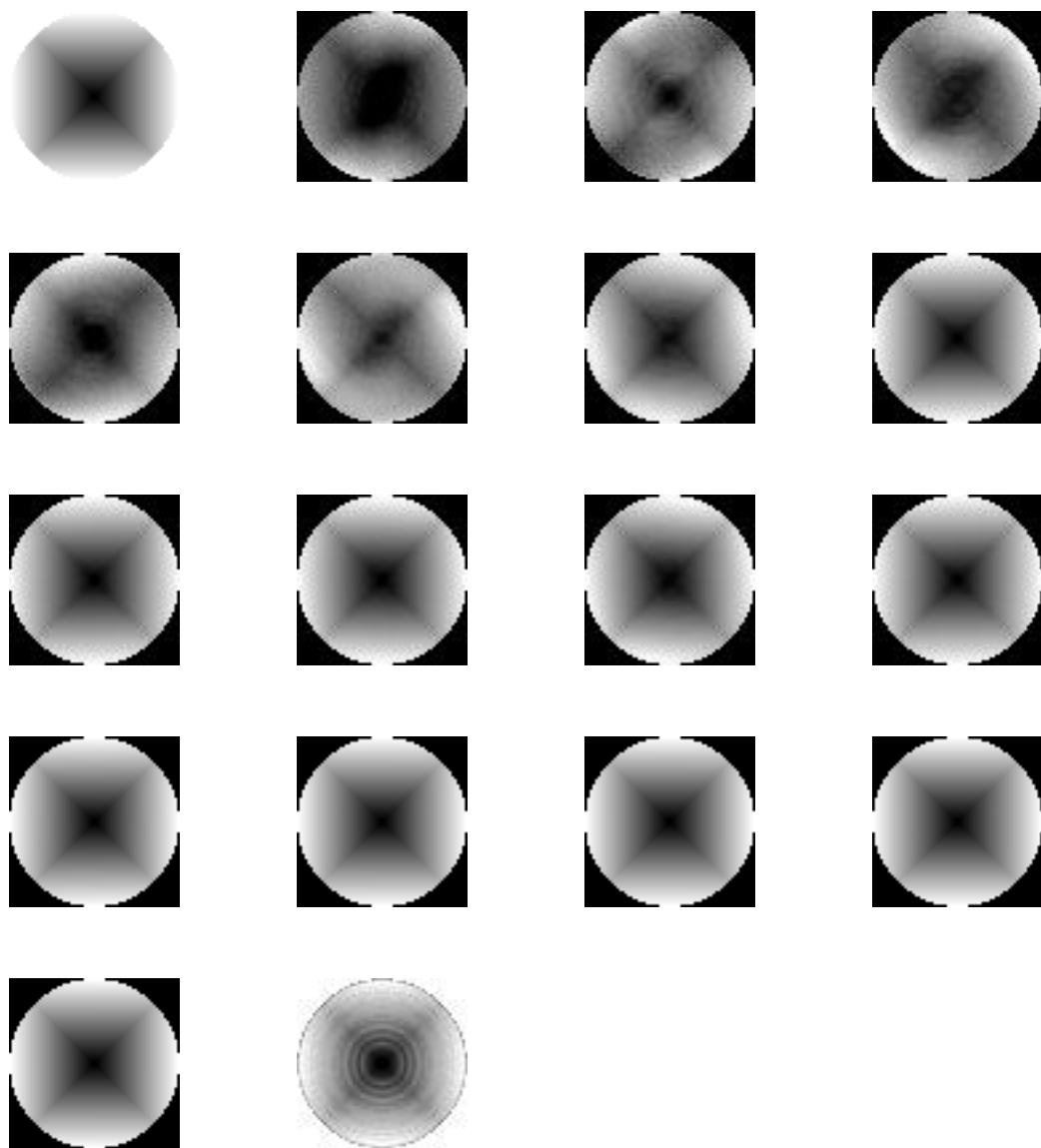


Figure 6.3: Comparison of reconstruction with CBP for PIC3

From Left to Right: Row1—Original image, Reconstruction by SMART in iteration 1, 2, 3 Row2—iteration 4, 5, 10, 15, Row3 – iteration 20, 25, 30, 35, Row4- 40, 45, 50, 55 Row5—iteration 60 and last image reconstructed by CBP.

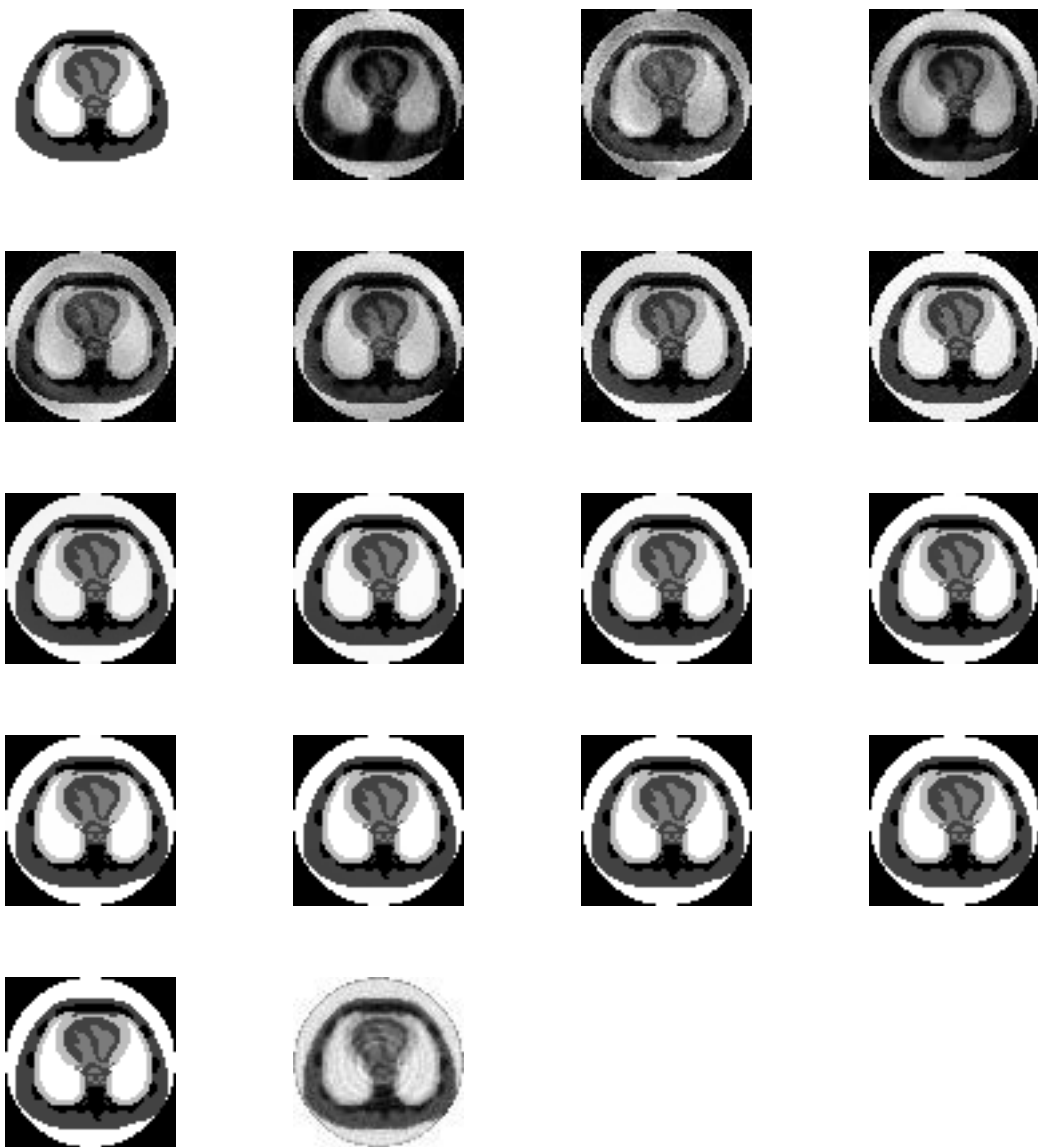


Figure 6.4: Comparison of reconstruction with CBP for PIC4

From Left to Right: Row1—Original image, Reconstruction by SMART in iteration 1, 2, 3 Row2—iteration 4, 5, 10, 15, Row3 – iteration 20, 25, 30, 35, Row4- 40, 45, 50, 55 Row5—iteration 60 and last image reconstructed by CBP.

6.3 CONVERGENCE WITH FEW PROJECTIONS

In this section we have tested the convergence and number of iterations required to get reconstruction with only four views. For experimentation we have taken an image of 8 X 8 e.g. n = 64 pixels with 4 detectors in the detector array, and the array is rotated through 4 views (horizontal, vertical, diagonal and antidiagonal) to produce m = 46 projections.

Starting with initial guess $f^{(0)}$ and projections p give in table 6.4.1 and 6.4.2 respectively.

18	16	19	10	08	06
12	09	15	12	07	23
18	14	17	05	23	09
14	17	22	24	28	13
19	12	10	27	26	24
12	29	26	15	16	12
21	24	19	09	12	13
11	10	23	14	0	0

Table 6.4.1 Given Projection Value (p)

0	0	0	0	0	0	0	0
0	0	0	0	0	0	0	0
0	0	0	0	0	0	0	0
0	0	0	0	0	0	0	0
0	0	0	0	0	0	0	0
0	0	0	0	0	0	0	0
0	0	0	0	0	0	0	0
0	0	0	0	0	0	0	0

Table 6.4.2 Initial Image Data ($f^{(0)}$)

We got the following image after 55th iteration (Table 6.4.3)

9.52	5.12	2.91	3.06	5.06	7.56	7.44	2.18
8.26	2.38	2.45	2.48	2.57	9.36	6.89	2.89
4.77	5.37	1.97	7.80	5.38	2.43	4.81	4.17
4.12	4.63	4.03	1.95	3.71	1.87	1.86	4.11
2.48	3.71	4.09	6.74	1.79	1.78	1.79	2.25
2.56	5.01	3.04	4.7	2.01	1.81	1.95	2.32
1.74	2.38	2.32	7.52	7.09	2.28	2.11	5.34
4.66	1.58	2.57	3.73	5.19	2.76	8.19	2.57

Table 6.4.3 Reconstructed Image after 55 iterations

The Figures 6.5.1, 6.5.2, 6.5.3, 6.5.4, 6.5.5. and 6.5.6. shows the reconstructed images at 1st, 10th, 20th, 30th, 50th and 55th iterations

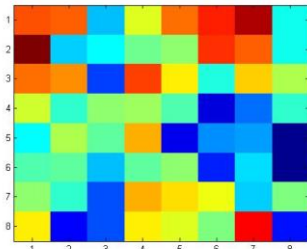


Figure 6.5.1

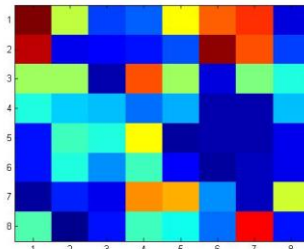


Figure 6.5.2

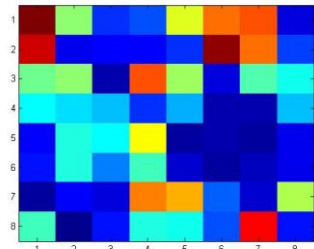


Figure 6.5.3

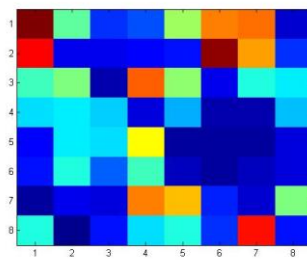


Figure 6.5.4

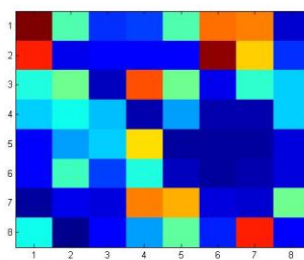


Figure 6.5.5

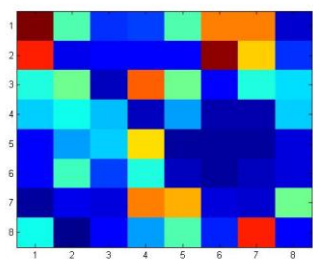


Figure 6.5.6

Figure 6.5: Reconstructed Image at different iterations

The errors EP1 and EP2 defined in Chapter V section 5.2.3 in projection data at each iteration are reported in Table 6.4.4 and Discrepancy in Consecutive Estimation of

image EF1 and EF2 defined in Chapter V section 5.2.3, successive iterations are reported in Table 6.4.5. The line graphs are shown in Figure 6.4.7, 6.4.8, 6.4.9 and 6.4.10 at iteration 1st, 15th, 25th and 55th respectively.

Iteration	$ p_{i+1} - p_i $	$(p_{i+1} - p_i)^2$
iteration 1	743.000000	552049.000000
iteration 2	299.375000	89625.390625
iteration 3	34.851563	1214.631444
iteration 4	7.800537	60.848377
iteration 5	2.252258	5.072666
iteration 6	1.376648	1.895160
iteration 7	1.503113	2.259349
iteration 8	0.413391	0.170892
iteration 9	0.408203	0.166630
iteration 10	0.084229	0.007095
iteration 11	0.162964	0.026557
iteration 12	0.281250	0.079102
iteration 13	0.287781	0.082818
iteration 14	0.296143	0.087701
iteration 15	0.178223	0.031763
iteration 16	0.026123	0.000682
iteration 17	0.151184	0.022857
iteration 18	0.176514	0.031157
iteration 19	0.169983	0.028894
iteration 20	0.170715	0.029144
iteration 21	0.112366	0.012626
iteration 22	0.139038	0.019332
iteration 23	0.039978	0.001598
iteration 24	0.069458	0.004824
iteration 25	0.083069	0.006900
iteration 26	0.085999	0.007396
iteration 27	0.069275	0.004799
iteration 28	0.086426	0.007469
iteration 29	0.016052	0.000258
iteration 30	0.037842	0.001432
iteration 31	0.045349	0.002057
iteration 32	0.049072	0.002408
iteration 33	0.051208	0.002622
iteration 34	0.053040	0.002813
iteration 35	0.054199	0.002938
iteration 36	0.055054	0.003031
iteration 37	0.055420	0.003071
iteration 38	0.055847	0.003119
iteration 39	0.165771	0.027480
iteration 40	0.128113	0.016413
iteration 41	0.078308	0.006132
iteration 42	0.049988	0.002499
iteration 43	0.032349	0.001046
iteration 44	0.020630	0.000426
iteration 45	0.041748	0.001743
iteration 46	0.018555	0.000344
iteration 47	0.109314	0.011950
iteration 48	0.098145	0.009632
iteration 49	0.060730	0.003688
iteration 50	0.039795	0.001584

Iteration	$ p_{i+1} - p_i $	$(p_{i+1} - p_i)^2$
iteration 51	0.025269	0.000639
iteration 52	0.015503	0.000240
iteration 53	0.008484	0.000072
iteration 54	0.003235	0.000010
iteration 55	0.000122	0.000000
iteration 56	0.003113	0.000010
iteration 57	0.005066	0.000026
iteration 58	0.016296	0.000266
iteration 59	0.008850	0.000078
iteration 60	0.012573	0.000158
iteration 61	0.014099	0.000199
iteration 62	0.013611	0.000185
iteration 63	0.013855	0.000192
iteration 64	0.013977	0.000195
iteration 65	0.014221	0.000202
iteration 66	0.013855	0.000192
iteration 67	0.014099	0.000199
iteration 68	0.013977	0.000195
iteration 69	0.014343	0.000206
iteration 70	0.013916	0.000194
iteration 71	0.013916	0.000194
iteration 72	0.013672	0.000187
iteration 73	0.013672	0.000187
iteration 74	0.013611	0.000185
iteration 75	0.013306	0.000177
iteration 76	0.013000	0.000169
iteration 77	0.013123	0.000172
iteration 78	0.012695	0.000161
iteration 79	0.012695	0.000161
iteration 80	0.012451	0.000155
iteration 81	0.012207	0.000149
iteration 82	0.011780	0.000139
iteration 83	0.011902	0.000142
iteration 84	0.011719	0.000137
iteration 85	0.011475	0.000132
iteration 86	0.011230	0.000126
iteration 87	0.010986	0.000121
iteration 88	0.010803	0.000117
iteration 89	0.010803	0.000117
iteration 90	0.010376	0.000108
iteration 91	0.010315	0.000106
iteration 92	0.010132	0.000103
iteration 93	0.010010	0.000100
iteration 94	0.009583	0.000092
iteration 95	0.009827	0.000097
iteration 96	0.009338	0.000087
iteration 97	0.009338	0.000087
iteration 98	0.009155	0.000084
iteration 99	0.008789	0.000077
iteration 100	0.008850	0.000078

Table 6.4.4. Error calculated in projection values in each iteration

Iterations	$ f_{i+1} - f_i $	$(f_{i+1} - f_i)^2$	Iterations	$ f_{i+1} - f_i $	$(f_{i+1} - f_i)^2$
iteration 1	260.593750	1196.627930	iteration 51	0.224570	0.001947
iteration 2	23.196289	13.700123	iteration 52	0.218310	0.001832
iteration 3	11.863609	3.781413	iteration 53	0.212647	0.001732
iteration 4	7.293658	1.328680	iteration 54	0.207277	0.001643
iteration 5	4.558233	0.521878	iteration 55	0.202114	0.001562
iteration 6	3.167742	0.264142	iteration 56	0.197140	0.001489
iteration 7	2.423008	0.162381	iteration 57	0.189942	0.001412
iteration 8	2.041324	0.120152	iteration 58	0.184316	0.001340
iteration 9	1.793079	0.097458	iteration 59	0.179717	0.001276
iteration 10	1.660157	0.085381	iteration 60	0.175271	0.001217
iteration 11	1.581798	0.077365	iteration 61	0.171076	0.001162
iteration 12	1.523060	0.071226	iteration 62	0.167109	0.001112
iteration 13	1.475091	0.066224	iteration 63	0.163492	0.001064
iteration 14	1.392426	0.058907	iteration 64	0.160142	0.001020
iteration 15	1.280310	0.049823	iteration 65	0.156920	0.000978
iteration 16	1.194516	0.044186	iteration 66	0.153788	0.000939
iteration 17	1.149647	0.040100	iteration 67	0.150822	0.000901
iteration 18	1.113286	0.036847	iteration 68	0.147948	0.000866
iteration 19	1.080504	0.034161	iteration 69	0.145214	0.000832
iteration 20	1.031179	0.031026	iteration 70	0.142620	0.000800
iteration 21	0.921514	0.026042	iteration 71	0.140079	0.000769
iteration 22	0.870406	0.023270	iteration 72	0.137586	0.000740
iteration 23	0.828576	0.021274	iteration 73	0.135143	0.000712
iteration 24	0.793581	0.019673	iteration 74	0.132742	0.000685
iteration 25	0.763604	0.018317	iteration 75	0.130393	0.000660
iteration 26	0.730673	0.016935	iteration 76	0.128084	0.000635
iteration 27	0.667299	0.014663	iteration 77	0.125825	0.000612
iteration 28	0.625723	0.013222	iteration 78	0.123611	0.000589
iteration 29	0.595970	0.012142	iteration 79	0.121439	0.000568
iteration 30	0.570434	0.011251	iteration 80	0.119310	0.000547
iteration 31	0.547994	0.010501	iteration 81	0.117219	0.000527
iteration 32	0.526815	0.009855	iteration 82	0.115158	0.000508
iteration 33	0.507945	0.009292	iteration 83	0.113141	0.000490
iteration 34	0.490216	0.008796	iteration 84	0.111161	0.000472
iteration 35	0.473685	0.008356	iteration 85	0.109214	0.000455
iteration 36	0.458431	0.007963	iteration 86	0.107293	0.000439
iteration 37	0.445886	0.007611	iteration 87	0.105417	0.000423
iteration 38	0.405795	0.006125	iteration 88	0.103568	0.000408
iteration 39	0.383962	0.005421	iteration 89	0.101752	0.000393
iteration 40	0.364060	0.005004	iteration 90	0.099965	0.000379
iteration 41	0.349298	0.004716	iteration 91	0.098218	0.000366
iteration 42	0.337096	0.004498	iteration 92	0.096495	0.000353
iteration 43	0.326862	0.004320	iteration 93	0.094801	0.000340
iteration 44	0.312715	0.004116	iteration 94	0.093147	0.000328
iteration 45	0.303181	0.003968	iteration 95	0.091513	0.000317
iteration 46	0.282642	0.003183	iteration 96	0.089912	0.000306
iteration 47	0.260532	0.002731	iteration 97	0.088335	0.000295
iteration 48	0.247859	0.002447	iteration 98	0.086793	0.000284
iteration 49	0.239172	0.002243	iteration 99	0.085267	0.000274
iteration 50	0.231610	0.002081	iteration 100	0.083781	0.000265

Table 6.4.5. Error calculated in Image pixel values in each iteration

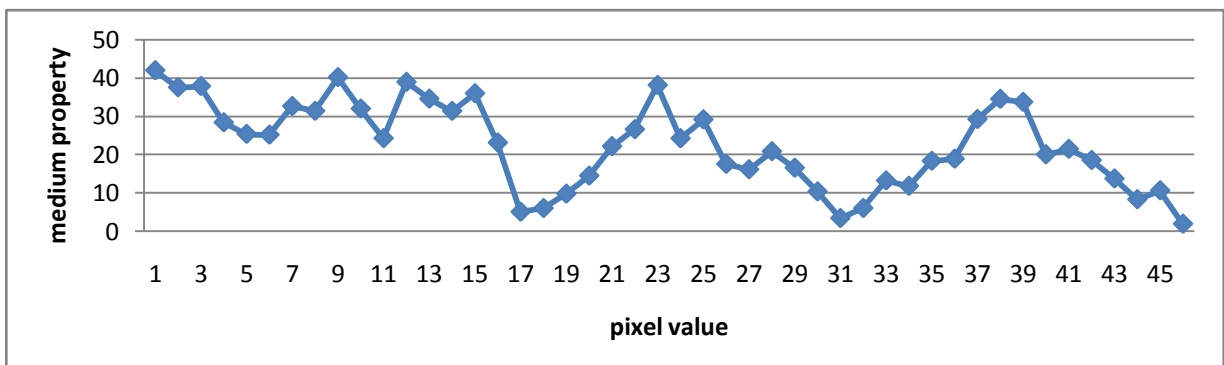


Fig 6.4.7. Image as a line Graph using ART after 01 iteration

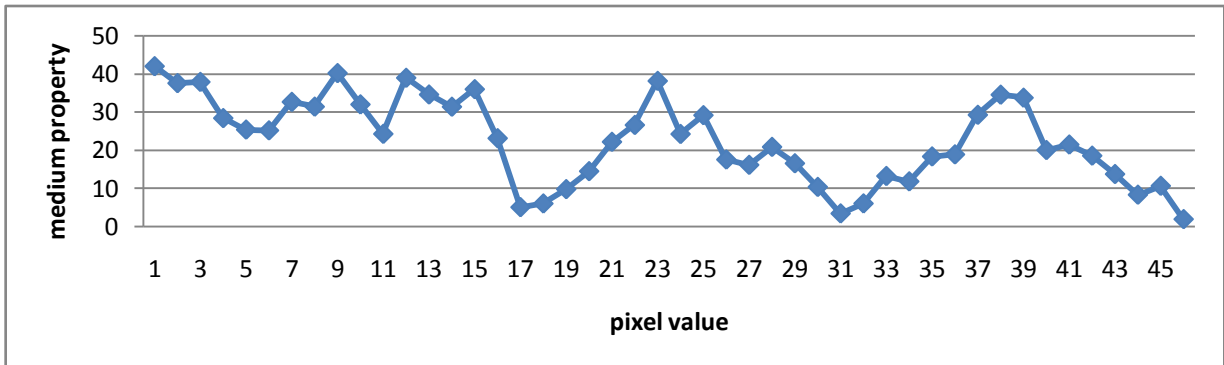


Fig 6.4.8. Image as a line Graph using ART after 15 iterations

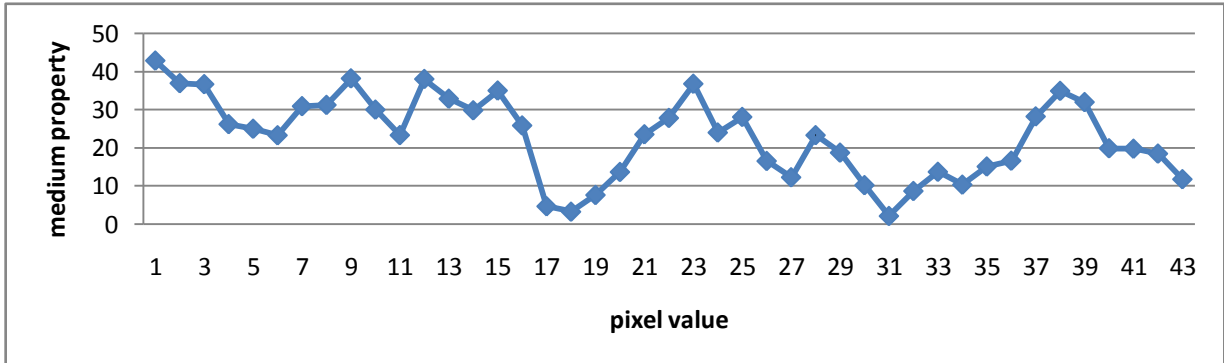


Fig 6.4.9. Image as a line Graph using ART after 25 iterations

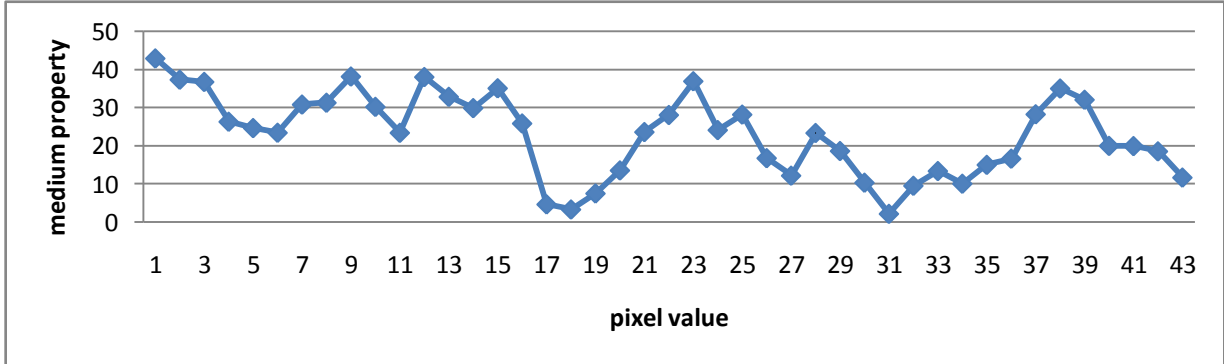


Fig 6.4.10. Image as a line Graph using ART after 55 iterations

The convergence is tested by difference in projection data at each iteration which is taken as EP1. The stopping criterion taken as EP2 is small enough or stabilizes. The accuracy is also tested by another measure, image difference at successive iterations i.e. EF1 and EF2. It is evident that after the difference in projection reaches at its minimum it again starts increasing, which says our stopping criterion should be guided by projection difference rather than a large number of iterations. In present example we reach at this minima in 55th iteration.

In next chapter conclusion and future research scope in the area is given.

CHAPTER VII: CONCLUSIONS AND FUTURE RESEARCH

7.1 CONCLUSION

The challenges of image reconstruction in medical imaging have been the motivation for this work. This thesis has demonstrated significant speedup for Modified Simultaneous Algebraic Reconstruction Technique (MSART) by an iterative approach. This method is used to reduce the number of iterations to produce good image quality using the various sets of views (projection data). It has been known for decades that the CBP reconstruction method produces unwanted streak artefacts and the final quantitative result is an approximation and therefore not very reliable. A CBP image is often also more noisy than images which are reconstructed iteratively. Therefore the MSART algorithm is developed that allows parallel beam geometry of the measured data and transmission dependent attenuation correction. In addition, the algorithm can use different amounts of iteration and change the order of the projection angles. The results reconstructed by MSART are more reliable and quantitatively more accurate than CBP results as demonstrated in this thesis. The MSART algorithm is a rapid method and therefore MSART may displace the CBP method. Iterations improve the contrast of the image, but increase the noise. Therefore the number of iterations has to be balanced to the final result. Quantitatively accurate and reliable results require increased matrix size and large number of projections. Main advantage of the MSART is that the number of iterations is not so critical as in CBP. Additional iterations improve the final result without increasing the noise. Iterative reconstruction algorithms improve the results of image

especially when the correct number of iterations and proper filtering are selected. The speed of the reconstruction process is not a problem when using accelerated computation algorithms and modern computers for the reconstruction. The present study revealed the improvement in image reconstruction and thus iterative reconstruction algorithms are recommended for image reconstruction in clinical situations. The comparison of MSART with CBP was carried out experimentally using four different types of image patterns. The convergence of this algorithm is shown geometrically. The results of MSART algorithm with convergence are reported. The comparison is done by error analysis with respect to the error considered for error analysis L_1 and L_2 errors in reconstruction at different iterations and original test image. They are represented as EL1 and EL2 in result tables. The reconstructions and errors with respect to both methods are reported and the convergence of ART is also tested with limited number of views.

7.2.2 FUTURE RESEARCH

From the discussion in last section it is evident that the proposed algorithm improves the quality of reconstruction upon convolution back projection algorithm both visually and in terms of error analysis. From table 6.1 to 6.4 it is observed that in terms of error analysis the quality of reconstruction is better as early as from 4th or 5th onwards. In pictorial view also the reconstruction by MSART is better than CBP. Further this algorithm can be modified for use in limited view projection data problems as well, where it looks to work better than transform methods.

REFERENCES:

- Agmon S. (1954): The relaxation method for linear inequalities, Can.J.Math., vol. 6, pp. 382-392.
- Ali A.M., Melegy Z., Morsy M., Megahid R.M., Bucherl T., Lehmann E.H. (2004): Image reconstruction techniques using projection data from transmission method. Annals of Nuclear Energy vol. 31, pp. 1415-1428.
- Andersen A. H. and Kak A. C. (1984): Simultaneous algebraic reconstruction technique (SART): A superior implementation of the ART algorithm, Ultrason. Imag., vol. 6, pp. 81–94.
- Andersen A.H. (1989): Algebraic Reconstruction in CT from Limited View, I IEEE Trans. On Medical Imaging, Vol. 8, pp 50-55.
- Badea C.T. and Gordon R. (2004). Experiments with the nonlinear and chaotic behavior of the multiplicative ART (MART) algorithm for computed tomography. Physics in Medicine and Biology 49(8), 1455-1474.
- Basu Samit and Bresler Yoram (2001): Error Analysis and Performance Optimization of Fast Hierarchical Backprojection Algorithms, IEEE Transaction on Image Processing, vol. 10, no. 7, pp 1103-1117.
- Bates R.H.T., Garden Kathryn L. and Peters Terence M. (1983): Overview of Computerized Tomography with Emphasis on Future Developments, Proceeding of the IEEE, vol 71 , pp 356-372.
- Belgacem Ben F., Kaber S.M. (2008): Quadratic optimization in ill-posed problems, Inverse problems, vol. 24 No. 5.
- Bloch Peter and Udupa Jayaram K. (1983): Application of Computerized Tomography to Radiation Therapy and Surgical Planning, Proceeding of the IEEE, vol 71 , pp 351-358.
- Bonnet Stephane, Peyrin Francoise, Turjman Francis and Prost Remy (2002): Multiresolution Reconstruction in Fan-Beam tomography, IEEE Transaction on Image Processing vol 11, pp 169-176.
- Boyd Jeffrey E. and Little James J. (1994): Complementary data fusion for limited angle tomography pp. 288-294.
- Bracewell R.N. (1956): Strip integral in radio astronomy. Australian Journal of Physics, 9, pp. 198-217.

Bracewell R.N. (1978): The Fourier Transforms and its Applications, McGraw Hill.

Bracewell R.N., Riddle A.C. (1967): Inversion of fan beam in Radio Astronomy, *Astrophys. J.* V150 pp.427-434.

Bregman L.M. (1967): The relaxation methods of finding the common point of convex sets and its application to the solution of problems in convex programming, *USSR Computat. Math. Phys.*, vol 7, pp. 427-434.

Bureau F.J. (1955): Divergent Integrals and Partial Differential Equations, *Comm. Pure Appl. Math* 8, pp. 143-202.

Censor Y. (1983): Finite series-expansion reconstruction methods, *Proceedings of the IEEE*, 71, pp. 409-419.

Chaganti S. Rao and Joshi R.C. (1997): Image Compression Using Wavelet Transform and Vector Quantization, International Conference on Computer Applications in Electrical Engg., Roorkee, India, pp 107-112.

Cormack A.M. (1973): Reconstruction of their densities from their projections with application in radiological physics, *Phys. Med. Biol.*, vol. 18, pp. 195-207.

Crowther R.A., DeRosier D.J. and Klug A. (1970): The reconstruction of a three dimensional structure from projections and its application to electron microscopy, *Proceeding of Royal Society of London, Ser A*, vol. 317, pp. 319-340.

Davison Mark E. (1983): The Ill-Conditioned Nature of the Limited Angle Tomography Problem, *Society for Industrial and Applied Mathematics*.

Deans, S.R. (1983): Radon Transform and some of its Applications, John Wiley and Sons, New York.

Delaney A.H., Bresler Y (1995): Efficient edge-preserving regularization for limited angle tomography, *Image processing, International conference on* vol. 3, pp. 176-179.

Delaney A.H., Bresler Y. (1996): A fast and accurate Fourier algorithm for iterative parallel-beam tomography, *Image processing IEEE transaction* vol. 5, pp. 740-753.

Delaney A.H., Bresler Y., Sunnyvale (1998): Globally convergent edge-preserving regularized reconstruction: an application to limited-angle tomography, *IEEE transaction* vol. 7, pp 204-221.

Demster A.P., Laird N.M. and Rubin D.B. (1977): Maximum likelihood from incomplete data via the EM algorithm, *Journal of Royal Statistical Society, Ser. B*, vol. 39, pp. 1-38.

Devaney A.J. (1989): The limited view problem in diffraction tomography, Inverse problem vol. 5 pp. 501-521.

Dhawan A. P., Rangayyan R. M., Gordon R. (1984): Image restoration by Wiener deconvolution in limited view computed tomography, Applied Optics, vol. 24, pp. 4013-4020.

Dorner, Bryan C. (1979): High speed array processing method applied to 2-D and 3-D image processing, vol. 26, pp. 2718-2719.

Douglas P. Boyd and Martin J. Lipton(1983): Cardiac Computed Tomography, Proceeding of IEEE, vol 71, No. 3, pp 298-312.

Faridani Adel, Erik L. Ritman and Kennan T. Smith (1992): Local Tomography, Society for Industrial and Applied Mathematics, vol 52, pp 459-484.

Farrokhi Farrok Rashid, Ray K.J., Berenstein Carlos A. and Walnut David (1997): Wavelet – Based Multiresolution local tomography, IEEE Transaction on Image Processing vol 6, pp 1412-1429.

Fishburn P., Schwander P., Schepp L., and Vanderbei R.J. (1997): The discrete radon transform and its approximate inversion via linear programming. Discrete Applied Mathematic, Vol. 75, pp. 39-61.

Frese Thomas, Bouman Charles A. and Sauer Ken (2002): Adaptive Wavelet Graph Model for Bayesian Tomographic Reconstruction, IEEE Transaction on Image Processing, vol. 11, no. 7, pp 756-768.

Galigekere R.R., Wiesent K., Mertelmeier T., Holdsworth D.W. (2000): on intermediate view estimation in Computed Tomography, circuits, systems and signals processing vol 19 pp. 279-299.

Gardner R. J. and Gritzmann P. (2001): Reconstructing polyatomic structures from discrete X-rays, Trans. Amer. Math. Soc. Vol. 349, pp. 2271-2295.

Gilbert P. (1972): Iterative methods for three-dimensional reconstruction of an object from projections, Journal of Theoretical Biology, 36, pp. 105-117.

Glenn F. Knoll (1983): Single-Photon Emission Computed Tomography, Proceeding of IEEE, vol 71, pp 320-332.

Gonzalez R.C. and Wintz P. (1977): Digital Image Processing, Addison-Wesley Publishing Co., Massachusetts.

Gordan R. and Herman G.T. (1974): Three dimensional reconstruction from projections: A review of algorithms, Int. Rev. Cytol, 01.38, pp. 111-151.

Gordon D. (2006): Parallel ART for image reconstruction in CT using processor arrays. The International journal of Parallel, Emergent and Distributed Systems, Vol. 21, pp. 365-380.

Gordon R. (1974): A tutorial on ART, IEEE Transaction on Nuclear Science, NS-21, pp. 78-83.

Gordon R. (1976): Dose reduction in computerized tomography. *Investigative*

Gordon R. (1985): Toward robotic "x-ray vision": new directions for computed tomography. Applied Optics 24(23), 4124-4133.

Gordon R. and Herman G.T. (1971): Reconstruction of pictures from their projections, Comm. Assoc. Compul. Machinery, Vo1.I4, pp. 759-768.

Gordon R., Bender R. and Herman G.T. (1970): Algebraic reconstruction techniques (ART) for three-dimensional electron microscopy and x-ray photography. J. Theor. Biol. 29(3), 471-481.

Greenleaf James F. (1983): Computerized Tomography with Ultrasound, Proceeding of IEEE, vol 71, No. 3, pp 330-341.

Grigoryan Artyom M. (2003): Method of paired transforms for reconstruction of images from projections: Discrete model. IEEE transaction on image processing vol. 12, pp 985-994.

Guan H. and Gordon R. (1994): A projection access order for speedy convergence of ART (Algebraic Reconstruction Technique): a multilevel scheme for computed tomography. Phys. Med. Biol. 39, 2005-2022.

Guan H. and Gordon R. (1996): Computed tomography using Algebraic Reconstruction Techniques (ARTs) with different projection access schemes: a comparison study under practical situations, Phys Med Biol 41(9), 1727-43.

Guan H., Gordon R. and Zhu Y. (1998): Combining various projection access schemes with the algebraic reconstruction technique for low-contrast detection in computed tomography. Phys Med Biol 43(8), 2413-21.

Gull S.F. and Daniell G.J. (1978): Image reconstruction from incomplete and noisy data, Nature, vol. 272, pp. 686-690.

Hanson K. M. (1990): Optimization of the Constrained Algebraic Reconstruction Technique for the Performance of a Variety of Visual Tasks, Processing in Medical Imaging, pp 45-57.

Herman G. T., Lent A. and Rowland S. W. (1973): ART: mathematics and applications (a report on the mathematical foundations and on the applicability to real data of the algebraic reconstruction techniques.); *J. Theor. Bioi.*, 42, pp. 1-32.

Herman G.T. (1973): Reconstruction of binary patterns from a few projections, International Symposium Davos, editors A Guenther et al North Holland Publ. co., pp. 371-379.

Herman G.T. (1980): Image Reconstruction from Projection: The Fundamental of Computerized Tomography, Academic Press.

Herman G.T. and Kuba Attila (2003): Discrete tomography in Medical Imaging, Proceedings of the IEEE, Vo1.91, No. 10, pp. 1612-1624.

Herman G.T. and Rowland S.W. (1973): Three methods for reconstructing objects from X-rays: A comparative study, *Comput. Graphics Image Process.*, vol. 2, pp. 151-178.

Hinshaw Waldo S. and Lent Arnold H. (1983): An Introduction to NMR Imaging: From the Bloch Equation to the Imaging Equation, Proceeding of IEEE, vol 71, No. 3, pp 338-354.

Hounsfield G.N. (1972): A method and apparatus for examination of a body by radiation such as X or gamma radiation, Patent Spec. 1283915, The Patent Offce, London, England.

Hounsfield G.N. (1973): Computerizes transverse axial scanning tomography part I, Description of the system, *British Journal of Radiology*, 46, pp. 1016-1022.

Hsiao Ing-tsung, Rangarajan Anand and Gindi Gene (2002): Joint-MAP Bayesian Tomographic Reconstruction with a Gamma-mixture Prior, *IEEE Transaction on Image Processing* vol 11, pp 1466-1477.

Inouye T. (1979): Image reconstruction with limited angle projection Data, *IEEE Transactions on Nuclear Science*, NS-26,pp. 2666-2669.

Jiang Ming and Wang Ge (2003): Convergence of the Simultaneous Algebraic Reconstruction Technique (SART), *IEEE Transaction on Image Processing*, Vol 12, pp 957-961.

John F. (1955): Planes wave and Spherical means applied to Partial Differential Equations, Interscience, Newyork.

Jorge LLacer (1990): On the Validity of Hypothesis Testing for Feasibility of Image Reconstruction, *IEEE Transaction on Medical Imaging*, vol. 9, No. 2, pp. 226-230.

Kaczmarz S. (1937): Angenherete Auflsung von System Linearer Gleichungen, Bull. Acad. Polon, Sci. Lett., A35, pp. 355-357.

Kak A.C. and Slaney Malcolm (2001): Principles of Computerized Tomographic Imaging, SIAM, Philadelphia.

Kenneth M. Hanson and George W. Wecksung (1983): Bayesian approach to limited angle reconstruction in computed tomography. Journal of the optical society of America vol. 73, pp 1501.

Kolaczyk Eric D. (1996): A wavelet shrinkage approach to topographic image reconstruction, Journal of the American Statistical Association, vol 91, pp 1079-1090.

Krimmel S., Baumann J., Kiss Z., Kuba A., Nagy A. and Stephan J. (2005): Discrete tomography for reconstruction from limited view angles in non-destructive testing. Discrete Mathematics vol. 20, pp. 455-474.

Laroque Samual J, Emil Y Sidky, Xiaochuan Pan (2008): Accurate image reconstruction from few-view and limited angle data in diffraction tomography, j.opt. society America, vol. 25, pp. 1772-1782.

Lautsch Michael (1989): A spline Inversion Formula for the Radon Transform, Society for Industrial and Applied Mathematics, vol 26, pp 456-467.

Leon Axel, Peter H. Arger and Robert A. Zimmerman(1983): Applications of Computerized Tomography to Diagnostic Radiology, Proceeding of IEEE, vol 71, No. 3, pp 293-300.

Lewitt R.M. (1983): Reconstruction algorithms: Transform methods, Proceedings of the IEEE, Vo1.71, pp. 390-405.

Lewitt Robert M. (1983): Reconstruction Algorithms: Transform Methods, IEEE proceeding vol. 71, pp 390-408.

Louis Alfred K. and Natterer Frank (1983): Mathematical Problems of Computerized Tomography, Proceeding of the IEEE, vol 71 , pp 379-389.

Macovski Albert (1983): Physical Problems of Computerized Tomography, Proceeding of the IEEE, vol 71 , pp 373-378.

Maitra Ranjan and O'Sullivan Finbarr (1998): Variability assessment in Positron Emission Tomography and Related Generalized Deconvolution Models, Journal of American Statistical Association, vol 93, pp 1340-1355.

Mazur E.J. and Gordon R. (1995). Interpolative algebraic reconstruction techniques without beam partitioning for computed tomography. *Med Biol Eng Comput* 33(1), 82-86.

Melvin Cameron (2006): Design, development and Implementation of a parallel algorithm for computed tomography using Algebraic reconstruction Techniques. University of Manitoba, Canada.

Melvin Cameron, Thulasiramam Parimala, Gordon R. (1995) Parallel Algebraic Reconstruction Technique for Computed Tomography, Medical and Biological Computing, volume 33, January 1995, 82-86.

Munshi P., Rathore R.K.S., Swamy S.T. and Dhariyal I.D. (1987): Tomographic Reconstruction of the Density Distribution using Direct Fan-Beam Algorithms, Nuclear Instruments and Methods in Physics Research A257, pp 398-405.

Nassi, Menahem, Brody, William R., Medoff, Barry P., Macovski, Albert (1982): Iterative Reconstruction a Reprojection: An Algorithm for Limited Data Cardiac-Computed Tomography Vol. 29, pp. 333 – 341.

Natterer F. (1980): A Sobolev Space Analysis of Picture Reconstruction, SIAM journal of Applied Mathematics, vol. 39, no. 3, pp 402-411.

Natterer F. and Wubbeling F. (2001): Mathematical Methods in Image Reconstruction, SIAM, Philadelphia.

Nievergelt Yves (1986): Exact Reconstruction Filters to Invert Radon transforms with finite Elements, Journal of Mathematical Analysis and Applications, vol. 120, pp. 288-314.

Nirvikar and Singh Raghuveer (2011): Reconstruction with Parallel Projections using ART, International Journal of Computer Applications, ISSN 0975- 8887, Volume 13, Number 1 (2011), pp 36–39.

Nirvikar and Srivastava Tanuja (2010): Reconstructions with 16 Projections using ART, 5th Uttarakhand State Science and Technology Congress-2010, pp. 215, Dehradun.

Nowak R.D. and Kolaczyk E.D.(2000): A statistical multiscale framework for Poisson inverse problems, IEEE Transaction on Information Theory, vol. 46, no. 5, pp 1811-1825.

Olson Tim and DeStefano Joe (1994): Wavelet Localization of the Radon Transform, IEEE Transactions on Signal Processing, vol 42, pp 2055-2067.

Oskoui P. and Stark Henry (1989): A Comparative Study of Three Reconstrucion Methods for a :Limited-view Computer Tomography Problem, IEEE Transaction on Medical Imaging Vol. 8, pp 43-49.

Paul Soble, Rangayyan, Rangaraj M., Richard G. (1985): Quantitative and Qualitative Evaluation of Geometric Deconvolution of Distortion in Limited-View Computed Tomography, IEEE vol. 32 pp. 330-335.

Phillips Peter R. (1989): Bayesian Statistics, Factors Analysis, and PET Image – Part I: Mathematical Background, IEEE Transaction on Medical Imaging, vol. 8, No. 2, pp 125-132.

Radon J. (1917): Über die Bestimmung von Funktionen durch ihre Integralwerte längs gewisser Mannigfaltigkeiten, Berichte Sächsische Akademie der Wissenschaften, Leipzig, Math Phys. Kl 69, pp. 262-267.

Ramakrishna R.S., Mullick S.K. and Rathore R.K.S. (1983): Iterative Image Restoration, IEEE processing, pp 1088-1091.

Ramakrishna R.S., Mullick S.K. and Rathore R.K.S. (1985): A New Iterative Algorithm for Image Restoration, Computer vision, Graphics and image processing, vol 30, pp 47-55.

Rangayyan R.M. and Gordon R. (1983): Computed tomography from ordinary radiographs for teleradiology. Med. Physics. 10(5), 687-690.

Rangayyan R.M., Dhawan A.P. and Gordon R. (1984): Algorithms for limited-view computed tomography: a survey. In: IEEE Int. Conf. on Computers, Systems and Signal Processing, Bangalore, India: IEEE Press, p. 1540-154.

Rangayyan R.M., Dhawan A.P. and Gordon R. (1985): Algorithms for limited-view computed tomography: an annotated bibliography and a challenge. Applied Optics 24(23), 4000-4012.

Rathore R.K.S. (1992): Total Error in the Discrete Convolution Backprojection Algorithm in Computerized Tomography, Journal of Computational and Applied Mathematics 54, pp 79-97.

Rathore R.K.S. and Singh Umesh (1993): On the CBP-Algorithm for Strip Integral Data in Computerized Tomography, ISIAM'92, University of Roorkee, Roorkee, pp 36-39.

Rathore R.K.S., Munshi P., Bhatia V.K. and Pandimani S. (1988): Filtered Bessel Functions in Computerized Tomography, Nuclear Engineering and Design 108, North-Holland, Amsterdam, pp 375-383.

Robb Richard A., Hoffman Eric A., Lawrence J. Sinak, Lowell D. Harris and Erik L. Rim(1983): High-Speed Three-Dimensional X-Ray Computed Tomography: The Dynamic Spatial Reconstructor, Proceeding of IEEE, vol 71, No. 3, pp 308-328.

Salina F.V., Mascarenhas N.D.A., Cruvinel P.E. (2002): A comparison of POCS algorithms for Tomographic reconstruction under noise and limited view. Digital Object Identifier, pp 342-346.

Schie Eddie Van and Middelhoek Jan (1989): Determination of 2D Implanted ION Distributions using Inverse Radon Transform Methods, Nuclear Instruments and Methods in Physics research B42, pp 109-121.

Shepp L.A., Logan B.F. (1974): The Fourier reconstruction of Head section, IEEE Trans Nuc. Sci. v NS-21, pp. 21-43.

Sidky Emil Y., Kao Chien-Min, Pan Xiaochuan (2006): Accurate image reconstruction from few-view and limited angle data in divergent beam Computed Tomography. Vol. 14 pp. 1095-9114 (online).

Srivastava Tanuja (1997): Image Reconstruction Technique in PET, Proceedings of XV ISMS Annual Conference, Jaipur.

Srivastava Tanuja (1997): Two Reconstruction Techniques in Computerized Tomography, Mathematics and its application in Engineering and Industry, (Narosa Publishings, New Delhi), pp. 255-262.

Srivastava Tanuja (1999): On Statistical Error Estimates for Convolution Back-projection Algorithm in Computerized Tomography, Proceedings of 86th India Science Congress, Jan, 3-7, Chennai.

Srivastava Tanuja (2001): Statistical Aspect of Computerized tomography, International Workshop CT2001 Computerized Tomography for Scientist and Engineer, Dec 12-13, I.I.T.Kanpur

Srivastava Tanuja (2003): Statistical Error Estimate in CBP: Inverse Theorem, International Journal of Tomography & Statistics. pp 1: 1-20.

Srivastava Tanuja (2003): Stochastic Modeling in Computerized Tomography, e-proceeding of DAAD Network Partnership Meeting, University of Colombo, Sri Lanka.

Srivastava Tanuja (2004): Statistical Method of Estimation of ESE in CBP, American Journal of Mathematical and Management Science, Vol. 24 pp.291-320.

Srivastava Tanuja (2006): Error analysis in convolution backprojection algorithm: An Empirical validation of Ω_c estimate.

Srivastava Tanuja and Rathore R. K.S. (2004): Characterization image by order of Error, International Journal of Tomography & Statistical, Vol. D-04 pp. 41-64.

Srivastava Tanuja, Nirvikar and Singh Raghuveer (2011): Convergence of ART in Few Projections, International Journal of Computer Science and Engineering, ISSN 0975-3397, Volume 3, Number 2 (2011), pp 726–734.

Srivastava Tanuja, Rathore R.K.S., and Dhariyal I.D. (1992): Direct Estimates of Statistical Error for Convolution Back-projection Algorithm in Computerized Tomography. Journal of Combination. Information and system Sciences, Vol. 17, pp. 271-287.

Srivastava Tanuja, Rathore R.K.S., and Dhariyal I.D. (1993): Inverse Theorem for Statistical error for Convolution Back-projection Algorithm in Computerized Tomography, Proceedings of First Annual Conference of ISIAM'92, pp 43-49.

Srivastava Tanuja, Rathore R.K.S., Dhariyal I. D., Munshi P., and Rastogi R. (1994): Design of Optimal Statistical Filter for Discrete Convolution Back-projection Method, American Journal of Mathematical and Management Science, Vol. 14, pp.229-265.

Srivastava Tanuja, Singh Raghuveer and Nirvikar (2010): ART for Image Reconstruction Using Parallel Beam Projection Data, International Journal of Information Sciences and Applications, ISSN 0974-2255 Volume 2, Number 4 (2010), pp. 627-630.

Srivastava Tanuja, Singh Raghuveer and Nirvikar(2010): ART with 3 Projections in CT, 1st National Conference on Emerging Trends in Advanced Computing & Informatics, CICON-2010, pp. 1-3, held at Shobhit University, Meerut.

Tanabe K. (1971): Projection methods for solving a singular system of linear equations and its applications, Numerische Mathematik, vol 17, pp 203-214.

Tom kwok C.: Limited angle imaging using lultiple energy scanning, United state patent.

Udupa Jayaram K. (1983): Display of 3D Information in Discrete 30 Scenes Produced by Computerized Tomography, Proceeding of IEEE, vol 71, No. 3, pp 420-434.

Vardi Y. and Lee D. (1998): Discrete Radon transform and its approximate inversion via the EM algorithm, Int. J Imaging Science Tech. Vol. 9, pp.155-173.

Vardi Y., Shepp L.A. and Kaufman L. (1985): A statistical model for Positron emission tomography, Journal of the American Statistical Association, vol. 80, pp. 8-37.

Wang Ge, Snyder Donald L., O'Sullivan Joseph. A. and Vannier Michael W. (1996): Iterative Deblurring for CT Metal Artifact Reduction, IEEE Transaction on Medical imaging, vol 15, pp 657-664.

Wei Yuchunan, Wang Ge, Hsieh Jiang (2005): Relation between the filtered backprojection algorithm and the backprojection algorithm in computed tomography, IEEE processing vol. 12 pp. 633-636.

Wood S.L. and More M. (1981): A fast implementation of a minimum variance estimator for computerized tomography image reconstruction, IEEE Transaction on Biomedical Engg., BME-28, pp. 56-68.

Yau Sze Fong, Wong Shum Him (1996): A linear sinogram extrapolator for limited angle tomography, Signal processing vol. 1, pp. 386-389.

Zhong Qu, Junhao Wen, Dan Yang, Yu Wu (2005): Algebraic Reconstruction Technique in Image Reconstruction with Narrow Fan-Beam, IEEE Transaction, pp 622-625.

Zhu Yang Ming, Zhuang Tian-ge and Chen Laigao M (1992): Virtual symmetry reconstruction algorithm for limited-view computed tomography, Vol. 1818, pp. 1294.

LIST OF REPRINTS

- ❖ Tanuja Srivastava, Nirvikar and Raghuveer Singh, “Convergence of ART in Few Projections”, International Journal of Computer Science and Engineering, ISSN 0975-3397, Volume 3, Number 2 (2011), pp 726–734.(online)
- ❖ Tanuja Srivastava, Raghuveer Singh and Nirvikar, “ART for Image Reconstruction Using Parallel Beam Projection Data”, International Journal of Information Sciences and Applications, ISSN 0974-2255 Volume 2, Number 4 (2010), pp. 627-630.
- ❖ Nirvikar and Raghuveer Singh, “Reconstruction with Parallel Projections using ART”, International Journal of Computer Applications, ISSN 0975-8887, Volume 13, Number 1 (2011), pp 36–39.
- ❖ Nirvikar and Tanuja Srivastava, “Reconstructions with 16 Projections using ART”, 5th Uttarakhand State Science and Technology Congress-2010, 10-12th Nov., 2010, pp. 215, Doon University, Dehradun.

Award:-

- ❖ **Young Scientist Award** for best oral presentation-2010 under the discipline Mathematics; Statistics & Computer Science, 5th Uttarakhand State Science and Technology Congress-2010 held at Doon University, 10-12 November, 2010.

Convergence of ART in Few Projections

Tanuja Srivastava¹

Department of Mathematics
Indian Institute of Technology
Roorkee, Uttarakhand

Nirvikar²

Department of CS & IT
Shobhit University
Meerut, UP

Raghuvir Singh³

Shobhit University
Meerut, UP

Abstract— Algebraic Reconstruction Technique (ART) is an iterative algorithm to obtain reconstruction from projections in a finite number of iterations. The present paper discusses the convergence achieved in small number of iteration even when projection data is available in only four directions.

Keywords-*ART, Image Reconstruction, Convergence, Projections, Computed Tomography*

I. INTRODUCTION

Computed Tomography (CT) is a diagnostic procedure that uses special x-ray equipment to obtain cross-sectional pictures of the body. The CT computer displays these pictures as detailed images of organs, bones, and other tissues. This procedure is also called CT scanning, computerized tomography, or computerized axial tomography (CAT) [1]. CT is a two step process of collecting the projection data, then calculating the attenuation values that could have generated these projection values (reconstruction). Two modalities that limit the radiation from Computed Tomography are then presentation: 3-D cone beam reconstruction, and limited view Computed Tomography.

Computed Tomography has a vital role in medical diagnostics as an imaging method that yields detailed information. As an X-ray technology, however, it exposes the patient to ionizing radiation that is known to be harmful. A challenge for this technology is to obtain the high quality images that have come to be expected from it, while limiting this harmful radiation. CT uses multiple X-ray views of the target for image reconstruction [2]. Each view is associated with a dose of radiation, hence limiting the number of views will reduce the radiation. Using a true 3-D reconstruction from 2-D views, rather than assembling from 2-D reconstructions of 1-D views, should theoretically reduce the number of views required. A second approach is to limit the number of views outright. Modifications of the commonly used convolution algorithms allow for some limited reconstruction in the third dimension, but these algorithms are not ideal for a full 3-D reconstruction [3]. Limiting the number of views outright causes the standard reconstruction algorithms to fail. The *Algebraic Reconstruction Technique* (ART) and similar *iterative* algorithms yield better quality reconstructions using limited views or a true 3-D reconstruction, but these algorithms are much more costly in execution time and memory. We can ameliorate this cost in execution time and memory by running the algorithm in parallel. Significant speed benefits are obtained compared to the sequential version of the ART algorithm. The iterative algorithms may have a role to play in limited view CT reconstruction or in 3-D CT reconstruction, and should not be rejected out of hand because of speed or memory limitations. These limitations are overcome significantly by implementing the algorithms in parallel, if communication is limited and an appropriate partitioning scheme is used.

The goal of medical imaging is to determine the internal structure of an organism with sufficient detail to yield diagnostic information. Imaging strives to achieve this in the least invasive manner possible, minimizing discomfort and harm to the patient. Two dimensional plain film X-ray pictures have been the standard medical imaging technique for a century, and remain a common technique today. An X-ray exposure of sufficient intensity and duration is used to project shadows of body tissues onto the detecting surface. The X-ray ‘beam’ is attenuated by scattering and absorption of the intervening tissue proportional to the distance the beam must traverse the tissue, the density of the tissue, and the atomic numbers of the contained elements. X-ray projections have at least three limitations: limited projection angles from which the X-ray view can be taken; inability to localize the 3-D position of a structure; and, most importantly, a lack of detail due to lack of contrast. The limitation of viewing angles is imposed by the target object and the imaging equipment.

There are two major families of reconstruction methods: filtered or Fourier backprojection (FBP), or convolution backprojection (CBP) methods, and iterative, or algebraic techniques. An image can be obtained by adding the detection value to every contributing voxel in the projection. If the target object has sharply defined contrasting regions, this *summation* method will cause these to be *blurred* much like a photograph out of focus. This summation is termed *backprojection* because it involves placing the projections back into the image. The terms *straight* backprojection or *unfiltered* backprojection is referred to the process when no other operations are performed on the backprojection image. We use the terms *Filtered backprojection (FBP)* or *convolution backprojection (CBP)* to refer to the whole group of filtered backprojection methods [4]. Although in principle the backprojected image could be deconvoluted using a 2-D filter, an equivalent transformation can be obtained by passing a 1D filter over the projection data *before* the backprojection in the case of parallel projections [5].

II. ALGEBRAIC RECONSTRUCTION TECHNIQUE (ART)

The Algebraic Reconstruction Technique (ART) was proposed by Gordon, Bender, and Herman as a method for the reconstruction of three-dimensional objects from electron-microscopic scans and X-ray photography [6]. There are number of variants which are known by the acronyms ART [7], SIRT (simultaneous iterative reconstruction technique) and SART (simultaneous algebraic reconstruction technique). In algebraic methods, the reconstruction is done by solving a system of linear equations. More precisely, ART can be written as a linear algebra problem, $Af = P$, where f is the unknown ($N^2 \times 1$) vector storing the values (f_1, \dots, f_N) of all $N = n^2$ surface elements or pixels in 2D or $N = n^3$ volume elements or voxels in 3D respectively, in the reconstruction grid. So, the image is represented as a single point in a N -dimensional space. P is the ($LK \times 1$) vector composed of the p_i values that represent the ray-sum measured with the i th ray, where L is number of views covering whole image suitable dispersed (equispaced on angular view) and K is the number of equispaced lines along each view, M is the total number of rays in all acquired projections. Finally, A is the ($M \times N$) weight (coefficient) matrix in which an emlement w_{ij} represents the contribution of the j th cell to the i th ray integral. The factor w_{ij} is equal to the fractional area of the j th image cell intercepted by the i th ray for one of the cells. The most of the w_{ij} 's are zero since only a small number of cells contribute to any given ray-sum. Algebraic Reconstruction Techniques (ART) was first published in the biomedical imaging literature in 1970 [7]. ART is a form of Gauss-Seidel iteration, and can be viewed as a generalization of the method of Kaczmarz in 1937 [8]. Algebraic Reconstruction Technique (ART) is a widely-used iterative method for solving sparse systems of linear equations. The main advantages of ART are its robustness, its cyclic convergence on inconsistent systems, and its relatively good initial convergence. ART is widely used as an iterative solution to the problem of image reconstruction from projections in computerized tomography (CT), where its implementation with a small relaxation parameter produces excellent results. It is shown that for this particular problem, ART can be implemented in parallel on a linear processor array [9].

The problem of CT reconstruction can be viewed as a system of linear equations. In this model, each pixel (voxel) j is assumed to have a homogenous attenuation f_j , an unknown value to be solved. The measured projection data is a set of attenuation sums P_i . Each P_i is the weighted sum of the attenuations of pixels along a given ray, also known as a ray integral or ray sum. Different variations of the model can be used to determine the weight w_{ij} that each pixel j contributes to the i th weighted attenuation sum P_i . Let us use a model where each weight w_{ij} is the product of the pixel's attenuation f_j and the length of the ray's intersection with the pixel (expressed in pixel widths). The weights can then be determined geometrically from the angle and position of the ray (these are determined from the geometry of the scanner) and the chosen pixel dimensions. As an example, we have an image of $N = 4$ pixels. There are 2 detectors in the detector array, and the array is rotated through 2 views (horizontal and vertical) to produce $M = 4$ ray sums [10]. We therefore have $M N = 16$ weights. The weights for raysum P_1 are calculated easily in this case. The ray traverses the width of pixel 1, so the weight of contribution of pixel 1 to the raysum is $w_{11} = 1$. Likewise, $w_{12} = 1$. Pixels 3 and 4 do not intersect ray 1, so $w_{13} = w_{14} = 0$. Similarly for the other rays in this example, all weights are 0 or 1, and the ray sum equations are as follows:

$$\begin{aligned} P_1 &= f_1 w_{11} + f_2 w_{12} + f_3 w_{13} + f_4 w_{14} = f_1 + f_2 \\ P_2 &= f_1 w_{21} + f_2 w_{22} + f_3 w_{23} + f_4 w_{24} = f_3 + f_4 \\ P_3 &= f_1 w_{31} + f_2 w_{32} + f_3 w_{33} + f_4 w_{34} = f_2 + f_4 \\ P_4 &= f_1 w_{41} + f_2 w_{42} + f_3 w_{43} + f_4 w_{44} = f_1 + f_3 \end{aligned} \quad (1)$$

In general, each ray P_i can be represented as:

$$P_i = \sum_{j=1}^N w_{ij} f_j, i = 1, 2, \dots, M \quad (2)$$

where M is the total number of rays(in all the projections) and w_{ij} is the weighting factor that represents the contribution of the j th image cell to the i th ray sum. The subscript i represents the projection index from a total of M projections. The subscript j represents the image index among N image cells. Half of the NM weights w_{ij} are zero. For the case of the 9 pixel Fig. 1 approximately two thirds of the weights are zero.

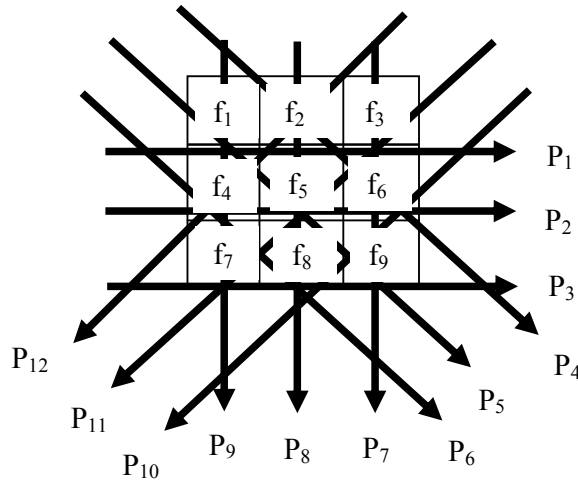


Fig. 1 The reconstruction problem as a system of linear equation

For the computer implementation of this method, we first make an initial guess at the solution. This guess, denoted by $\mathbf{f}^{(0)}$, is represented vectorially by $\mathbf{f}^{(0)}$ in the N -dimensional space. In most cases, we simply assign a value of zero to all the f_i 's. This initial guess is projected on the hyperplane represented by the equation in (2). When we project the $(i - 1)$ th solution onto the i th hyperplane [i th equation in (2)] the gray level of the j th element, whose current value is $f_j^{(i-1)}$, is obtained by correcting its current value by Δf_j , where

$$\Delta f_j = \frac{p_i - q_i}{\sum w_{ij}} \quad (3)$$

Note that while p_i is the measured ray-sum along the i th ray, q_i may be considered to be the computed ray-sum for the same ray based on the $(i - 1)$ th solution for the image gray levels. The correction Δf_j to the j th cell is obtained by first calculating the difference between the measured ray-sum and the computed ray-sum, normalizing this difference by $\sum w_{ij}$, and then assigning this value to all the image cells in the i th ray, each assignment being weighted by the corresponding w_{ij} . In general, for large images, a substantial portion of the weights are zero, because many of the pixels make no contribution to a particular raysum. One approach to solving large systems of equations, iterative approximations, forms the basis of the *iterative* or *algebraic* methods. Successive adjustments are made to the attenuation values until a solution is reached that is consistent with the projection values by some criterion. Iterative methods compare the computed ray sums of an estimated image with the original projection measurements and use the error obtained from this comparison to correct the estimated image. Though there is unlikely to be an exact solution because of inconsistencies, this method yields an approximate solution to the attenuation values.

III. ART EXAMPLE

ART consists of three steps:

1. Make an initial guess at the solution
2. Compute projections based on the guess
3. Refine the guess on the weighted difference between the actual projections and desired projections:

$$p^{(i+1)} = p^{(i)} + w(\text{desired} - \text{actual})$$

We have an image of 8×8 e.g. $N = 64$ pixels. There are 3 detectors in the detector array, and the array is rotated through 4 views (horizontal, vertical, diagonal and antidiagonal) to produce $M = 46$ raysums.

Starting with initial guess $\mathbf{f}^{(0)}$ and projections \mathbf{p} .

Table 1. Given Projection Value (

18	16	19	10	08	06
12	09	15	12	07	23
18	14	17	05	23	09
14	17	22	24	28	13
19	12	10	27	26	24
12	29	26	15	16	12
21	24	19	09	12	13
11	10	23	14	0	0

Table 2. Initial Image Data (

0	0	0	0	0	0	0	0
0	0	0	0	0	0	0	0
0	0	0	0	0	0	0	0
0	0	0	0	0	0	0	0
0	0	0	0	0	0	0	0
0	0	0	0	0	0	0	0
0	0	0	0	0	0	0	0
0	0	0	0	0	0	0	0

Table 3. Reconstructed Image after 55 iterations

9.52	5.12	2.91	3.06	5.06	7.56	7.44	2.18
8.26	2.38	2.45	2.48	2.57	9.36	6.89	2.89
4.77	5.37	1.97	7.80	5.38	2.43	4.81	4.17
4.12	4.63	4.03	1.95	3.71	1.87	1.86	4.11
2.48	3.71	4.09	6.74	1.79	1.78	1.79	2.25
2.56	5.01	3.04	4.7	2.01	1.81	1.95	2.32
1.74	2.38	2.32	7.52	7.09	2.28	2.11	5.34
4.66	1.58	2.57	3.73	5.19	2.76	8.19	2.57

Table 4. Error calculated in Image pixel values in each iteration

Iterations	$ f_{i+1} - f_i $	$(f_{i+1} - f_i)^2$	Iterations	$ f_{i+1} - f_i $	$(f_{i+1} - f_i)^2$
iteration 1	260.593750	1196.627930	iteration 51	0.224570	0.001947
iteration 2	23.196289	13.700123	iteration 52	0.218310	0.001832
iteration 3	11.863609	3.781413	iteration 53	0.212647	0.001732
iteration 4	7.293658	1.328680	iteration 54	0.207277	0.001643
iteration 5	4.558233	0.521878	iteration 55	0.202114	0.001562
iteration 6	3.167742	0.264142	iteration 56	0.197140	0.001489
iteration 7	2.423008	0.162381	iteration 57	0.189942	0.001412
iteration 8	2.041324	0.120152	iteration 58	0.184316	0.001340
iteration 9	1.793079	0.097458	iteration 59	0.179717	0.001276
iteration 10	1.660157	0.085381	iteration 60	0.175271	0.001217
iteration 11	1.581798	0.077365	iteration 61	0.171076	0.001162
iteration 12	1.523060	0.071226	iteration 62	0.167109	0.001112
iteration 13	1.475091	0.066224	iteration 63	0.163492	0.001064
iteration 14	1.392426	0.058907	iteration 64	0.160142	0.001020
iteration 15	1.280310	0.049823	iteration 65	0.156920	0.000978
iteration 16	1.194516	0.044186	iteration 66	0.153788	0.000939
iteration 17	1.149647	0.040100	iteration 67	0.150822	0.000901
iteration 18	1.113286	0.036847	iteration 68	0.147948	0.000866
iteration 19	1.080504	0.034161	iteration 69	0.145214	0.000832
iteration 20	1.031179	0.031026	iteration 70	0.142620	0.000800
iteration 21	0.921514	0.026042	iteration 71	0.140079	0.000769
iteration 22	0.870406	0.023270	iteration 72	0.137586	0.000740
iteration 23	0.828576	0.021274	iteration 73	0.135143	0.000712
iteration 24	0.793581	0.019673	iteration 74	0.132742	0.000685
iteration 25	0.763604	0.018317	iteration 75	0.130393	0.000660
iteration 26	0.730673	0.016935	iteration 76	0.128084	0.000635
iteration 27	0.667299	0.014663	iteration 77	0.125825	0.000612
iteration 28	0.625723	0.013222	iteration 78	0.123611	0.000589
iteration 29	0.595970	0.012142	iteration 79	0.121439	0.000568
iteration 30	0.570434	0.011251	iteration 80	0.119310	0.000547
iteration 31	0.547994	0.010501	iteration 81	0.117219	0.000527
iteration 32	0.526815	0.009855	iteration 82	0.115158	0.000508
iteration 33	0.507945	0.009292	iteration 83	0.113141	0.000490
iteration 34	0.490216	0.008796	iteration 84	0.111161	0.000472
iteration 35	0.473685	0.008356	iteration 85	0.109214	0.000455
iteration 36	0.458431	0.007963	iteration 86	0.107293	0.000439
iteration 37	0.445886	0.007611	iteration 87	0.105417	0.000423
iteration 38	0.405795	0.006125	iteration 88	0.103568	0.000408
iteration 39	0.383962	0.005421	iteration 89	0.101752	0.000393
iteration 40	0.364060	0.005004	iteration 90	0.099965	0.000379
iteration 41	0.349298	0.004716	iteration 91	0.098218	0.000366
iteration 42	0.337096	0.004498	iteration 92	0.096495	0.000353
iteration 43	0.326862	0.004320	iteration 93	0.094801	0.000340
iteration 44	0.312715	0.004116	iteration 94	0.093147	0.000328
iteration 45	0.303181	0.003968	iteration 95	0.091513	0.000317
iteration 46	0.282642	0.003183	iteration 96	0.089912	0.000306
iteration 47	0.260532	0.002731	iteration 97	0.088335	0.000295
iteration 48	0.247859	0.002447	iteration 98	0.086793	0.000284
iteration 49	0.239172	0.002243	iteration 99	0.085267	0.000274
iteration 50	0.231610	0.002081	iteration 100	0.083781	0.000265

Table 5. Error calculated in projection values in each iteration

Iteration	$ p_{i+1} - p_i $	$(p_{i+1} - p_i)^2$	Iteration	$ p_{i+1} - p_i $	$(p_{i+1} - p_i)^2$
iteration 1	743.000000	552049.000000	iteration 51	0.025269	0.000639
iteration 2	299.375000	89625.390625	iteration 52	0.015503	0.000240
iteration 3	34.851563	1214.631444	iteration 53	0.008484	0.000072
iteration 4	7.800537	60.848377	iteration 54	0.003235	0.000010
iteration 5	2.252258	5.072666	iteration 55	0.000122	0.000000
iteration 6	1.376648	1.895160	iteration 56	0.003113	0.000010
iteration 7	1.503113	2.259349	iteration 57	0.005066	0.000026
iteration 8	0.413391	0.170892	iteration 58	0.016296	0.000266
iteration 9	0.408203	0.166630	iteration 59	0.008850	0.000078
iteration 10	0.084229	0.007095	iteration 60	0.012573	0.000158
iteration 11	0.162964	0.026557	iteration 61	0.014099	0.000199
iteration 12	0.281250	0.079102	iteration 62	0.013611	0.000185
iteration 13	0.287781	0.082818	iteration 63	0.013855	0.000192
iteration 14	0.296143	0.087701	iteration 64	0.013977	0.000195
iteration 15	0.178223	0.031763	iteration 65	0.014221	0.000202
iteration 16	0.026123	0.000682	iteration 66	0.013855	0.000192
iteration 17	0.151184	0.022857	iteration 67	0.014099	0.000199
iteration 18	0.176514	0.031157	iteration 68	0.013977	0.000195
iteration 19	0.169983	0.028894	iteration 69	0.014343	0.000206
iteration 20	0.170715	0.029144	iteration 70	0.013916	0.000194
iteration 21	0.112366	0.012626	iteration 71	0.013916	0.000194
iteration 22	0.139038	0.019332	iteration 72	0.013672	0.000187
iteration 23	0.039978	0.001598	iteration 73	0.013672	0.000187
iteration 24	0.069458	0.004824	iteration 74	0.013611	0.000185
iteration 25	0.083069	0.006900	iteration 75	0.013306	0.000177
iteration 26	0.085999	0.007396	iteration 76	0.013000	0.000169
iteration 27	0.069275	0.004799	iteration 77	0.013123	0.000172
iteration 28	0.086426	0.007469	iteration 78	0.012695	0.000161
iteration 29	0.016052	0.000258	iteration 79	0.012695	0.000161
iteration 30	0.037842	0.001432	iteration 80	0.012451	0.000155
iteration 31	0.045349	0.002057	iteration 81	0.012207	0.000149
iteration 32	0.049072	0.002408	iteration 82	0.011780	0.000139
iteration 33	0.051208	0.002622	iteration 83	0.011902	0.000142
iteration 34	0.053040	0.002813	iteration 84	0.011719	0.000137
iteration 35	0.054199	0.002938	iteration 85	0.011475	0.000132
iteration 36	0.055054	0.003031	iteration 86	0.011230	0.000126
iteration 37	0.055420	0.003071	iteration 87	0.010986	0.000121
iteration 38	0.055847	0.003119	iteration 88	0.010803	0.000117
iteration 39	0.165771	0.027480	iteration 89	0.010803	0.000117
iteration 40	0.128113	0.016413	iteration 90	0.010376	0.000108
iteration 41	0.078308	0.006132	iteration 91	0.010315	0.000106
iteration 42	0.049988	0.002499	iteration 92	0.010132	0.000103
iteration 43	0.032349	0.001046	iteration 93	0.010010	0.000100
iteration 44	0.020630	0.000426	iteration 94	0.009583	0.000092
iteration 45	0.041748	0.001743	iteration 95	0.009827	0.000097
iteration 46	0.018555	0.000344	iteration 96	0.009338	0.000087
iteration 47	0.109314	0.011950	iteration 97	0.009338	0.000087
iteration 48	0.098145	0.009632	iteration 98	0.009155	0.000084
iteration 49	0.060730	0.003688	iteration 99	0.008789	0.000077
iteration 50	0.039795	0.001584	iteration 100	0.008850	0.000078

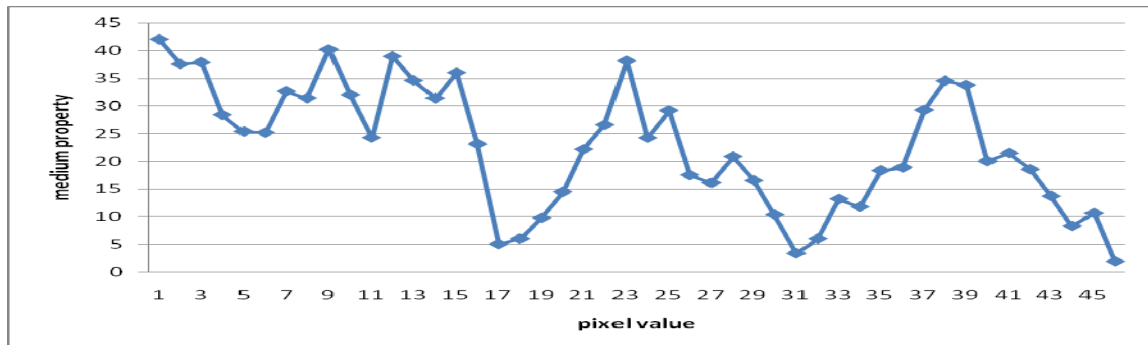


Fig 1. Image as a line Graph using ART after 01 iteration

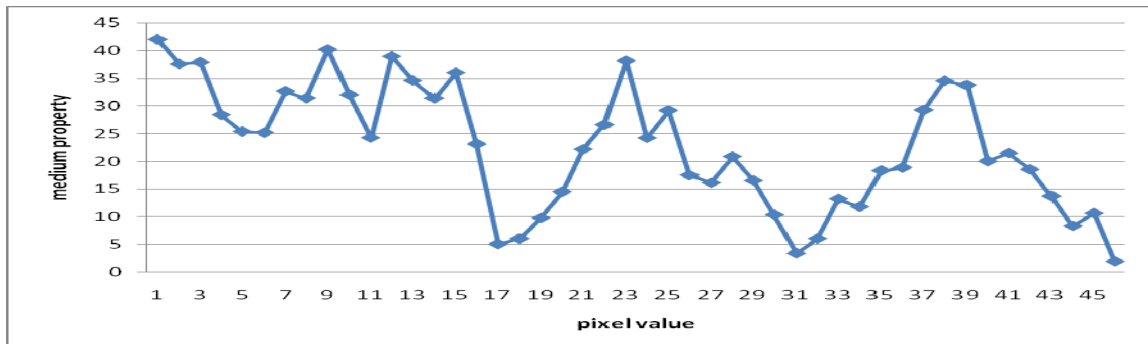


Fig 2. Image as a line Graph using ART after 15 iterations

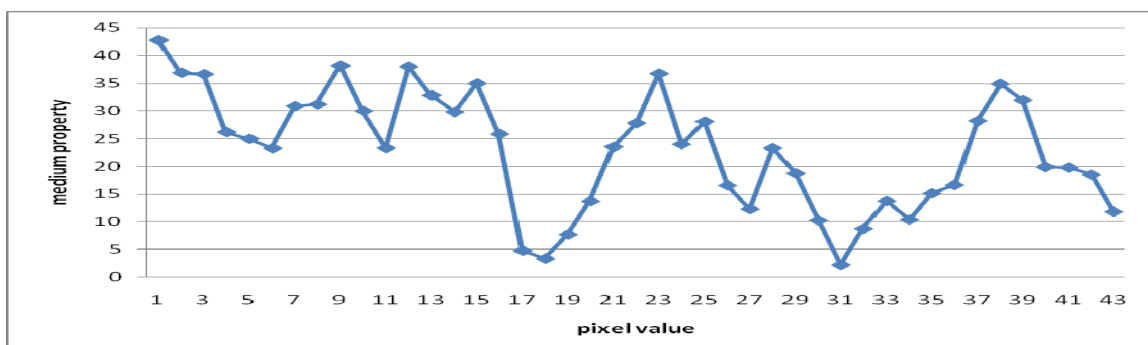


Fig 3. Image as a line Graph using ART after 25 iterations

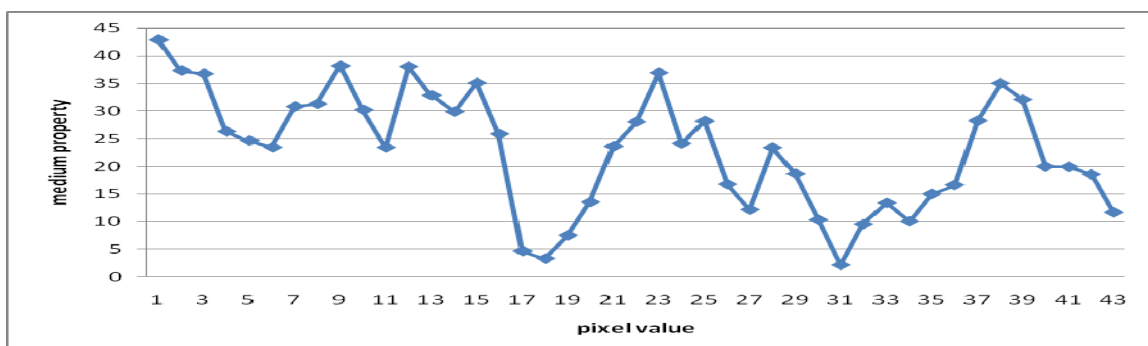


Fig 4. Image as a line Graph using ART after 55 iterations

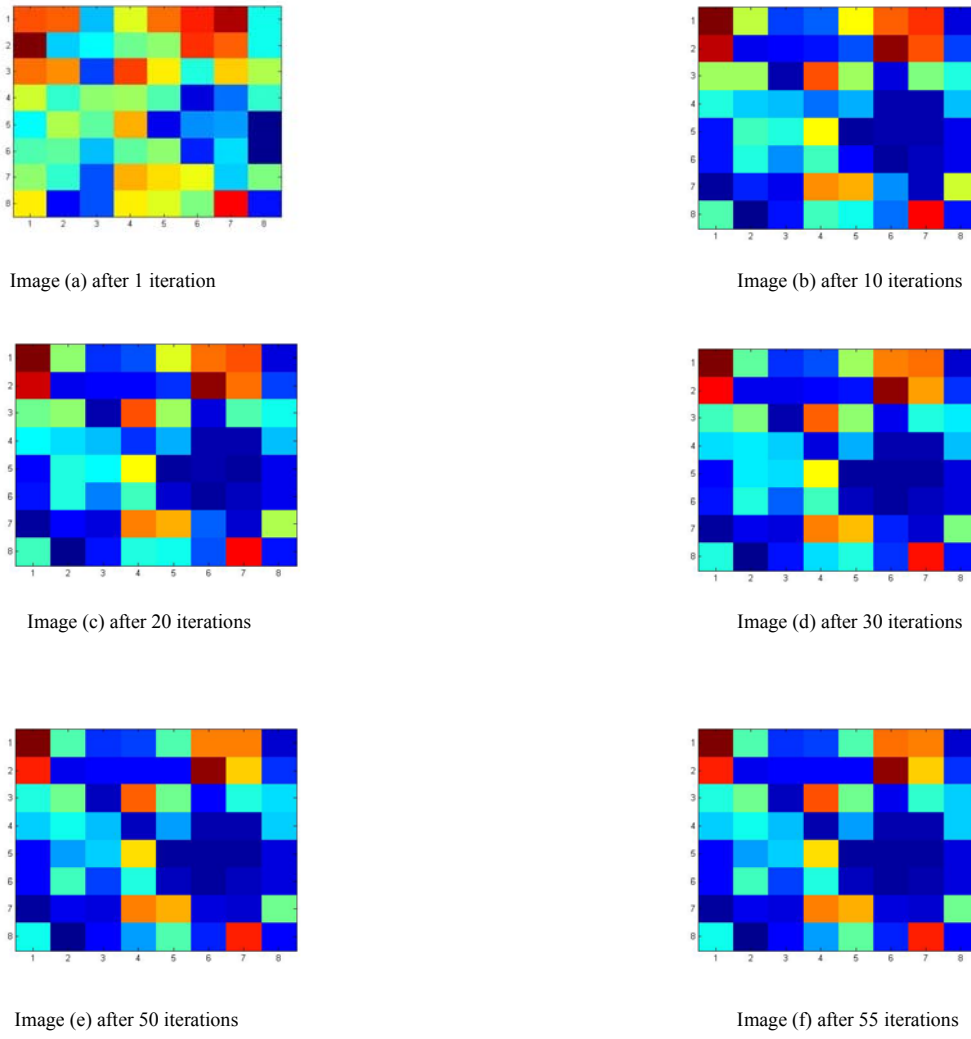


Fig.5 Reconstruction at different iterations

CONCLUSION

The convergence is tested by difference in projection data at each iteration which is taken as $\sum_{i=1}^M |p_i - p_i^{(k)}|$ and $\sum_{i=1}^M (p_i - p_i^{(k)})^2$ at k^{th} iteration ($k = 1, 2, 3, \dots$). The stopping criterion taken as $\sum_{i=1}^M (p_i - p_i^{(k)})^2$ is small enough or stabilizes. The accuracy is also tested by another measure, image difference at successive iterations i.e. $\sum_{i=1}^M |f_i^{(k+1)} - f_i^{(k)}|$ and $\sum_{i=1}^M (f_i^{(k+1)} - f_i^{(k)})^2$. These results for our example are given in table 5 and table 4 respectively. We observe that after the difference in projection reaches at its minimum it again starts increasing, which says our stopping criterion should be guided by projection difference rather than a large number of iterations. In present example we reach at this minima in 55th iteration.

REFERENCES

- [1] Seeram E. Computed tomography, physical principles – clinical applications, and quality control. 2nd edition, WB Saunders Co. 2000; 1-8.
- [2] Shepp, L.A. and Kruskal, J.B., “Computerized tomography: The new medical x-ray technology”, Am. Math. Monthly, 85, pp. 420-439, 1978.
- [3] J. Friedhoff, Aufbereitung von 3D-Digitalisierdaten für den Werkzeug-, Formen-und Modellbau, Vulkan Verlag, Essen 1997.
- [4] C. Kak, M. Slaney, *Principles of Computerized Tomography*, Society for Industrial and Applied Mathematics, 2001, pp49-60, 275-285
- [5] Robert M. Lewitt (1983): Reconstruction Algorithms: Transform Methods, IEEE proceeding vol. 71, pp 390-408.
- [6] R. Gordon *et al.*, “Three-Dimensional Reconstruction from Projections: A Review of Algorithms”, International Review of Cytology, Vol. 38, p. 111 (1974).

- [7] R. Gordon, R. Bender, and G. T. Herman, "Algebraic reconstruction techniques (ART) for three-dimensional electron microscopy and X-ray photography," *J. Theoret. Biol.*, vol. 29, pp. 471-482, 1970.
- [8] S. Kaczmarz, "Angentihre Auflösung von Systemen linearer Gleichungen," *Bull. Int. Acad. Pol. Sei. Lett., A*, vol. 35, pp. 355-357, 1937.
- [9] Dan Gordan, "Parallel ART for image reconstruction in CT using processor arrays", *The International Journal of Parallel, Emergent and Distributed Systems*, Vol. 21, No. 5, October 2006, 365-380.
- [10] Tanuja Srivastava, Raghveer Singh and Nirvikar, "ART for Image Reconstruction Using Parallel Beam Projection Data", *International Journal of Information Sciences and Applications*, ISSN 0974-2255 Volume 2, Number 4 (2010), pp. 627-630.

AUTHORS PROFILE

NIRVIKAR

Research Scholar

School of CS & IT

Shobhit University, Meerut (UP), India

- ❖ Pursuing Ph.D. from School of Computer Engg. & IT, SHOBHIT UNIVERSITY, MEERUT on the topic of "Algebraic Reconstruction Technique for Computerized Tomography using Parallel Beam Projection Data".

ART for Image Reconstruction Using Parallel Beam Projection Data

Tanuja Srivastava¹, Raghuveer Singh² and Nirvikar³

¹Department of Mathematics, IIT Roorkee, Uttarakhand, India

²Shobhit University, Meerut, UP, India

³Department of CSE, Shobhit University, Meerut, UP, India

Abstract

Algebraic Reconstruction Technique (ART) is a method for reconstructing images for CT from projections. It is widely used in applications such as Computed Tomography (CT). CT is a method to reconstruct cross sections of the interior structure of an object without destructing or damaging the object.

Keywords: ART, CT, Image processing, Projections, Reconstruction

Introduction

The initial use of computed tomography (CT) for applications in radiological diagnostics during the seventies sparked a revolution in the field of medical engineering. More recently, however, medical imaging has also been successfully accomplished with radioisotopes, ultrasound, and magnetic resonance. There are numerous nonmedical imaging application, which lend themselves to the methods of CT like the mapping of underground resources via crossboreholes imaging (e.g. estimation of depth to water table, geological and hydrological mapping etc.), some specialized cases of cross sectional imaging for nondestructive testing, the determination of the brightness distribution over a celestial sphere, and three dimensional imaging with electron microscopy. And even throughout the eighties, a CT examination lost little if any of its special and exclusive character. In the meantime, however, times have changed. Today computed tomography represents a perfectly natural and established technology which has advanced to

become an indispensable and integral component of routine work in clinics and medical practices.

The classic application of industrial X-ray computed tomography (CT) is the inspection and three-dimensional measurement of metal and plastic castings. However, phoenix x-ray's high-resolution X-ray technology opens up a variety of new applications in fields such as sensor technology, electronics, materials science, and many other natural sciences.

In the last years, industrial computed tomography (CT) in Switzerland had its main application in scientific examinations. Specific fields of interest were flaw detection, analysis of failure, dimensional measurements of not accessible geometrical features, inspection of assemblies or statistical investigations of material properties as density distribution. Single slices were taken at well-defined places and used for further analysis[4].

Today, the most important application of CT has become scanning for 3D-digitizing purposes [5]. First of all, automotive and motorcycle industries as well as their suppliers and the medical technology show a very strong interest in the new possibilities that CT offers. Using this new technology it is possible to reduce the time to market for development of new products. Thus companies can realise substantial competitive advantages.

Algebraic Reconstruction Technique (ART)

The Algebraic Reconstruction Technique (ART) introduced by Gordan, Bender and Herman[1]

uses three or more projections to reconstruct the 2-dimensional beam density distribution. They have shown that the improvement in the quality of the reconstruction is pronounced when a third projection is added, but additional projections add much less to the reconstruction quality. Algebraic Reconstruction Techniques (ART) was first published in the biomedical imaging literature in 1970 [2]. From the mathematical point of view, they are variations of the iterative method for solving a system of simultaneous equations introduced by Kaczmarz in 1937 [3].

ART can produce high-quality reconstructions with excellent computational efficiency. The Algebraic Reconstruction Technique (ART) uses three or more projections to reconstruct 3-dimensional density profiles.

The ART algorithms have a simple intuitive basis. Each projected density is thrown back across the reconstruction space in which the densities are iteratively modified to bring each reconstructed projection into agreement with the measured projection. Assuming that the pattern being reconstructed is enclosed in a square space of $n \times n$ array of small pixels, p_j ($j = 1, \dots, n^2$) is grayness or density number, which is uniform within the pixel but different from other pixels. A "ray" is a region of the square space which lies between two parallel lines. The weighted ray sum is the total grayness of the reconstruction figure within the ray. The projection at a given angle is then the sum of non-overlapping, equally wide rays covering the figure. The ART algorithm consists of altering the grayness of each pixel intersected by the ray in such a way as to make the ray sum agree with the corresponding element of the measured projection.

The ART algorithm begins with some initial estimate of the image to be reconstructed (usually taken as a uniformly gray image). It modifies this estimate repeatedly until the pixel values appear to converge by some criterion. ART decides how to modify the image by summing the pixels along some straight path and comparing this sum to the measured ray sum (referred to earlier as an "X-ray projection"). The difference between projections calculated from the image estimate, and the measured ray is calculated, and the adjustment is divided among the pixels in the ray sum.

The methods of algebraic reconstruction techniques (ART) in computerized tomography are based on a representation of the projection line integrals as discrete ray-sums [2][6][7]. Let p_i be the ray-sum measured with the i th ray then the

relationship between the f_j 's and p_i 's may be expressed as

$$P_i = \sum_{j=1}^N w_{ij} f_j, i = 1, 2, \dots, M \quad (1)$$

where M is the total number of rays(in all the projections) and w_{ij} is the weighting factor that represents the contribution of the j th cell to the i th ray integral. The subscript m represents the projection index from a total of M projections. The subscript n represents the ray index among N rays within each projection.

For large values of M and N there exist very attractive iterative methods for solving (1). These are based on the "method of projections" as first proposed by Kaczmarz [3], and later elucidated further by Tanabe [8]. To explain the computational steps involved in these methods, we first write (1) in an expanded form:

$$w_{11}f_1 + w_{12}f_2 + \dots + w_{1N}f_N = p_1 \\ w_{21}f_1 + w_{22}f_2 + \dots + w_{2N}f_N = p_2$$

$$\dots \\ w_{M1}f_1 + w_{M2}f_2 + \dots + w_{MN}f_N = p_M \quad (2)$$

Therefore, an image, represented by (f_1, f_2, \dots, f_N) , may be considered to be a single point in an N -dimensional space. In this space each of the above equations represents a hyperplane. When a unique solution to these equations exists, the intersection of all these hyperplanes is a single point giving that solution.

The computational procedure for locating the solution consists of first starting with an initial guess, projecting this initial guess on the first line, reprojecting the resulting point on the second line, and then projecting back onto the first line, and so forth. If a unique solution exists, the iterations will always converge to that point.

For the computer implementation of this method, we first make an initial guess at the solution. This guess, denoted by $f_1^{(0)}, f_2^{(0)}, \dots, f_N^{(0)}$, is represented vectorially by $\vec{f}^{(0)}$ in the N -dimensional space. In most cases, we simply assign a value of zero to all the f_i 's. This initial guess is projected on the hyperplane represented by the first equation in (2).

As mentioned before, the computational procedure for algebraic reconstruction consists of starting with an initial guess for the solution,

taking successive projections on the hyperplanes represented by the equations in (2), eventually yielding $\tilde{f}^{(M)}$. In the next iteration, $\tilde{f}^{(M)}$ is projected on the hyperplane represented by the first equation in (2), and then successively onto the rest of the hyperplanes in (2), to yield $\tilde{f}^{(2M)}$, and so on. Tanabe [8] has shown that if there exists a unique solution \tilde{f}_s to the system of equations (2), then

$$\lim_{n \rightarrow \infty} \tilde{f}^{(kn)} = \tilde{f}_s. \quad (3)$$

When we project the $(i - 1)$ th solution onto the i th hyperplane [i th equation in (2)] the gray level of the j th element, whose current value is $f_j^{(i-1)}$, is obtained by correcting its current value by $\Delta f_j^{(i)}$, where

$$\Delta f_j^{(i)} = f_j^{(i)} - f_j^{(i-1)} = \frac{p_i - q_i}{\sum_{k=1}^N w_{ik}^2} w_{ij} \quad (4)$$

Note that while p_i is the measured ray-sum along the i th ray, q_i may be considered to be the computed ray-sum for the same ray based on the $(i - 1)$ th solution for the image gray levels. The correction Δf_j to the j th cell is obtained by first calculating the difference between the measured ray-sum and the computed ray-sum, normalizing this difference by $\sum_{k=1}^N w_{ik}^2$, and then assigning this value to all the image cells in the i th ray, each assignment being weighted by the corresponding w_{ij} .

In many ART implementations the w_{ik} 's in (4) are simply replaced by 1's and 0's, depending upon whether the center of the k th image cell is within the i th ray. This makes the implementation easier because such a decision can easily be made at computer run time. In this case the denominator in (4) is given by $\sum_{k=1}^N w_{ik}^2 = N_i$ which is the number of image cells whose centers are within the i th ray. The correction to the j th image cell from the i th equation in (2) may now be written as

$$\Delta f_j^{(i)} = \frac{p_i - q_i}{N_i} \quad (5)$$

The approximation in (5), although easy to implement, often leads to artifacts in the reconstructed images, especially if N_i isn't a good approximation to the denominator. Superior reconstructions may be obtained if (5) is replaced by

$$\Delta f_j^{(i)} = \frac{p_i - q_i}{L_i} \quad (6)$$

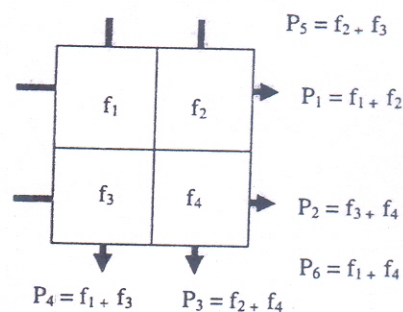
where L_i is the length (normalized by δ) of the i th ray through the reconstruction region.

ART reconstructions usually suffer from salt and pepper noise, which is caused by the inconsistencies introduced in the set of equations by the approximations commonly used for w_{ik} 's. It is possible to reduce the effects of this noise in ART reconstructions by relaxation, in which we update a pixel by $\alpha \cdot \Delta f_j^{(i)}$, where α is less than 1. In some cases, the relaxation parameter α is made a function of the iteration number; that is, it becomes progressively smaller with increase in the number of iterations. The resulting improvements in the quality of reconstruction are usually at the expense of convergence.

ART consists of three steps:

- Make an initial guess at the solution
- Compute projections based on the guess
- Refine the guess on the weighted difference between the actual projections and desired projections:

$$p^{i+1} = p^i + g \text{ (desired - actual)}$$



For example, if we have our favorite small image and its projections

$$\begin{bmatrix} w & x \\ y & z \end{bmatrix} \begin{bmatrix} 1 & 1 \\ 1 & 1 \end{bmatrix}$$

$$6 \ 10 \quad 8 \ 12$$

then:

1. Initial guess and projections

$$\begin{bmatrix} 0 & 0 \\ 0 & 0 \\ 0 & 0 \end{bmatrix} \begin{bmatrix} 0 & 0 \\ 0 & 0 \\ 0 & 0 \end{bmatrix}$$

2. Refine projection I, view 1, $\theta=0^0$ (assume $g = 1$)

$$\begin{bmatrix} w \\ x \\ y \\ z \end{bmatrix} = \begin{bmatrix} 0 + \frac{11 - 0}{2} \\ 0 + \frac{11 - 0}{2} \\ 0 + \frac{7 - 0}{2} \\ 0 + \frac{7 - 0}{2} \end{bmatrix} = \begin{bmatrix} 5.5 \\ 5.5 \\ 3.5 \\ 3.5 \end{bmatrix}$$

3. Refine projection II, view 2, $\theta=90^0$

$$\begin{bmatrix} w \\ x \\ y \\ z \end{bmatrix} = \begin{bmatrix} 5.5 + \frac{10 - 9}{2} \\ 5.5 + \frac{8 - 9}{2} \\ 3.5 + \frac{10 - 9}{2} \\ 3.5 + \frac{8 - 9}{2} \end{bmatrix} = \begin{bmatrix} 6 \\ 5 \\ 4 \\ 3 \end{bmatrix}$$

4. Refine projection III, view 3, $\theta=45^0$

$$\begin{bmatrix} w \\ x \\ y \\ z \end{bmatrix} = \begin{bmatrix} 6 + \frac{12 - 9}{2} \\ 5 + \frac{6 - 9}{2} \\ 4 + \frac{12 - 9}{2} \\ 3 + \frac{6 - 9}{2} \end{bmatrix} = \begin{bmatrix} 7.5 \\ 3.5 \\ 2.5 \\ 4.5 \end{bmatrix}$$

$$\begin{bmatrix} 7.5 & 3.5 \\ 2.5 & 4.5 \end{bmatrix} \begin{bmatrix} 11 \\ 7 \end{bmatrix}$$

$$\begin{bmatrix} 6 & 10 \\ 8 & 12 \end{bmatrix}$$

We are now done; the image data and projections match.

In general, M and N are quite large. For example, when reconstructing an image size of 256×256 pixels, from 256 detector measurements in each of 256 views, N and M are both 65,536. In such cases the weight matrix size is $65,536 \times 65,536 = 4,294,967,296$. We require algorithms that are efficient in terms of both time and memory requirements to solve this on a computer without increasing turnaround time in the CT suite.

Conclusion

We have tested an iterative algorithm for reconstructing images with three projections using the algebraic reconstruction technique. The algorithm now experimented with more numbers of projections to find the image data.

References

- [1] R. Gordon *et al.*, "Three-Dimensional Reconstruction from Projections: A Review of Algorithms", International Review of Cytology, Vol. 38, p. 111 (1974).
- [2] R. Gordon, R. Bender, and G. T. Herman, "Algebraic reconstruction techniques (ART) for three-dimensional electron microscopy and X-ray photography," *J. Theoret. Biol.*, vol. 29, pp. 471-482, 1970.
- [3] S. Kaczmarz, "Angentirte Auflosung von Systemen linearer Gleichungen," *Bull. Int. Acad. Pol. Sci. Lett., A*, vol. 35, pp. 355-357, 1937.
- [4] Flisch *et al.*, ETH Zürich "Industrial Computed Tomography in Reverse Engineering Applications" Industrial Applications and Image Processing in Radiology March, 15 - 17, 1999 Berlin, Germany.
- [5] J. Friedhoff, Aufbereitung von 3D-Digitalisierdaten für den Werkzeug-, Formen-und Modellbau, Vulkan Verlag, Essen 1997.
- [6] Herman, G.T., Image Reconstruction from Projections: The Fundamentals of Computerized Tomography, Academic Press, New York, 1980.
- [7] C. N. Hounsfield, "A method of and apparatus for examination of a body by radiation such as X or Gamma radiation." Patent Specification 1283915, London, 1968.
- [8] K. Tanabe, "Projection method for solving a singular system," *Numer. Math.*, vol. 17, pp. 203-214, 1971.
- [9] A. H. Andersen and A. C. Kak, "Simultaneous algebraic reconstruction technique (SART): A superior implementation of the art algorithm," *Ultrason. Imaging*, vol. 6, pp. 81-94, Jan. 1984.

Reconstruction with Parallel Projections using ART

Nirvikar
Shobhit University
Meerut, India

Raghuvir Singh
Shobhit University
Meerut, India

ABSTRACT

Algebraic Reconstruction Technique (ART) is most accurate method for image reconstruction. In present paper the accuracy of ART is shown with parallel projections, in all only 16 projections with about 60 iterations are used to obtain reconstruction.

Keywords

ART, CT, Image processing, Projections, Reconstruction

1. INTRODUCTION

The word *tomography* means “reconstruction from projections”, i.e. the recovery of a function from its line or (hyper) plane integrals (from the Greek – slice and –to write). In the applied sense, it is a method to reconstruct cross sections of the interior structure of an object without destructing or damage the object. The term often occurs in the combination *computerized (computed) tomography* (CT) or *computer-assisted tomography* (CAT), since for performing the reconstruction in practice one needs the use of a digital computer. The initial use of computed tomography (CT) for applications in radiological diagnostics during the seventies sparked a revolution in the field of medical engineering [3][7]. More recently, however, medical imaging has also been successfully accomplished with radioisotopes, ultrasound, and magnetic resonance. There are numerous nonmedical imaging application, which lend themselves to the methods of CT like the mapping of underground resources via crossboresholes imaging (e.g. estimation of depth to water table, geological and hydrological mapping etc.), some specialized cases of cross sectional imaging for nondestructive testing, the determination of the brightness distribution over a celestial sphere, and three dimensional imaging with electron microscopy. And even throughout the eighties, a CT examination lost little if any of its special and exclusive character. In the meantime, however, times have changed. Today computed tomography represents a perfectly natural and established technology which has advanced to become an indispensable and integral component of routine work in clinics and medical practices.

The classic application of industrial X-ray computed tomography (CT) is the inspection and three-dimensional measurement of metal and plastic castings. However, phoenix x-ray's high-resolution X-ray technology opens up a variety of new applications in fields such as sensor technology, electronics, materials science, and many other natural sciences.

In last years, industrial computed tomography (CT) in Switzerland had its main application in scientific examinations. Specific fields of interest were flaw detection, analysis of failure, dimensional measurements of not accessible geometrical features, inspection of assemblies or statistical investigations of material properties as

density distribution. Single slices were taken at well-defined places and used for further analysis[4].

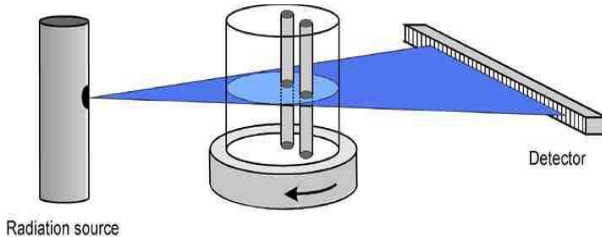


Fig 1. Computed Tomography Scan Process

Today, the most important application of CT has become scanning for 3D-digitizing purposes [5]. First of all, automotive and motorcycle industries as well as their suppliers and the medical technology show a very strong interest in the new possibilities that CT offers. Using this new technology it is possible to reduce the time to market for development of new products. Thus companies can realize substantial competitive advantages.

2. ALGEBRAIC RECONSTRUCTION TECHNIQUE (ART)

The Algebraic Reconstruction Technique (ART) introduced by Gordan, Bender and Herman[1] uses a large number of projections to reconstruct the 2-dimensional beam density distribution. Algebraic Reconstruction Techniques (ART) was first published in the biomedical imaging literature in 1970 [2]. From the mathematical point of view, they are variations of the iterative method for solving a system of simultaneous equations introduced by Kaczmarz in 1937 [3]. ART can produce high-quality reconstructions with excellent computational efficiency.

The ART algorithms have a simple intuitive basis. Each projected density is thrown back across the reconstruction space in which the densities are iteratively modified to bring each reconstructed projection into agreement with the measured projection. Assuming that the object being reconstructed is enclosed in a square space of $n \times n$ array of small pixels, p_j ($j = 1 \dots n^2$) is grayness or density number, which is uniform within the pixel but different from other pixels. A “ray” is a region of the square space which lies between two parallel lines. The weighted ray sum is the total grayness of the reconstruction figure within the ray. The projection at a given angle is then the sum of non-overlapping, equally wide rays covering the object. The ART algorithm consists of altering the grayness of each pixel intersected by the ray in such a way as to make the ray sum agree with the corresponding element of the measured projection.

The ART algorithm begins with some initial estimate of the image to be reconstructed (usually taken as a uniformly gray image). It modifies this estimate repeatedly until the pixel values appear to converge by some criterion. ART decides how to modify the image by summing the pixels along some straight path and comparing this sum to the measured ray sum (referred to earlier as an “X-ray projection”). The difference between projections calculated from the image estimate, and the measured ray is calculated, and the adjustment is divided among the pixels in the ray sum.

The methods of algebraic reconstruction techniques (ART) in computerized tomography are based on a representation of the projection line integrals as discrete ray-sums [2][6][7]. Let p_i be the ray-sum measured with the i th ray then the relationship between the f_j 's and p_i 's may be expressed as

$$p_i = \sum_{j=1}^N w_{ij} f_j, i = 1, 2, \dots, M \quad (1)$$

where M is the total number of rays(in all the projections) and w_{ij} is the weighting factor that represents the contribution of the j th cell to the i th ray integral. The subscript m represents the projection index from a total of M projections. The subscript n represents the ray index among N rays within each projection.

For large values of M and N there exist very attractive iterative methods for solving (1). These are based on the “method of projections” as first proposed by Kaczmarz [3], and later elucidated further by Tanabe [8]. To explain the computational steps involved in these methods, we first write (1) in an expanded form:

$$\begin{aligned} w_{11}f_1 + w_{12}f_2 + \dots + w_{1N}f_N &= p_1 \\ w_{21}f_1 + w_{22}f_2 + \dots + w_{2N}f_N &= p_2 \end{aligned}$$

$$w_{M1}f_1 + w_{M2}f_2 + \dots + w_{MN}f_N = p_M \quad (2)$$

Therefore, an image, represented by (f_1, f_2, \dots, f_N) , may be considered to be a single point in an N -dimensional space. In this space each of the above equations represents a hyperplane. When a unique solution to these equations exists, the intersection of all these hyperplanes is a single point giving that solution.

The computational procedure for locating the solution consists of first starting with an initial guess, projecting this initial guess on the first line, reprojecting the resulting point on the second line, and then projecting back onto the first line, and so forth. If a unique solution exists, the iterations will always converge to that point.

For the computer implementation of this method, we first make an initial guess at the solution. This guess, denoted by $f_1^{(0)}, f_2^{(0)}, \dots, f_N^{(0)}$, is represented vectorially by $\vec{f}^{(0)}$ in the N -dimensional space. In most cases, we simply assign a value of

zero to all the f_i 's. This initial guess is projected on the hyperplane represented by the first equation in (2).

As mentioned before, the computational procedure for algebraic reconstruction consists of starting with an initial guess for the solution, taking successive projections on the hyperplanes represented by the equations in (2), eventually yielding $\vec{f}^{(M)}$. In the next iteration, $\vec{f}^{(M)}$ is projected on the hyperplane represented by the first equation in (2), and then successively onto the rest of the hyperplanes in (2), to yield $\vec{f}^{(2M)}$, and so on. Tanabe [8] has shown that if there exists a unique solution \vec{f}_s to the system of equations (2), then

$$\lim_{k \rightarrow \infty} \vec{f}^{(kM)} = \vec{f}_s. \quad (3)$$

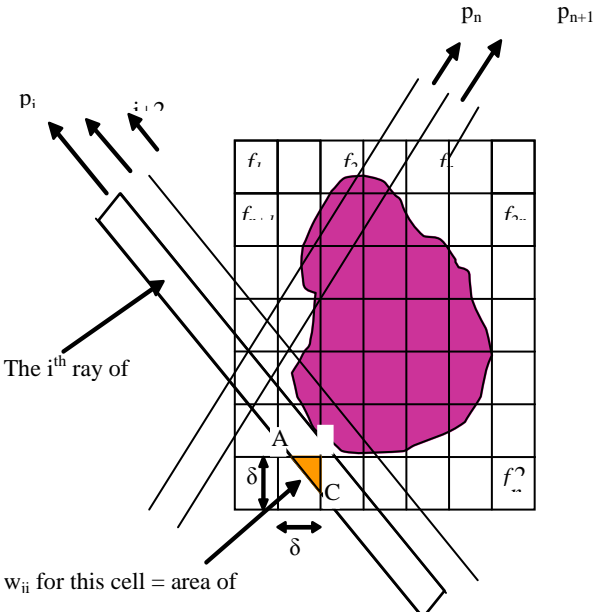


Fig 2. Image with a grid superimposed onto it, where image values are assumed to be constant within a cell.

When we project the $(i - 1)$ th solution onto the i th hyperplane [i th equation in (1)] the gray level of the j th element, whose current value is $f_j^{(i-1)}$, is obtained by correcting its current value by $\Delta f_j^{(i)}$, where

$$\Delta f_j^{(i)} = f_j^{(i)} - f_j^{(i-1)} = \frac{p_i - q_i}{\sum_{k=1}^N w_{ik}^2} w_{ij}. \quad (4)$$

where p_i is the measured ray-sum along the i th ray, q_i is the computed ray-sum for the same ray based on the $(i - 1)$ th solution for the image gray levels. The correction Δf_j , to the j th cell is obtained by first calculating the difference between the measured ray-sum and the computed ray-sum, normalizing this difference by $\sum_{k=1}^N w_{ik}^2$ and then assigning this value to all the image cells in the i th ray, each assignment being weighted by the corresponding w_{ij} .

- Generic ART procedure:
1. Prepare an initial estimate
 2. Compute projections based on the guess
 3. Refine the guess on the weighted difference between the actual projections and desired projections
 4. Perform Steps 2 and 3 for all rays available
 5. Repeat steps 2-4 as many times as required

Different variations of the model can be used to determine the weight w_{ij} that each pixel j contributes to the i th weighted attenuation sum P_i . Let us use a model where each weight w_{ij} is the product of the pixel's attenuation f_j and the length of the ray's intersection with the pixel (expressed in pixel widths). The weights can then be determined geometrically from the angle and position of the ray (these are determined from the geometry of the scanner) and the chosen pixel dimensions.

ART simple example,

we have an image of $N = 9$ pixels. There are 3 detectors in the detector array, and the array is rotated through 4 views (horizontal, vertical, diagonal and antidiagonal) to produce $M = 16$ raysums.

- make initial guess
- while convergence not reached //
- iteration for each projection
- for each ray
- compute back-projection
- compute difference to measured projection
- distribute difference
- end for
- end for
- end while

Starting with initial guess $f^{(0)}$ and projections p .

Table 1. Initial Image Data ($f^{(0)}$)

0	0	0
0	0	0
0	0	0

Table 2. Initial Projection Value (p)

2	6	8	7
9	7	2	1
3	9	2	6
8	7	9	7

After 4 iteration

Table 3. Final Reconstructed Image

2.74	5.97	1.65
2.47	2.59	5.68
4.71	3.25	3.96

Table 4. Projection data of final reconstructed image

10.36	10.74	11.92	9.92
11.81	11.29	4.71	5.72
9.29	11.65	1.65	2.74
8.44	8.95	8.93	3.96

Table 5. Error calculated in Image pixel values for every iteration

Iteration	$ f_{i+1} - f_i $	$(f_{i+1} - f_i)^2$
1	33.9999	143.9506
2	4.6913	3.4226
3	1.6872	0.5149
4	0.8254	0.1038

We are now done; because in this example the image has only nine pixels, it is convenient to present it as a line graph.

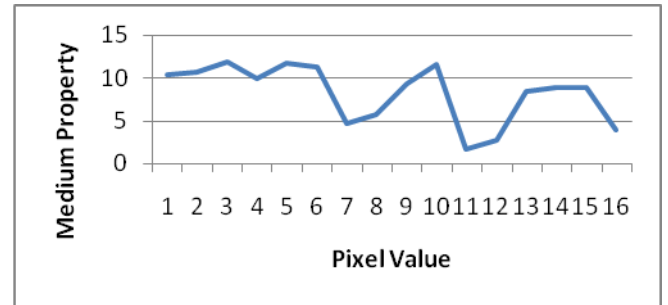


Fig 3. Image as a line Graph using ART with 4 iteration

In general, M and N are quite large. For example, when reconstructing an image size of 256×256 pixels, from 256 detector measurements in each of 256 views, N and M are both 65,536. In such cases the weight matrix size is $65,536 \times 65,536 = 4,294,967,296$. We require algorithms that are efficient in terms of both time and memory requirements to solve this on a computer without increasing turnaround time in the CT suite.

3. CONCLUSION

We have tested the algorithm on 3×3 image in which, we obtained four reconstructions iterative where errors in successive iterations are reducing very fast as it is evident from table 5. The algorithm now experimented with more numbers of projections to find the image data.

4. REFERENCES

- [1] R. Gordon et al., "Three-Dimensional Reconstruction from Projections: A Review of Algorithms", International Review of Cytology, Vol. 38, p. 111 (1974).
- [2] R. Gordon, R. Bender, and G. T. Herman, "Algebraic reconstruction techniques (ART) for three-dimensional

- electron microscopy and X-ray photography," J. Theoret. Biol., vol. 29, pp. 471-482, 1970.
- [3] F.Natterer, " The Mathematics of Computed Tomography", John Wiley and Sons, New York, 1986.
- [4] A.H. Andersen, "Algebraic Reconstruction in CT from Limited Views" , IEEE Trans. On Medical Imaging, Vol. 8, pp 50-55, 1989.
- [5] S. Kaczmarz, "Angentirte Auflösung von Systemen linearer Gleichungen," Bull. Int. Acad. Pol. Sei. Lett., A, vol. 35, pp. 355-357, 1937.
- [6] Flisch et al, ETH Zürich "Industrial Computed Tomography in Reverse Engineering Applications" Industrial Applications and Image Processing in Radiology March, 15 – 17, 1999 Berlin, Germany.
- [7] J. Friedhoff, Aufbereitung von 3D-Digitalisierdaten für den Werkzeug-, Formen-und Modellbau, Vulkan Verlag, Essen 1997.
- [8] Herman, G.T., Image Reconstruction from Projections: The Fundamentals of Computerized Tomography, Academic Press, New York, 1980.
- [9] C. N. Hounsfield. "A method of and apparatus for examination of a body by radiation such as or Gamma radiation." Patent Specification 1283915, London, 1968.
- [10] K. Tanabe, "Projection method for solving a singular system," Numer. Math., vol. 17, pp. 03-214, 1971.
- [11] A. H. Andersen and A. C. Kak, "Simultaneous algebraic reconstruction technique (SART): A superior implementation of the art algorithm," Ultrason. Imaging, vol. 6, pp. 81-94, Jan. 1984.
- [12] Tanuja Srivastava, Raghav Singh, Nirvikar, " ART with 3 projections in CT", CICON – 2010, pp. 1-3, May 8-9, 2010.



10 International Year of Biodiversity

5th

UTTARAKHAND
STATE SCIENCE AND
TECHNOLOGY
CONGRESS



10 - 12 NOVEMBER, 2010

RECONSTRUCTION WITH 16 PROJECTIONS USING ART

Nirvikar* and Tanuja Srivastava

Department of Mathematics, College of Engineering Roorkee, Roorkee

Email: nirvikarlohan@yahoo.com

The word *tomography* means "reconstruction from projections", i.e. the recovery of a function from its line or (hyper) plane integrals (from the Greek – slice and –to write). In the applied sense, it is a method to reconstruct cross sections of the interior structure of an object without destructing or damaging the object. The initial use of computed tomography (CT) for applications in radiological diagnostics during the seventies sparked a revolution in the field of medical engineering. Medical imaging has also been successfully accomplished with radioisotopes, ultrasound, and magnetic resonance. There are numerous nonmedical imaging application, which lend themselves to the methods of CT like the mapping of underground resources via crossboreholes imaging.

The Algebraic Reconstruction Technique (ART) introduced by Gordan, Bender and Herman, uses a large number of projections to reconstruct the 2-dimensional beam density distribution. The ART algorithm begins with some initial estimate of the image to be reconstructed and modifies this estimate repeatedly until the pixel values appear to converge by some criterion. ART

decides how to modify the image by summing the pixels along some straight path and comparing this sum to the measured ray sum. The difference between projections calculated from the image estimate, and the measured ray is calculated, and the adjustment is divided among the pixels in the ray sum. The methods of algebraic reconstruction techniques (ART) in computerized tomography are based on a representation of the projection line integrals as discrete ray-sums. Let p_i be the ray-sum measured with the i th ray then the relationship between the f_j 's and p_i 's may be expressed as:

$$P_i = \sum_{j=1}^N w_{ij} f_{j,i} = 1, 2, \dots, M \quad (1)$$

where M is the total number of rays (in all the projections) and w_{ij} is the weighting factor that represents the contribution of the j th cell to the i th ray integral. When we project the $(j-1)$ th solution onto the i th hyperplane [j th equation in (1)] the gray level of the j th element, whose current value is $f_j^{(i-1)}$, is obtained by

$$\Delta f_j^{(i)} = f_j^{(i)} - f_j^{(i-1)} = \frac{p_i - q_i}{\sum_{k=1}^N w_{ik}^2} w_{ij} \quad (2)$$

where p_i is the measured ray-sum along the j th ray, q_i is the computed ray-sum for the same ray based on the $(j-1)$ th solution for the image.

ART simple example,

We have an image of $N = 9$ pixels with 4 detectors in the detector array, and the array is rotated through 4 views (horizontal, vertical, diagonal and anti diagonal) to produce $M = 16$ ray sums. Starting with initial guess at $f^{(0)} = (0, 0, 0, 0, 0, 0, 0, 0, 0)$ with given projections

$p = (3, 7, 9, 8, 56, 4, 4, 9, 7, 4, 9, 4, 2, 6, 4, 1)$, after 4 iterations we found the final image data and projection match.

$$\begin{aligned} f &= (2.78, 0.00, 3.04, 3.67, 2.33, 0.67, 8.22, \\ &3.67, 1.78) \\ p &= (5.81, 6.67, 13.67, 14.67, 6.00, 5.48, \\ &8.22, 7.34, 6.89, 0.67, 3.04, 1.78, 4.54, \\ &13.59, 3.67, 2.78) \end{aligned}$$

The algorithm is now experimented with more numbers of projections to find the image data. The proposed research work is very important as it provides solution to real work problems, which will be better than existing known solutions. As well; this will provide an algorithm which can be directly applied to the problem to get solution. So this will reduce to get implementation errors which occur when an analytic solution is implemented on real world problems.

COMMON FIXED POINTS UNDER CONTRACTIVE CONDITION IN FUZZY METRIC SPACE

Sanjay Kumar Padaliya* and Achin Jain

Department of Mathematics, SGRR (PG) College, Pathri Bagh, Dehradun

Email: spadaliya12@rediffmail.com

The aim of this paper is to consider a new approach for obtaining common fixed point theorems in Fuzzy metric spaces by subjecting new contractive condition, property (E.A) introduced by Aamri and Moutawakil [1], which is independent of the known contractive definitions. We give examples and initiate the application of Property (E.A) for investigating fixed points of mappings in fuzzy metric space.

YOUNG SCIENTIST Award



u
cost
राजीव गांधी दून विश्वविद्यालय

Govt. of Uttarakhand

This is to certify that

NIRVIKAR

has been awarded

Young Scientist Award for Best Oral Presentation-2010

under the discipline

Mathematics; Statistics & Computer Science

5TH UTTARAKHAND STATE SCIENCE AND TECHNOLOGY CONGRESS-2010

SCIENCE AND TECHNOLOGY FOR DEVELOPMENT

Doon University, Dehradun, Uttarakhand
10-12 November, 2010
Uttarakhand State Council for Science & Technology (UCOST)

(Prof. Girijesh Pant)
Vice Chancellor

Doon University
Dehradun, Uttarakhand

(Dr. Rajendra Dobhal)
Director
Uttarakhand State Council for Science & Technology
Dehradun, Uttarakhand